2012

Conversion of a Micro, Glow-Ignition, Two-Stroke Engine from Nitromethane-Methanol Blend Fuel to Military Jet Propellant (JP-8)

Andrew L. Wiegand
Michigan Technological University

CONVERSION OF A MICRO, GLOW-IGNITION, TWO-STROKE ENGINE FROM NITROMETHANE-METHANOL BLEND FUEL TO MILITARY JET PROPELLANT (JP-8)

By

Andrew L. Wiegand

A THESIS

Submitted in partial fulfillment of the requirements for the degree of

MASTER OF SCIENCE

In Mechanical Engineering

MICHIGAN TECHNOLOGICAL UNIVERSITY

2012

This thesis has been approved in partial fulfillment of the requirements for the Degree of MASTER OF SCIENCE in Mechanical Engineering.

Department of Mechanical Engineering – Engineering Mechanics

Thesis Co-Advisor:	Dr. Scott A. Miers
Thesis Co-Advisor:	Dr. Jason R. Blough
Committee Member:	Dr. Wayne W. Weaver
Department Chair:	Dr. William W. Predebon

Table of Contents

Appendices

List of Figures

List of Tables

Disclaimer

Reference herein to any specific commercial company, product, process, or service by trade name, trademark, manufacturer, or otherwise, does not necessarily constitute or imply its endorsement, recommendation, or favoring by the United States Government or the Department of the Army (DoA). The opinions of the authors expressed herein do not necessarily state or reflect those of the United States Government or the DoA, and shall not be used for advertising or product endorsement purposes.

Copyright Permission

Abstract

The goal of the thesis “Conversion of a Micro, Glow-Ignition, Two-Stroke Engine from Nitromethane-Methanol Blend Fuel to Military Jet Propellant (JP-8)” was to demonstrate the ability to operate a small engine on JP-8 and was completed in two phases. The first phase included choosing, developing a test stand for, and baseline testing a nitromethane-methanol-fueled engine. The chosen engine was an 11.5 cc, glow-ignition, two-stroke engine designed for remote-controlled helicopters. A micro engine test stand was developed to load and motor the engine. Instrumentation specific to the low flow rates and high speeds of the micro engine was developed and used to document engine behavior. The second phase included converting the engine to operate on JP-8, completing JP-8-fueled steady-state testing, and comparing the performance of the JP-8-fueled engine to the nitromethane-methanol-fueled engine. The conversion was accomplished through a novel crankcase heating method; by heating the crankcase for an extended period of time, a flammable fuel-air mixture was generated in the crankcase scavenged engine, which greatly improved starting times. To aid in starting and steady-state operation, yttrium-zirconia impregnated resin (i.e. ceramic coating) was applied to the combustion surfaces. This also improved the starting times of the JP-8-fueled engine and ultimately allowed for a 34-second starting time. Finally, the steady-state data from both the nitromethane-methanol and JP-8-fueled micro engine were compared. The JP-8-fueled engine showed signs of increased engine friction while having higher indicated fuel conversion efficiency and a higher overall system efficiency. The minimal ability of JP-8 to cool the engine via evaporative effects, however, created the necessity of increased cooling air flow. The conclusion reached was that JP-8-fueled micro engines could be viable in application, but not without additional research being conducted on combustion phenomenon and cooling requirements.

Acknowledgements

My mother has a plaque that reads, “A journey of a thousand miles begins with a single step.” Cliché? Certainly. True? Undoubtedly so.

This thesis is the end of my thousand mile journey, and along the way I have encountered many individuals that have helped me through. Some of them followed me along the way and others were only part of my journey for a brief moment. All of them, however, deserve my thanks. Without them, that “journey” may have never happened.

First, I must thank Dr. Scott Miers, my advisor, for pulling me into graduate school. I had no intention of continuing my education beyond my bachelor’s degree until his enthusiasm drew me back into academics. Without him, I would have never had this journey for which I am especially thankful.

Thanks are also due to the many faculty and staff at Michigan Technological University. Dr. Jason Blough, my co-advisor, could always be counted on for creative solutions. Mr. Marty Toth, the mechanical engineering department’s machinist, could always be counted on to figure out my occasionally odd requests. Ms. Nancy Barr more than twice reviewed my long-winded papers out of the kindness of her heart. And of course, my thanks goes to all of the staff of the mechanical engineering department for their various efforts in helping me to succeed.

A thousand miles is a long journey, and my journey would not have been possible without the close friendship of John Armstead and Denise Rizzo. Through the many disappointments, distractions, and failures, they were both there to keep me focused and keep me moving; they were the ones that reminded me to keep taking the next steps.

Finally, I must thank the two people that got me to where I am in the first place. A special thanks to my mother and father, Jackie and Mark Wiegand, for their continued support. They engrained me with work ethic, pushed me to realize my potential, and were always supportive when I was unsure of the path my journey was taking.

It is safe to say that without the influence of these and many others, I would not be successful. I would have never taken the first steps, the correct steps, or the last steps without all of their help.

Thank you.

Chapter 1 Introduction

1.1 Project Origins

In June 2011, a research project was initiated at Michigan Technological University. It was funded through MTU's Keweenaw Research Center (KRC) where Mr. Geoff Gwaltney of the KRC was the Principle Investigator (PI), Dr. Scott Miers of MTU was the Research Lead and I, Andrew L. Wiegand, was the Graduate Research Assistant. This project was focused on the conversion of a micro, glow-ignition, internal combustion engine from nitromethane-methanol blend fuel to military jet propellant (JP-8).

JP-8 is the common fuel in combat operations, specified by the United States Department of Defense Directive 4140.25 [1]. The use of JP-8 as the fuel for a micro engine opens up application possibilities because JP-8 is available commercially as Jet-A fuel and is similar to kerosene. These fuels are safer and more commonly available compared to the stock nitromethane-methanol blend fuels of micro engines, which would make placing micro engines in applications easier.

1.2 Motivation

A glow-ignition, crankcase scavenged, two-stroke engine architecture has many advantages that make exploring it for compact applications worth considering. Glow ignition engines, which are common in the hobby aircraft industry, have no electronic ignition system, making them robust as there are fewer components susceptible to failure. Additionally, crankcase scavenged two-stroke engines are mechanically simple which allows them to be lightweight and durable; this would be an extremely important feature for applications that are highly mobile and work under the most critical of circumstances. Crankcase scavenged two-strokes are also especially compact and simple to maintain, which makes them appealing for mobile applications. While they are inherently inefficient, applications involving steady-state conditions could be tuned for that operating point in the engine, helping to eliminate the inefficiencies of a crankcase scavenged, two-stroke engine.

The objective of JP-8-fueled operation was motivated by the "Single Fuel Forward" concept. First implemented by the U.S. military in 1986, the "Single Fuel Forward" concept is simple; all land-based vehicles should be capable of using a single fuel to simplify fuel support logistics. Specifically, the newest directive (Department of Defense Directive 4140.25, "DoD Management Policy for Energy Commodities and Related Services") states:

"Primary fuel support for land-based air and ground forces in all theaters (overseas and in the Continental United States) shall be accomplished using a single kerosene-based fuel, in order of precedence: JP-8, commercial jet fuel (with additive package), or commercial jet fuel (without additives), as approved by the Combatant Commander. Fuel support for ground forces may also be accomplished using commercially available diesel fuel when supplying jet fuel is not practicable or cost effective." -DoD 4140.25, April 12, 2004

This directive therefore eliminates the possibility of using the stock nitromethane-methanol blend fuel in any land-based military application.

The positive implications of using a kerosene-based fuel can be extended into the civilian field applications, as well. The stock nitromethane-methanol fuel is not only corrosive, but is also highly flammable. Kerosene type fuel is far more stable due to its higher flash point and would likely be preferred for applications where explosions, damage, and fire are prevalent. Kerosene type fuels are also cheaper and more common than nitromethane-methanol blend fuels.

One final note is necessary when describing the motivation for this project. There is a lack of objectives and constraints for the fuel conversion of the engine because this project was intended to act as a first step in the development of an improved JP-8-fueled engine. The underlying goal of this project was to identify future issues and methods of improvement for the JP-8 fuel conversion, which ultimately will allow for a more robust finished product.

1.3 Project Phases and Accompanying Objectives

The primary goal of the project was to demonstrate the ability to operate a small (less than 20 cubic centimeters), internal combustion engine on JP-8 fuel. The process of completing this conversion was to be accomplished in two phases.

The first step of phase 1 was to choose a commercial off-the-shelf (COTS) engine for conversion. The only three requirements for the COTS engine was the ability to be modifiable to operate on JP-8 fuel, to be less than 20 cubic centimeters, and to be capable of producing 250 W of power.

The second step of phase 1 was to design a test stand capable of providing and absorbing power from the engine with appropriate instrumentation and the ability to log the data during steady-state conditions. Additional specifications including maximum power and speed for power dissipation were not initially identified and were developed at a later date. The required instrumentation and data was all the information necessary to fully document the conversion.

The final step of phase 1 involved testing the chosen COTS engine in its stock form and with the fuel it was designed for as a baseline. Performance, combustion, and fuel flow data were specifically required from the stock COTS engine.

With phase 1 complete, phase 2 could be started. The first step of phase 2 was to understand the challenges of and develop a method for converting the COTS engine to JP-8. No specific constraints or objectives were initially outlined, other than the objective of a successful JP-8 conversion.

The second step of phase 2 included documenting the converted engine's performance over a variety of speeds and loads. The desired speeds and loads were not initially specified, and a durability study was not anticipated. It was implied that the same performance measurements collected with the stock fuel before the conversion were to be collected after the conversion for comparison reasons.

The final step of phase 2 was to document any future work that was deemed necessary and suggest routes to improvement of the JP-8-fueled engine.

Note that the project lacked specific numerical objectives or constraints; these were developed as the project progressed and are discussed in the appropriate sections.

1.4 Summary

The purpose of this thesis is to fully understand and document the conversion of a small, COTS internal combustion engine from the fuel it was designed for to JP-8. This purpose implies necessity of the development of a test stand capable of high speed, low flow rate, high precision measurements, the testing of a COTS engine in its stock form, developing features to allow operation on JP-8, and, finally, comparing the performance of the JP-8-fueled engine to its stock form.

Chapter 2 Background

2.1 Glow-Ignition, Centimeter Scale, Two-Stroke Engines

The engine used in this fuel conversion project was a glow-ignition, centimeter scale, crankcase scavenged, two-stroke engine normally fueled by a nitromethane-methanol blend of fuel. For brevity, this type of engine will be referred to as a “micro engine” henceforth. Micro engines present a number of unique behaviors and challenges that must be understood in order to operate and modify the engine successfully. The fuel’s role in the engine and the way the ignition is initiated, specifically, differ from conventional internal combustion engines.

In a conventional engine, the fuel’s primary role is to provide energy for the combustion process. The fuel also provides some mild cooling effect, especially in small engines, but this is usually a secondary role for the fuel. In two-stroke engines, namely those engines that run a fuel that is premixed with oil, the fuel also acts as a lubricant. These fuel roles are understood and applied in many engines, but micro engines rely on these roles of the fuel more heavily than most engines. The fuel in a micro engine is crucial to the engine’s operation not only in providing energy for conversion, but equally for cooling and lubricating effects.

Micro engines commonly use a nitromethane-methanol blend of fuel. The methanol in the fuel has a high latent heat of vaporization, meaning that it takes considerable energy for the methanol to vaporize. Micro engines typically take advantage of this fact by using the vaporization energy to cool the engine. As the fuel moves through the crankcase, through the transfer ports, and into the combustion chamber, it absorbs heat energy and vaporizes. By running a fuel-rich mixture through the engine, the vaporization effect is used as the primary source of cooling. In fact, micro engines typically run fuel-rich enough that raw fuel droplets are readily observed in the engine’s exhaust stream.

Lubrication in a micro engine is especially critical for engine durability due to the high rotational speeds and the lack of natural lubricity in the nitromethane-methanol blend fuel. The micro engine used in this research (the O.S. Engines 70SZ-H) is capable of up to 18,000 RPM. This speed is not unusual for micro engines and other micro engines may operate in excess of 25,000 RPM. This sort of rotational speed demands excellent lubrication as even short durations without lubrication at these speeds could be catastrophic. Additionally, because of the short amount of time spent in the engine, the premixed fuel and oil must be sufficiently oil-rich that the oil has a chance to penetrate the appropriate interfaces. Nitromethane and methanol also act as solvents,

providing minimal lubricity in the engine. For these reasons, oil percentages near 20% are common in nitromethane-methanol blend fuels used in micro engines. The oil used can be either castor oil, synthetic oil, or a combination of the two oils. Selection of the oils is largely based on operator preference.

Ignition in a micro engine is a complex process that can be initiated by multiple sources and can be changed by multiple conditions. The ignition process in a micro engine can be initiated by heat from the compression process, the heat supplied by a filament style glow plug, or a catalytic reaction of methanol with the platinum coating applied to the glow plug [2]. Note, however, that none of these processes of ignition can be intelligently controlled, making optimal tuning of the engine for multiple operating conditions nearly impossible. Additionally, as ambient conditions, fuel constituents, and carburetor tuning change, the phasing of the fuel-air charge ignition changes. Ambient air temperature and pressure affect the heat generated in compression. The fuel constituents change the ignition behavior of the fuel/air charge. The carburetor tuning affects how much heat is lost from the glow plug. All of these conditions alter the ignition process. In practice, operators of micro engines regularly alter their tuning settings to achieve the desired operating characteristics.

By understanding the importance of the fuel's role in the ignition process in a micro engine, successful modifications can be made. In this project, the fuel was modified, but with the understanding that lubrication and heat rejection had to be accounted for. Likewise, the loss of methanol from the fuel resulted in the loss of the ability to start ignition by catalytic reaction. By understanding these basic principles of micro engine operation, a successful fuel conversion could be made.

2.2 Fuel Properties

Converting a micro engine from nitromethane-methanol blend fuel to JP-8 fuel required careful fuel property consideration. Specifically, the lubricity of the fuel-oil blends and the thermodynamic properties of the fuels were necessary to document while converting the engine from nitromethane-methanol blend fuels to JP-8.

2.2.1 Methods of Determining Lubricity

(1) Overview

Lubrication in micro engines is accomplished through a premixed blend of fuel and lubricating oil. While the amount and type of lubricant in commercially available nitromethane-methanol blend fuels is usually available, a quantifiable measure of the lubricity of those fuels is not published. For the fuel conversion process, it was necessary to have a quantifiable measure of the fuel lubricity. Therefore, two ASTM fuel lubricity testing methods were explored.

Based on thorough research, it seems that there is no standard way to document the lubricity of premixed fuel-oil combinations in the application of two-stroke engines. Premixed fuel and oil is a somewhat archaic method of lubricating an engine and is reserved for only the lowest cost applications. Additionally, it seems that the low cost of these engines means destructive testing is the standard measure of durability. As destructive testing would not be acceptable for the micro engine conversion project, additional fuel lubricity information was sought out.

In the 1980's and 1990's there was research conducted in the field of fuel lubricity for diesel engines that resulted in multiple lubricity measurement standards. As the chemical content of commercial diesel fuel was changed to produce lower emissions, the abrasiveness of diesel fuel increased. This was especially problematic for the new high pressure fuel systems of the time being used to comply with increased diesel emission regulation. In order to quantify the lubricity of the fuels and ensure component durability, the ASTM standards D6078 and D6079 were developed [3]. As these tests are still used for diesel fuel lubricity measurements, they seemed a good fit for quantifying the lubricity of the fuel-oil blends used in the micro engine fuel conversion project.

(2) ASTM D6078 – Scuffing Load Ball-on-Cylinder Lubricity Evaluator

The first testing method examined was the ASTM D6078 standard, known as the scuffing load ball-on-cylinder lubricity evaluator (SLBOCLE). The SLBOCLE is a test used to examine the lubricity properties of diesel fuels in applications where the fuel acts as a lubricant between surfaces with tangential friction forces [4]. This would include interfaces commonly seen in rotating machinery, such as fuel pumps and bearing surfaces. The results of the SLBOCLE are also generally considered a good indication of the test specimen's lubricity in any additional friction interfaces.

The SLBOCLE test apparatus holds a prepared test cylinder in contact with a 2.7 mm ball while the test cylinder is partially submerged in a 50 mL sample of the fuel being tested. The fuel is kept in an environment with a specific relative humidity, air flow rate, and temperature. The test cylinder is rotated at 525 RPM while the ball is in contact with the cylinder and a load is applied to the ball. The apparatus is instrumented to record the tangential friction force between the test ball and test cylinder. Essentially, the load applied to the ball is increased or decreased until the tangential friction coefficient is equal to 0.175. This load is recorded in grams and is reported as the final result of the test. Figure 2-1 shows a simplified diagram of the SLBOCLE apparatus, where the "Test Load" is the load reported when the friction coefficient is equal to 0.175. Note that additional detail can be found in ASTM D6078.

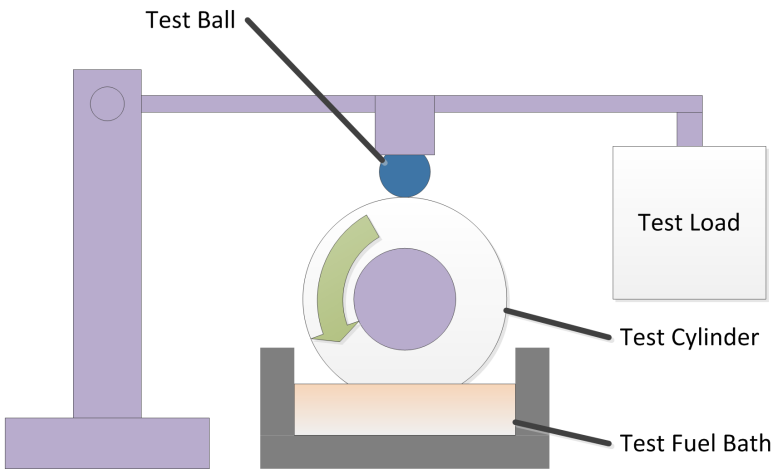

Figure 2-1: SLBOCLE simplified representation

(3) ASTM D6079 – High Frequency Reciprocating Rig

Another method for documenting diesel fuel lubricity is ASTM D6079, known as the high frequency reciprocating rig (HFRR) test. The HFRR test is also used to evaluate diesel fuel lubricity, but the results are more applicable to boundary lubrication conditions; due to the short stroke of the reciprocation, the effects of viscosity are minimized, creating a condition where viscous effects (assumedly hydrodynamic lubrication) are eliminated [5]. The ASTM standard does not specify where this type of wear could exist, but one can reasonably deduce that conditions where oscillation occurs are good examples of where boundary lubrication is crucial.

Such cases could include piston ring-cylinder liner interfaces. No direct correlation between ASTM D6078 and D6079 exists, though they both are used to generally quantify diesel fuel lubricity.

The HFRR test apparatus is similar to the SLBOCLE apparatus in that it holds a small sample of the test fuel under specific atmosphere conditions while it loads a ball against a test specimen. The difference between the tests is that instead of the ball being in contact with a rotating cylinder, the ball is held against a fixed flat disk and is oscillated 1 mm at 50 Hz for 75 minutes. Upon test completion, the ball is removed and examined with a microscope. The wear scar on the ball, caused by the contact with the plate, is documented and reported in microns. Figure 2-2 shows a simplified diagram of the HFRR apparatus. Again, note that a more specific testing procedure is available in ASTM D6079.

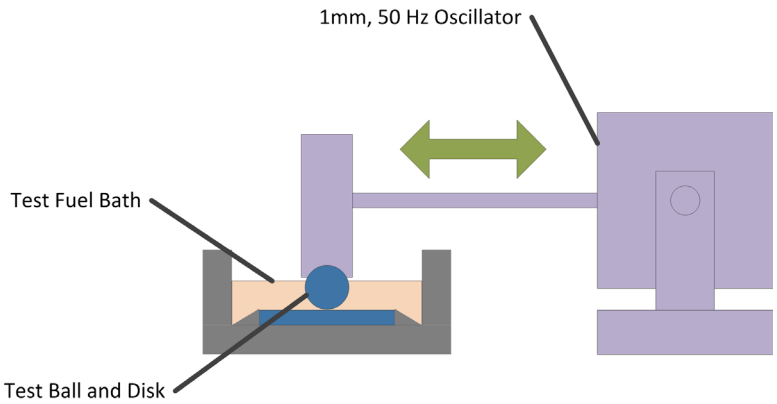

Figure 2-2: HFRR simplified representation

2.2.2 Thermodynamic Properties of Investigated Fuels

Nitromethane-methanol-fueled micro engines rely on their fuel for cooling, starting, and general run characteristics far more than conventional engines. Micro engines run fuel-rich to provide cooling to the entire engine. Likewise, they rely on the reactivity of their fuel for starting and ignition. These engines do not have any sort of intelligent control of their ignition timing, so the fuel often acts as a primary modifier of the engine's behavior. Therefore, in order to successfully convert the micro engine from nitromethane-methanol blend fuel to JP-8, the physical properties of the fuels must be documented and compared. The physical properties compared here were selected because they best represent the varied fuel behaviors crucial to the micro engine fuel conversion. These properties include liquid density, net heat of combustion, latent heat of

vaporization, stoichiometric air-to-fuel mass ratio, flash point, and autoignition temperature. Each of these properties can be summarized as follows:

- Liquid density – This is the density in kilograms per liter of fuel in its liquid state. The density is crucial in understanding the amount of energy available per liter of fuel and also when calculating the mass ratios in the nitromethane-methanol blend fuels.
- Net heat of combustion – The net heat of combustion is a measure of the amount of energy in a fuel with some specific conditions and is also commonly called the lower heating value of the fuel. The conditions placed on the net heat of combustion are that all of the fuel is completely oxidized so that all carbon is part of a carbon dioxide molecule, all hydrogen is part of a water molecule, and all sulfur is part of a sulfur dioxide molecule. Additionally, the term “net” is used to indicate that the water in the products remains in a vapor form and has not been condensed into a liquid. If the water was condensed into a liquid form, the amount of energy released by the fuel would be greater due to the additional energy from the water’s heat of vaporization. This energy is called the gross heat of combustion or higher heating value [6].
- Heat of Vaporization – Also called the enthalpy of vaporization or the latent heat of vaporization, this is a measure of the amount of heat energy required to vaporize a given mass of saturated liquid into a saturated vapor state. In the provided properties, the heat of vaporization is given at atmospheric conditions. This property is crucial in understanding how the fuel is used to cool the engine as well as how difficult it may be to produce a flammable fuel vapor mixture [6].
- Stoichiometric air-to-fuel mass ratio (AFR_s) – This is the ratio of the mass of air to the mass of fuel required for complete, ideal combustion. The AFR_s is calculated using chemical stoichiometry where one mole of the fuel is completely oxidized using atmospheric air (where 1 mole of atmospheric air is composed of 1 mole of diatomic oxygen plus 3.773 moles of diatomic nitrogen) into carbon dioxide, water, and diatomic nitrogen. Once a balanced chemical equation is produced for the complete combustion of the fuel, the mass of the required atmospheric air is divided by the mass of the fuel to yield the AFR_s [7]. The AFR_s is used as a baseline to compare the amount of fuel required for the combustion process given a set amount of air mass taken into the engine.
- Flash point temperature – The flash point of a fuel is defined as the temperature at which the fuel can produce a flammable mixture with air under controlled conditions. Note that the flash point is the temperature where a flammable mixture is present, not necessarily

where combustion occurs. In simple terms, this is the temperature where an ignition source could ignite the fuel. It is commonly used to determine whether a substance is flammable or combustible for transportation reasons and can be measured by many standards [8]. While flash point is not a commonly reported property for engine testing, it proved to be useful for the micro engine fuel conversion.

- Autoignition temperature – The temperature at which a fuel combusts in air without a distinct ignition source is called the autoignition temperature. The autoignition temperature can vary widely based on the apparatus used for its determination, but when compared qualitatively can be used to predict the readiness of fuel to autoignite [9].

A collection of these physical properties are presented here for JP-8, heavy diesel fuel (approximately equivalent to diesel fuel #2), methanol, nitromethane and for a 15 vol% blend of nitromethane in methanol in Table 2-1. However, due to the nature of these fuels, some further clarification is necessary when discussing these values.

Table 2-1: Physical properties for investigated fuels [10] [7] [11] [12] [13] [14]

Property		JP-8	Heavy Diesel	Methanol	Nitromethane	15 vol% Nitromethane-Methanol Blend
Liquid Density	(kg/L)	0.775 - 0.840	0.820-0.880	0.792	1.139	0.862
Net Heat of Combustion	(MJ/kg)	42.8 (min)	42.9	19.6	10.5	17.8
Heat of Vaporization	(kJ/kg)	250*	230	1100	561	991
Stoichiometric Air/Fuel Mass Ratio	(-)	14.8*	14.4	6.5**	1.7**	4.2**
Flash Point	(°C)	38	51.7	16.1	43.3	~16
Autoignition Temperature	(°C)	220*	329.4	463.9	418.3	~418
* - Value for Kerosene, ** - Calculated Value						

The first point that needs to be made is that the properties of JP-8 are difficult to provide due to how the US military standard MIL-DTL-83133H is written. In this military standard, specifications of the chemical and physical properties as well as the test methods for determining those properties are provided. However, values are presented as a minimum and maximum value, if

they are specified at all. By reducing the amount of requirements of the fuel, it is likely to be cheaper and easier to produce. However, because JP-8 is a kerosene-based fuel, it seems plausible for this qualitative analysis to present properties of kerosene for the values not specified in the military standard. These values are denoted with a single asterisk in Table 2-1.

Next, explanation of the heavy diesel fuel values is necessary. These values are also a range of values as diesel fuel's physical properties can vary. Additionally, these values are presented for heavy diesel, which is approximately equivalent to diesel fuel #2. The values for heavy diesel are included for comparison purposes to show that while heavy diesel is similar to JP-8, it would be more difficult to combust in the micro engine. Note that diesel fuel #1 (not shown) is very similar to kerosene and therefore would be directly comparable to JP-8.

The properties of methanol and nitromethane are the properties of these neat fuel constituents in a high state of purity. The values presented for the 15 vol% nitromethane in methanol blend, however, are a combination of the properties of its two neat fuel constituents. This fuel blend, which was used in the micro engine testing, does not have published values for any of the properties given. In order to approximate the properties of this fuel combination, a number of assumptions were made. First, it was assumed that the commercial "15%" nitromethane content was a volume percent (vol%) defined as the volume of nitromethane divided by the total fuel volume. Next, the volume percentage was converted into a mass percentage. The properties of the nitromethane and methanol were then linearly combined, weighted by the mass percentage, into a single approximate value for the nitromethane-methanol blend; this was completed for the density, net heat of combustion, and heat of vaporization. For the temperatures, it was assumed that the lowest value of the two constituents would likely be the primary contributor to the respective behavior and listed that value for the blended fuel. These approximations cannot be confirmed without experimental testing and assume that no chemical changes occur when nitromethane and methanol are blended.

The final note necessary to present is the calculation of the stoichiometric air-to-fuel mass ratios. These ratios were calculated using ideal combustion stoichiometry for the methanol and nitromethane fuels. Additionally, by converting the volume percentage into a molar ratio, the combustion stoichiometry was calculated for the 15 vol% nitromethane-methanol blend fuel. The values in Table 2-1 that were calculated this way are denoted with a double asterisk. The value for heavy diesel is a reported value commonly accepted in practice and the value for JP-8 was assumed to be approximately equal to the value for kerosene.

2.2.3 Qualitative Examination of Fuel Properties

Having presented the quantitative properties of the fuel, a qualitative analysis of the fuels' behaviors can be presented.

The density and net heat of combustion of the fuels are important to the micro engine project because of the end application; a benefit of converting the engine to JP-8 is that because the energy density is higher for JP-8, less fuel must be theoretically carried in the final application. Consider the calculations presented below. Multiplying the liquid fuel density by the net heat of combustion provides a value of how much energy is available per unit of volume. These calculations show that there is approximately double the amount of available energy in a unit volume of JP-8 compared to a unit volume of 15 vol% nitromethane-methanol blend (abbreviated as NM in the calculations).

$$Liquid\ Density * NHoC = available\ energy\ per\ liter\ fuel$$

$$0.775 \frac{kg\ JP8}{L\ JP8} * 42.8 \frac{MJ}{kg\ JP8} = 33.17 \frac{MJ}{L\ JP8}$$

$$0.862 \frac{kg\ NM}{L\ NM} * 17.8 \frac{MJ}{kg\ NM} = 15.34 \frac{MJ}{L\ NM}$$

Next, consider the amount of energy delivered into the engine for a unit of air. By inverting the AFR_S, the mass of fuel per unit mass of air is obtained; this is called the stoichiometric fuel-to-air ratio (FAR_S). Assuming the engine runs with similar air intake behavior on both fuels, this value can be multiplied by the net heat of combustion to provide an amount of energy delivered into the engine per unit mass of intake air at stoichiometric conditions.

$$\frac{1}{AFR_s} = FAR_s \rightarrow Mass\ of\ fuel\ per\ unit\ mass\ of\ air$$

$$FAR_S * NHoC = Energy\ per\ unit\ mass\ of\ air$$

Completing this equation for JP-8 and the 15 vol% nitromethane-methanol blend and comparing the values, it is clear that converting from nitromethane-methanol blend to JP-8 will result in a 46.5% reduction in the amount of energy delivered into the cylinder at stoichiometric conditions.

Combine this fact with the fact that JP-8 combusts bests in fuel-lean conditions while nitromethane-methanol can combust at especially fuel-rich conditions and it is clear that there would be a significant reduction in energy potential provided to the micro engine after it has been converted to JP-8.

$$\left(\frac{1}{14.8}\ kg\ JP8\right) * 42.8 \frac{MJ}{kg\ JP8} = 2.892\ MJ$$

$$\left(\frac{1}{4.2}\ kg\ NM\right) * 17.8 \frac{MJ}{kgNM} = 4.238\ MJ$$

$$Percent\ Change = \frac{2.892 - 4.238}{2.892} = \mathbf{-46.5\%}$$

In most homogenous charge engines, fuel has a role of absorbing heat energy as it is introduced into the charge that will be combusted. This generally provides a slight cooling effect for the engine components and also increases the air-fuel charge density. More importantly, however, is that as the liquid fuel absorbs the surrounding heat energy it transitions into a vapor phase, creating a combustible mixture. The property that characterizes the amount of energy necessary to vaporize the liquid fuel is called the heat of vaporization.

Micro engines rely heavily on the high heat of vaporization of the nitromethane-methanol blend fuels that they operate on for engine cooling. From Table 2-1, a 15 vol% nitromethane in methanol blend needs 991 kilojoules per kilogram of fuel to vaporize from a saturated liquid state. This is almost a four-fold increase in the amount of energy required to vaporize a kilogram of fuel compared to JP-8. Because the nitromethane-methanol blend fuels require so much energy to vaporize, they provide a substantial cooling effect to the micro engine. The micro engine, in turn, can be made with less cooling fin surface area which allows for lighter engines. This is a substantial challenge when converting micro engines to JP-8, however, as they are not designed to operate without this dramatic cooling effect. One advantage of JP-8's low heat of vaporization, however, is that less heat is required to form a fuel vapor-air mixture.

This topic of flammable mixture transitions into flash point property. From Table 2-1, the flash point of methanol is only 16.1°C. This means that at room temperature, the vapors surrounding liquid methanol are flammable. JP-8, however, is designed to have a minimum flash point of 38°C. This makes it far safer to transport and store because it requires a relatively high temperature before a flammable mixture exists.

The disadvantage of JP-8 in the micro engine is this high flash point. The mixture preparation on a micro engine is poor due to the use of a carburetor and pooling of liquid fuel in the crankcase. At room temperature, methanol forms a combustible mixture, so poor mixture preparation is not problematic. JP-8's higher flash point is problematic, though, because even though it requires less energy to vaporize, it requires a higher surrounding temperature in order to form a mixture that is combustible. Note that the heat of vaporization and the flash point are not directly linked and flash point is not commonly used for predicting engine starting performance.

The final comparison to be made is the autoignition temperature. This property is used primarily for safety reasons; a fuel should never come close to its autoignition temperature outside of a combustion vessel. In the micro engine conversion, there were cases where the fuel and fuel-air charge were heated. Care was taken to ensure that the temperature of the fuel and fuel-air charge was not greater than the autoignition temperature to avoid potential fires or explosions.

Comparison of NM blend fuel to JP-8 yields a number of interesting results because these two fuels are quite different. However, care must be taken as the properties of both of these fuels are only an approximation without laboratory analysis of the fuels. The first observation that can be made is that JP-8 is substantially less volatile than the NM blend fuels, shown by an increased flash point. JP-8 also has a lower latent heat of vaporization, which could be detrimental to a micro engine's operation. Next, consider the energy density of JP-8; JP-8 has roughly twice the energy per unit volume as NM fuels, which could be an advantage in the application of a mobile engine platform. The advantage of NM fuels, however, is that they can be combusted at a faster rate for a fixed amount of air, evident in their low AFR_s. This means that for a given amount of air, NM blend fuels can produce roughly twice the energy output as JP-8, suggesting they would allow an engine to produce a higher power density.

This comparison yields mixed results. While JP-8 is less volatile than NM fuel, it requires less energy to vaporize. Also, while JP-8 has more energy per unit volume, less energy can be delivered for a given amount of air. These mixed results made it difficult to predict the performance of JP-8 in a micro engine.

2.3 Previous Micro Engine Test Stands

One part of the micro engine conversion was to develop a test stand capable of documenting the conversion process. The test stand had to be able to load and control the engine as well as document any flow rates, power output, or any other operating behavior of the engine. On a

larger, more common research engine, this control and documentation can be accomplished with many commercially available hardware and instrumentation options. On a micro engine, however, this is not a simple task. The output of these engines is low, demanding sensitive loading equipment. The fuel and air flow rates into these engines are very low and highly variable. Simply installing instrumentation can be difficult with micro engines due to the limited space. Therefore, a literature search was conducted to look for ways to address the demanding instrumentation and loading requirements of a micro engine. Three micro engine test stands were identified and used as inspiration for the JP-8 conversion micro engine test stand.

The first micro engine test stand examined was a small, cost-effective micro engine dynamometer that was designed for testing the micro engines of model aircraft and for teaching. This test stand consisted of a propeller mounted to a micro engine while the engine was held in a reaction cradle load measurement system. This simulated the true application of the micro engine by documenting the performance of the engine for a given propeller; the amount of power produced by the engine could be back-calculated knowing the propeller type, speed, and engine reaction torque. A bubble-velocity-type measurement was used for the fuel flow. Micro engines typically operate with a fuel system pressurized by the exhaust; as fuel leaves the fuel tank, it is replaced with exhaust gas. Water droplets were introduced in the exhaust pressure line and their velocity was measured. Knowing the area of the exhaust pressure tube and the speed of the bubble, a volumetric flow rate was calculated. The only other flow measurement was the exhaust gas flow rate, which was measured using an adaptor for the engine's muffler and a large plastic garbage bag. When the exhaust flow rate was desired, the adapter was fixed to the engine and the bag was filled with exhaust gas for a given amount of time. The volume of the bag was later measured after it was removed from the engine. The exhaust gas composition was also analyzed from this sample volume. The final measurement was the engine speed, which was collected using a hand-held optical tachometer [15]. While the authors were confident with the results of their testing and presented data to support their measurement, this system seemed too uncertain for the JP-8 micro engine conversion.

The next micro engine test stand that was identified was a simple test stand used for making observations of the combustion characteristics of a 5 cc, four-stroke, glow ignition engine while operating on various NM fuels. For this testing, only in-cylinder pressure, engine speed, and load were measured. The load was provided by a Magtrol brand hysteresis dynamometer through a gear reduction system. A Citizens brand in-cylinder pressure transducer and charge amplifier were used to measure the in-cylinder pressure while a rotary encoder signal was fed through a

frequency to voltage (F-V) converter. These two signals were then passed to an oscilloscope for documentation. While appreciable data was collected which provided valuable insight into the combustion of glow-ignition engines, no additional engine performance metrics were collected [16]. This made it difficult to fully understand the behavior of the micro engine, and this simple approach appeared unacceptable for the JP-8 conversion project. However, this test stand did show a successful application of combustion analysis to micro engine combustion.

The final micro engine test stand identified was a more substantial test stand. This test stand was developed to understand the output and fuel efficiency of multiple micro engines and to try to relate how micro engine performance scales with engine size. Loading for this test stand was also accomplished using a Magtrol hysteresis brake with a gear reduction system and a reaction cradle. The fuel flow was documented using a positive displacement type meter for larger engines or a manual fuel mass measurement at 30 second intervals for smaller micro engines. The airflow measurement was accomplished using a thermal mass flow meter with a plenum chamber before the carburetor. Finally, a magnetic encoder signal was processed through an F-V converter to document engine speed [17]. Overall, this stand was well set up and provided low-uncertainty data for analysis of performance scaling. However, the lack of combustion analysis or exhaust gas analysis made documentation of the engines internal behavior, such as scavenging and combustion quality, impossible to assess.

While none of the micro engine test stands identified provided the level of accuracy and variety of measurements necessary for the JP-8 conversion, they all proved insight into the final design. The cost effective micro engine test stand showed the limitations of propeller-type loading and demonstrated creative measurement techniques. The 5 cc combustion analysis test stand showed that combustion analysis was possible with micro engines. Finally, the performance scaling test stand showed that accurate steady-state measurements on low-flow, high-variability micro engines were possible. By observing the benefits and limitations of each of these test stands, the micro engine test stand could be developed with a more thoughtful understanding.

2.4 Previous Engines Converted to JP-8

Before commencing the micro engine conversion to JP-8, previous engine fuel conversions to JP-8 were examined. Three specific sources were identified, but all of these sources focused on the conversion of a spark-ignition (SI) gasoline engine to JP-8 fuel; no sources were identified of a nitromethane-methanol-fueled micro engine being converted to JP-8. This is likely because most military applications appear to require higher power output, where gasoline-fueled engines are

more common. Nonetheless, the information presented from these conversions was valuable in understanding the micro engine JP-8 conversion. Each of these three sources identified theories of operation on JP-8 vaporization and ignition behavior that could be interpreted and applied to the micro engine conversion.

The first source identified was actually quite similar to the micro engine JP-8 conversion. The paper was called “Catalytically Assisted Combustion of JP-8 in a 1 kW Low-Compression Genset” and focused on the conversion a 1000 W portable generator from gasoline to JP-8. The 50 cc, four-stroke, SI engine in the genset was converted from gasoline to JP-8 using the concept of a “catalytic plasma torch” (CPT). The CPT concept is similar to the glow plug concept in a micro engine and replaces the spark plug in the SI engine [18].

The CPT consisted of a small “pre-chamber” that houses a heating element encased in a ceramic coating. This ceramic coating was then coated with platinum catalysis paint. During the compression stroke of the engine, a small amount of the fresh air-fuel charge was pushed through small nozzles into the pre-chamber of the CPT. There, the heated platinum coated ceramic element catalyzed a small amount of the fuel-air charge into intermediate fuel species. When sufficient pressure builds in the pre-chamber, these catalyzed intermediate species were pushed back through the nozzles into the primary combustion chamber, creating a “torch-style” ignition system. These “torch” flames moved into the remaining air-fuel charge, resulting in robust combustion. For cold-start and part-load operation, the CPT was powered to ensure a strong torch flame, but under higher load operating points, this process was self-sustaining. This was similar to the operation of a glow plug in a micro engine [18].

The result of the CPT addition to the 50 cc generator yielded results similar to the results observed later in the micro engine JP-8 conversion. First, while the generator could produce 1000 W when fueled by gasoline, only 500 W could be produced with JP-8. The authors mention that the power output of the JP-8 operation could be increased to 700 W if additional power was supplied to the CPT’s heating element, but speculated that the CPT may not be durable enough to handle sustained electrical power input. The overall system efficiency, defined as the electrical power output divided by the fuel energy input (a calculation also used in the micro engine conversion), ranged from 3-14% for the JP-8-fueled generator; these results were very close to the results obtained with the gasoline powered engine. Another observation made in the micro engine conversion was an extreme sensitivity to carburetor settings. The author notes in the paper that even a small adjustment in the carburetor needle position drastically changed the behavior of the JP-8-fueled engine [18].

The next source identified was a patented combustion system currently used in the ScanEagle UAV system. This system is produced by Sonnex Research, Inc. and is called the Sonex Combustion System (SCS). In the paper “Conversion of a Homogenous Charge Air-Cooled Engine for Operation on Heavy Fuels,” the application of the SCS to 20 and 40 hp, two-stroke, aircraft engines to enable operating on JP-8 was presented. While these engines are much larger than the micro engine, this paper states that the ScanEagle UAV system uses a similar system on a 1.9 hp engine [19].

The SCS for these applications consists of three primary components including an aluminum cylinder head, a mild-steel bowl insert in the cylinder head, and commercial diesel engine glow plugs. The aluminum cylinder head was machined to accept the mild steel bowl, which is placed around the spark plug. The glow plugs are then placed behind the bowl insert through the aluminum cylinder head to provide heat to the cylinder head and allow for better starting performance. Sonnex Research, Inc. claims that this modification provides increased chemical and turbulent effects in the fuel-air charge. The mild-steel bowl, thanks to its decreased thermal conductivity, holds more heat from previous combustion events than the remaining aluminum head. This heat helps vaporize the fuel near the spark plug late in the compression stroke allowing for combustion of the heavy fuel. The turbulent effects appear to be the result of tuning combustion chamber shape to allow more of the two-stroke engines exhaust gases to remain in the cylinder. This allows more heat energy to be delivered to the fresh fuel-air charge and also allows for unburned fuel components in the exhaust to be retained. These unburned components generally are shorter hydrocarbons, which have increased volatility and combust easier than the operating fuel [19].

The result of the SCS application to the 20 and 40 hp aircraft engines was a successful and robust conversion from gasoline to JP-8-fueled combustion. The test setup for this conversion had inherently high uncertainty because it was a propeller-based loading system, but the authors claim that the indicated mean effective pressure (IMEP) was statistically unchanged between the unmodified gasoline, SCS gasoline, and SCS JP-8 tests. Another note from the SCS conversion was that the cylinder head temperature was reduced while operating on JP-8. The authors speculated that this could be due to JP-8’s lower laminar flame temperature compared to gasoline or differences in the amount of fuel and air delivered to the engine [19].

The final conversions identified, outlined in the two-stroke section of the paper “The Application of Air-Assist Direct Injection for Spark-Ignited Heavy Fuel 2-Stroke and 4-stroke Engines,” were a series of two-stroke engines converted from gasoline to JP-5 through the use of air-assisted

direct injection systems. The engines converted included 50 cc, 625 cc, and 700 cc engines. All of these engines were converted from and compared to their original two-stroke, gasoline SI, carbureted configurations [20]. JP-5 is similar to JP-8, but has a higher flashpoint; it is used in environments were flammability must be minimized, such as on aircraft carriers.

An air-assisted direct injection system consists of three components: a low pressure fuel injector, a high pressure air injector, and a small mixing area for the fuel and air. Essentially, fuel is injected into this small mixing area which is pressurized with an air supply. Then, the air injector injects the mixture of fuel and air directly into the engine's cylinder through a nozzle. When the fuel and air exit through the nozzle, there are strong fluid shearing effects. As a result, much of the momentum of the injected charge is lost, but the fuel and air are well mixed. This translates into poor fuel-air charge penetration into the cylinder but small fuel droplet size [20].

The results of this application to the 50 cc, 625 cc, and 700 cc two-stroke engines was a propensity for fuel-air autoignition and lubrication issues while having good starting and run characteristics. Because the fuel and air was mixed so well, there was increased probability that the fuel would autoignite (commonly known as engine "knock"). To combat the presence of knock in the engine, the compression ratio of the engines equipped with the air-assisted direct injection had to be reduced and the spark timing had to be retarded. This resulted in lower power output from the engines across most of the speed-load range. Typically, the torque output was reduced by 5-15% at the measured speed-load points compared to the gasoline carbureted engine [20].

Another issue observed with these small two-stroke engines was that without additional lubrication considerations, piston seizure was observed within 10 hours of operation on the engines operated on heavy fuels. To address this issue additional "lubricant channels or ports" were added to supply lubrication to the piston-cylinder interface [20].

The results of using the air-assisted direct injection system seemed mixed. The 50 cc engine showed reduced fuel consumption with the direct injection system for both the gasoline and JP-5 fueled engines compared to the carbureted gasoline-fueled engine. There was no apparent improvement observed by using the direct injection system and switching to JP-5 over gasoline. The 700 cc engine, however, showed increased fuel consumption when powered by JP-5 compared to gasoline for all the tested speed load points. The final result presented for two-strokes was the starting time for a 3,000 cc, V6 two-stroke engine running on JP-5. This engine

was able to start at -10°C in 4 seconds when equipped with air-assisted direct injection. No results were presented for a non-direct injection engine [20].

These three sources show that conversion of SI gasoline engines to JP-8 is possible. Although no specific instances of a nitromethane-methanol-fueled micro engine were documented, the results and methods of these conversions provided insight and inspiration for the nitromethane-methanol-fueled engine conversion. The CPT converted engine results showed that the CPT had to be powered under part load and cold conditions, which was also observed with powering the glow plug on the micro engine. The SCS was inspiration for cylinder head heating and the use of a steel cylinder head to reduce heat transfer out of the combustion charge. Finally, the air-assisted direct inject system provides a possibility for future modifications to the JP-8-fueled micro engine.

Chapter 3 Micro JP-8 Burn: Phase 1

3.1 Commercial, Off-the-Shelf Engine Selection

Before completing any of the many objectives of the Micro JP-8 Burn directive, a COTS engine had to be selected. Choosing the engine would allow a specific test stand to be designed and modifications to be focused on the selected engine's specific design. Only two specific requirements were made:

1. The engine should be a small (less than 20 cubic centimeters), internal combustion engine.
2. The engine should be modifiable to operate on JP-8 fuels.

These requirements allowed for extreme flexibility in engine choice. The size requirement essentially limited the qualified COTS engines to light-duty and hobby applications. The second requirement really implied no restriction, only the implied suggestion of choosing engines that were "over-built" for their application, allowing them to be more durable.

In order to provide the truly desired product, multiple discussions were initiated with those people involved with the project. From these discussions, some new objectives and constraints became clear:

3. The engine should be capable of producing 250 W of electrical power.
4. It would be preferable if the engine was a two-stroke for simplicity.
5. The engine's designed purpose should be a steady-state application.
6. Hobby, glow-ignition, nitromethane-methanol-fueled, two-stroke engines provided a wide range of sizes and accessories, making them appealing to a generic application.

A clearer direction was formed in selecting the COTS engine after this discussion. However, the choice of available engine was still quite vast. To narrow the selection further, two aspects of the engine were considered. Engine operating speed was considered first. Hobby glow-ignition engines typically operate at very high speeds, occasionally in excess of 25,000 revolutions per minute (RPM). It was felt that a high engine speed could be detrimental in future applications because it would be difficult to design application couplings and reductions for speed requirement. Additionally, because higher speeds mean higher friction, operation at a lower engine speed would enhance efficiency and also reduce engine wear. The second aspect considered was the original engine application. Steady-state operation generally implies long

operating times with low airflow for cooling (compared to non-stationary applications). Operating at steady-state suggested a hobby aircraft type engine because hobby aircraft typically operate within a relatively narrow engine speed range. The low airflow expected in this application is similar to the conditions found in hobby remote controlled (RC) helicopters, where the engine is typically shrouded in a cowling, limiting airflow.

From these considerations, large-bore, RC helicopter engines were investigated. The larger displacement engines would allow lower operating speeds and possibly lower operating temperatures. Additionally, these engines were assumed to be more robust due to the inherent lack of cooling and operation in helicopter applications. Searching consumer information for large-bore, RC helicopter engines showed that the brand O.S. Engines was well respected and provided a wide array of engine choices. O.S. Engines offers six glow-ignition, two-stroke, RC helicopter engines ranging from 6-17 cc.

The O.S. Engines 70SZ-H model, which falls in the center of the O.S. Engines product line, appeared to be a good choice for the JP-8 fuel conversion project. Specifications for the O.S. 70SZ-H engine are shown in Table 3-1. This engine possessed a few unique features that could have been advantageous to the conversion and also appeared capable of the desired power output of 250 W at lower engine speeds. First, it was supplied with a three-adjustment carburetor (main jet, middle jet, and idle adjustment) which would allow a better chance of operation on JP-8 without fuel delivery modifications. Another feature of the 70SZ-H was extra crankcase webbing for heat dissipation, which could have been advantageous in the stationary application heat rejection and also enhances crankcase rigidity for any possible fuel conversion modifications. Mounting the 70SZ-H is accomplished through six mounting lugs, whereas many RC aircraft engines have only four mounting lugs. This was suspected to help shaft alignment and provide more flexibility in future applications. All of these features and capabilities suggested that the 70SZ-H was a good choice for the JP-8 fuel conversion.

Table 3-1: O.S. Engines' 70SZ-H published specifications [21]

Total Displacement	11.5	cc
Bore	25.8	mm
Stroke	22	mm
Practical RPM Range	2,000-18,000	RPM
Rate Power	1842	W
Rated Speed	16,000	RPM
Weight without Muffler	553	g

There was some uncertainty when selecting the 70SZ-H engine, but it was determined to be the best choice given the unknown path of the conversion project. Some of the uncertainty came from the fact that the information listed in Table 3-1 was the only published information available. O.S. Engines does not supply additional information on their website and, upon request, informed us that additional information was not given to the public. At the early stages of the project there was also uncertainty as to how the engine would be converted to JP-8 operation. Many options were plausible, but no clear path had been identified yet. These uncertainties were overlooked, however, as they would have been common to any engine chosen for the conversion.

3.2 Micro Engine Test Stand Development

3.2.1 Overview

The bulk of phase 1 was comprised of the micro engine test stand development. Because the project was a demonstration project, many different stand configurations and choices in instrumentation were available for selection. In order to design a more focused system, the stand was broken into three subsystems including the power system architecture, the test stand instrumentation, and the test stand software.

3.2.2 Power System Architecture

(1) Design Criteria

The first step in testing the micro engine was developing a method to physically load the engine using a power absorption system. Traditional force measurement to calculate torque was expected to be problematic for the high-speed, high-vibration engine. Additionally, the purpose of the project was to convert an engine to JP-8 operation and provide a comparison of that engine running on its stock fuel versus JP-8 for a given operating condition. Both of these considerations suggest the measurement of electric power.

Measuring electric power simplified the development of the power system architecture. First, measuring electric power was easier to accomplish with regard to hardware. Measuring brake engine power requires torque measurement, which requires a more complex apparatus such as a reaction cradle. Electric power can also be easier to measure from an acquisition and signal processing viewpoint because the power calculation is directly from Ohm's law, whereas a torque measurement requires calibration. These simplifications allow lower material and development costs. From this reasoning, the first constraint was developed:

- The test stand design should produce and measure steady-state electrical, not engine, power.

The next constraints and objectives were introduced by the power requirements and engine selection. Specifying maximum speed and power was crucial when selecting different components of the power system, and later the instrumentation. From internal discussion, the target to be generated was 250 W of electrical power (that is, electrical power available after generation and conversion in the electric circuit). However, in anticipation of possible higher power testing, we increased the limit of maximum power to be generated to 350 W. Engine speed was also a concern. During initial research, it was difficult to identify components capable of over 10,000 RPM and, therefore, choosing a maximum rotational speed greater than 10,000 RPM appeared unrealistic. Note that the chosen 70SZ-H model engine was rated for 1842 W at 16,000 RPM and the stand would be undersized and unable to completely map the engines behavior with these speed/power ratings. This was intentional, however, because the engine was intended to operate at much lower speed than its rated power. This discussion determined two objectives:

- The stand should be able to generate and dissipate at least 350 W of electrical power.
- The stand should be capable of at least 10,000 RPM at the engine crankshaft.

Some additional criteria had to be considered in power system architecture based on some general engineering assumptions. These included:

- Engine-generator alignment and coupling – It was assumed that excessive misalignment would cause significant losses in engine power. Since the power was low and the speed was high, the resistance caused by high misalignment would likely result in significant losses in conversion efficiency between the engine power and the generated electric power. Therefore, the best possible alignment was desired for the power system architecture.
- Re-configurability – Because the O.S. 70SZ-H engine choice was not fully justified and because limited background was available on micro engine test stands, it was likely that the power system would need to be reconfigured. This reconfiguration had to be quick and cost effective, due to the project timeline and budget. This led to the self-applied constraint of developing an easily, quickly, and cost-effectively re-configurable power system.

- Test stand isolation – The single-cylinder, two-stroke, high-speed engine was assumed to produce strong vibrations, which could be detrimental to both the stand durability and the instrumentation accuracy. Maximizing the isolation of the engine to the other components was made a priority for this reason.

(2) Electric Circuitry and Components

With design criteria established, the power system was developed starting with the electric power generation hardware and circuitry. This development included selecting a generator motor, converting that generator's output to absorbable power, absorbing that electrical power, and finally providing an integrated system to start and motor the engine.

Selecting an electric machine to act as the generator was simplified based on the purpose and criteria of the project. Specific electric machines have advantages and disadvantages, but because the project goal was a demonstration engine capable of JP-8 operation, the actual selection of the electric machine was not crucial. In effect, the only constraints of the motor were the ability to motor the engine and generate 350W up to 10,000 RPM. The simplest choice, therefore, was to look at commonly available hobby, sensor-less, brushless direct current (BLDC) motors as they typically operate at the same speeds and loads as nitromethane-methanol-fueled engines and are also inexpensive relative to the micro engine. The Cobra brand C-4130-14 hobby BLDC motor appeared to meet the design criteria. Specifications for the C-4130-14 can be seen in Table 3-2.

Table 3-2: Cobra C-4130-14 specifications [22]

Motor Configuration	BLDC, External Rotor
Motor Kv	450 RPM/VDC
Max Continuous Current Draw	60 A
Max Continuous Power at 18.5 VDC	1110 W
Weight	400 g
Stator Diameter	41 mm
Stator Thickness	30 mm

The Cobra C-4130-14 appeared to provide the basic necessary performance for the motor/generator application. First, with a Kv of 450, up to 22.2 VDC could be produced at 10,000 RPM, avoiding high voltage circuitry. Additional Cobra 4130 models are available with other Kv values, allowing flexibility in the design if an even higher voltage is desired in the future. The

current and power limits of the Cobra C-4130-14 also suggested that ample starting torque and generating ability were available.

There were three significant uncertainties in selecting a hobby BLDC motor. The first two potential issues were related to the motor's capabilities. First, we were uncertain if the motor would be able to generate the desired 350W continuously without overheating and failing. Second, there was insufficient information to determine if the motor would have enough torque to actually motor the engine from a resting state. The final uncertainty focused on the actual output of the BLDC motor. BLDC motors actually operate by applying (or generating) voltage in an alternating fashion between coils (called phases) in the motor. In the case of the Cobra motor, there are three phases so the power out of the motor is essentially a three-phase, variable-frequency, alternating current. This sort of output is not readily regulated or absorbed with simple electronics. Therefore, using the BLDC motor would require some method of converting the power generated into an easily regulated and absorbed DC power.

The hobby BLDC motor had three significant advantages that made these uncertainties negligible, however. First, as mentioned, the speed and power ratings were similar to the actual engine due to their shared application. Second, hobby BLDC motors are readily available and repairable thanks to hobbyist demand. Finally, and most importantly, the motors are inexpensive. The Cobra C-4130-14 has a retail price of $149.99, which makes it an excellent value for the power produced.

After minimal experimentation, the uncertainties revolving around the hobby BLDC motor were resolved. Initially, a Cobra C-4120-22 motor was selected and tested in the test stand. While this motor was sufficient, the next larger Cobra brand motor (the 4130 model) was selected to provide improved performance, especially in starting torque. With the C-4130-14 motor, 350 W could be easily generated with no heat issues for extended periods of time. Additionally, the C-4130-14 motor provided excellent starting torque with increased compression ratios on the engine (up to 13:1 geometric compression ratio). The final uncertainty of how to regulate and absorb the power produced by the BLDC motor was resolved through a recommendation from an external source, who had experimented and shown that hobby, sensor-less, BLDC motor controllers could also absorb the energy from the BLDC and output DC voltage. For this project, a Castle Creations Phoenix ICE 50 motor controller (capable of 30 VDC and 50 A) was purchased and used to both provide power to and absorb power from the Cobra C-4130-14. The controller accepted a 50 Hz square wave with a 1-2 ms pulse to control the electric motor throttle setting. Additionally,

software from Castle Creations allowed starting torque, direction, and other motor parameters to be controlled.

Having selected a generator/controller combination that produced DC voltage, a method to load the generator and the associated engine could be selected. Initially, resistive circuit designs were explored to load the engine. However, it was believed that this would not provide sufficient flexibility or control in the amount of power absorbed and limited experience existed with designing high-power circuits. Through minimal research, a programmable DC load bank was identified as a potential option as an electric load. Programmable DC load banks are used commonly in battery testing and are available in many different configurations. Many offer programmatic control as well as constant voltage, current, resistance and power modes of operation. Ultimately, a BK Precision model 8510 DC load was chosen and purchased for its load capacity, cost effectiveness, and ability to be controlled programmatically through LabVIEW. Table 3-3 shows specifications for the 8510 model. Note that the current, voltage, and power limits of the model 8510 exceed our requirements to allow hardware flexibility for potential future projects.

Table 3-3: B&K Precision model 8510 specifications [23]

Operating Modes	Constant Current, Voltage, Resistance, and Power
Control Inputs	RS232 or USB
Voltage Range	0-120 VDC
Max Current	120 A
Max Power	600 W

Finally, the motor/generator (MG), sensor-less BLDC motor controller, and DC load bank were configured in a simple circuit with a 12 VDC marine-grade battery and a 20A, 100 VDC solid-state relay to form the power system electric circuit. The marine-grade battery was chosen because it was cost effective and had a 115 Ah rating, providing ample starting and motoring power. The relay was used in conjunction with the LabVIEW software to act effectively as a single-throw, double-pole switch. With the battery switched into the circuit and the DC load disabled, the motor and controller were powered and acted as the engine starter. With the battery switched out of the circuit and the DC load enabled, the load bank could absorb all of the power being produced by the motor/generator. A simplified representation of this circuit can be seen in Figure 3-1. Additionally, the true wiring diagram can be seen in Figure 3-2.

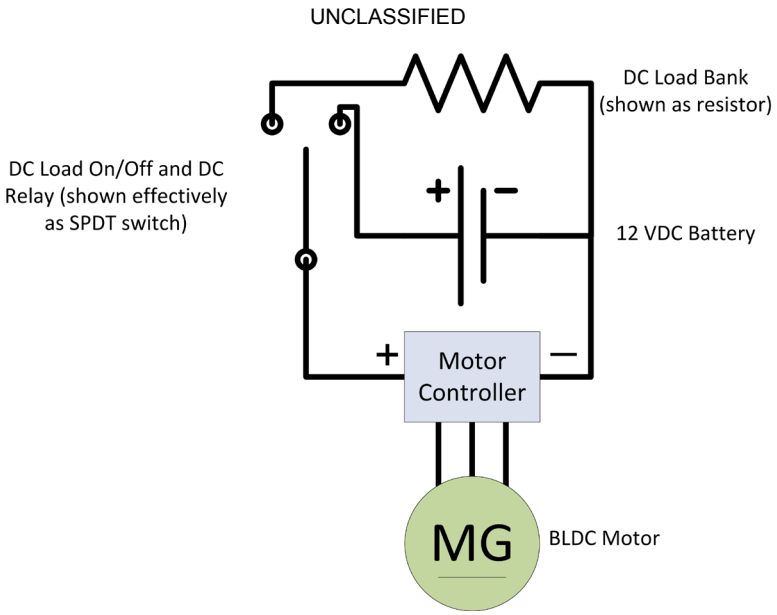

Figure 3-1: Simplified representation of BLDC dynamometer setup. Note system is shown in neutral state.

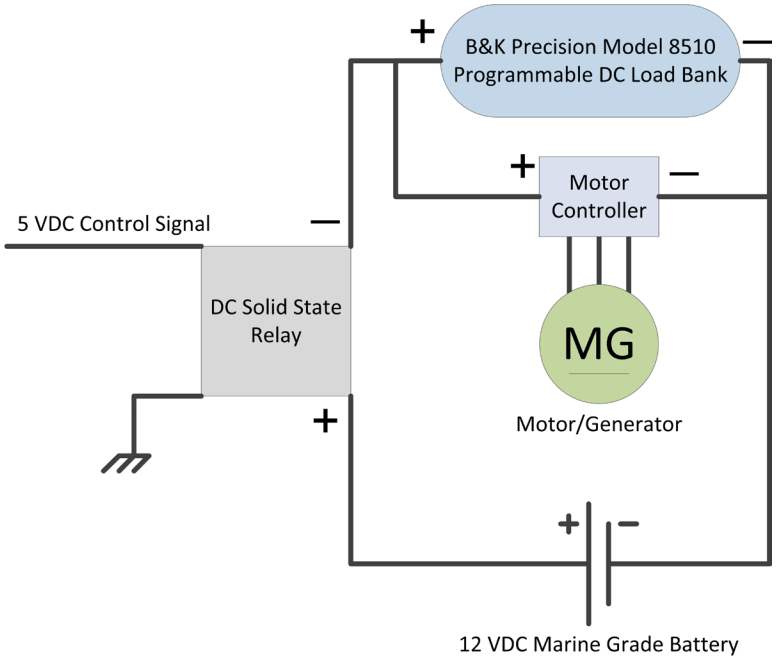

Figure 3-2: True power system architecture wiring diagram

This final power system electronic circuit and hardware proved effective and durable in operation. No issues were observed with the circuit's operation and all of the hardware proved sufficient.

The only modification that had to be made was cooling air had to be circulated by a fan around the motor controller to keep it at a stable operating temperature; this cooling air was provided by the fan used to cool the engine.

One final note on the power system electronic circuit should be made. This circuit was effective, offered excellent control, and succeeded in enabling engine testing. However, the addition of the B&K Precision DC Load bank greatly increased the cost of the system (MSRP $2,125). Also, while the motor controller proved sufficient for generating electric power, it is likely not the most optimal method of converting the BLDC motor's output to DC voltage. With some basic electronic circuit design background, a more efficient and less expensive method of rectifying the BLDC motor output and absorbing that output could potentially be produced. This circuit could potentially reduce the system costs to a level where this power system could be used in mass testing or an educational setting.

(3) Mounting Configuration

Developing a mounting configuration was next in designing the power system architecture. The chosen BLDC motor allowed for a direct drive configuration between the motor and the engine, rather than some sort of flexible drive system (belt, differential, etc.). This would allow the most efficient and simplest power system architecture possible because the number of additional components, and their associated losses, was minimized.

With this direct drive system, three criteria were critical to the mounting configuration design: shaft-to-shaft alignment, test stand isolation, and ease of modification. Shaft alignment was critical due to the size and power of the engine/motor combination. A small misalignment causes a set amount of energy loss in the system. For a large engine, a small misalignment leads to a small percentage of the energy from the engine being lost. However, that same amount of lost energy on a micro engine could be a significant amount of the total power produced. Therefore, alignment was crucial in making the system as efficient as possible. System isolation was important for durability and instrumentation reasons. Single cylinder, two-stroke, micro engines produce a significant imbalance during operation, leading to the transmission of significant vibration to whatever they are attached too. Durability and instrumentation accuracy can be greatly reduced if severe vibration is introduced to a system, which made it critical to isolate the engine from the rest of the stand. Finally, the ability to quickly manipulate the test stand was crucial due to the uncertainty in the component selection at the beginning of the project. Initially,

it was not known if the engine and motor choice were sufficient, so the test stand had to be capable of quick and economical reconfiguration.

To best accommodate these criteria, a “generator structure” was designed. This structure consisted of an engine cradle, an electric motor mount, and a base plate to which the cradle and mount attached. The base plate was configured with press-fit dowel pins which matched piece-specific patterns on the engine cradle and electric motor mount. The dowel pins allowed precise alignment of the cradle and motor mount along a common axis, minimizing misalignment in all degrees of freedom except in the translational direction perpendicular to the base plate mounting surface. The vertical alignment was held by precisely machining the height of both the engine cradle and motor mount. Once aligned, both the cradle and mount were fastened to the baseplate by hex head cap screws that went through holes in the base plate. Figure 3-3 shows the CAD representation of this system.

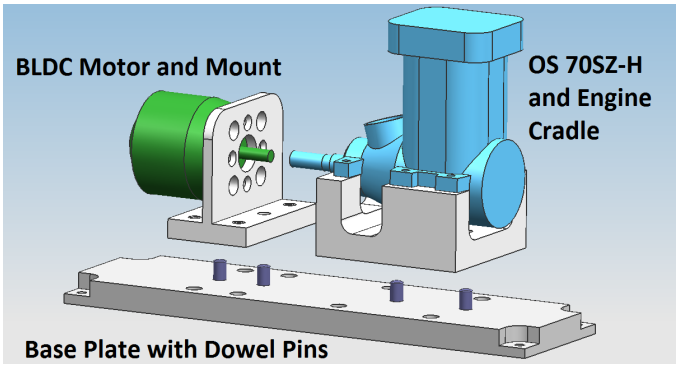

Figure 3-3: CAD representation of generator structure, shown in exploded view with engine and motor

Additionally, a hobby servo (Futaba brand, model S3003) was attached to the generator structure to ensure proper throttle linkage alignment at all times. Once assembled, the generator structure was mounted using four compression isolation mounts (Advanced Antivibration Components brand, model V10Z 2-301A) to a larger bed plate. This structure satisfied the requirements of the mounting stand in three ways.

- By fixing the engine and motor rigidly to a base plate, their alignment could be held nearly constant. This allowed more flexibility in coupler choices.

- By mounting the engine, motor, and throttle servo to the same structure, the mass of the system was increased. Additionally, because the remaining connections were flexible (fuel hoses, wires, etc.), soft isolation mounts could be used. This moved the mounted natural frequency well below the firing frequency of the engine.

The simple designs of the three components (engine cradle, motor mount, and base plate) meant that any of the components could be re-machined within a few hours, enabling fast reconfiguration times.

(4) Coupling

The final component necessary to tie the power system architecture together was a coupler to directly connect the engine and motor shafts. The requirements for the coupler were relatively minimal; it had to be capable of absorbing the torque pulses of the engine/motor system and absorbing some potential misalignment. In the initial phases of the power system design, it was also specified that the coupler be zero backlash, in the event that there was not sufficient room for an encoder on the engine crankshaft. That requirement was later dropped when a suitable encoder was found. Though the coupler itself should have been one of the simplest components to select, it proved problematic in both design and application.

Coupler selection was based around three specifications: speed rating, torque, and shaft size. Speed ratings and the range of specific shaft sizes a coupler type can accommodate were easily identified and specified. The speed range was limited from the power system architecture constraints to 10,000 RPM. The shaft size was specified from the chosen engine and motor (5/16-24 UNF thread and 6 mm smooth shaft, respectively). Torque, however, was difficult to predict. In the early phases of the project, the only information known about the engine was its rated power of 1842W at 16,000 RPM and that it was a single cylinder, two-stroke engine. Although the engine was never intended to run at rated power, this was the only information available and was used to calculate an average torque of 1.1 Nm using the equation below.

$$T = \frac{P}{2 * \pi * \left(\frac{N}{60}\right)}$$

$where$:
$T = Average\ torque\ (N * m)$
$P = Power\ (W)$
$N = Engine\ speed\ (RPM)$

Previous industry experience led to investigation of Zero-Max Inc. for coupler solutions. A Zero-Max ServoClass© coupler is a zero-backlash, clamp-style coupler that uses 304 stainless steel disc packs to transmit torque while allowing some misalignment. The shaft is surrounded by a hub that has a small slot cut in it. A clamping screw extends through the hub across the slot. When tightened, the screw causes the hub to deform in a controlled fashion, creating eccentricity. This eccentricity interferes with the inserted shaft, creating a large contact patch that fastens the coupler to the shaft through contact friction. From product information, the ServoClass© SC030R was identified as a good potential option. Specifications for the SC030R can be seen in Table 3-4. Additionally, a representative image of a SC model ServoClass© coupler is shown in Figure 3-4.

Table 3-4: Zero-Max Inc. ServoClass© SC030R specifications [24]

Bore Ranges	5.0-14.0	mm
Maximum RPM	10,000	RPM
Operating Torque	4.00	Nm
Parallel Misalignment Capacity	0.18	mm
Angular Misalignment Capacity	1.00	deg
Axial Misalignment Capacity	0.40	mm

Figure 3-4: Zero-Max Inc. ServoClass© SC style coupler [24]

The bore ranges, maximum RPM, and misalignment capacity all suited the power system well. The operating torque specification provided a safety factor of 3.6. A good reference could not be located on how to specify a torque safety factor for coupling small engines early in the test stand development; in order to move the design forward, the assumption was made that the SC030R would be capable of withstanding the engine torque pulses.

Ultimately, this assumption proved to only be correct with a number of modifications which warrant further explanation. This narrative is shown through

Table 3-5, where each iteration's problem, the cause of the problem, and the final solution to that specific problem is listed.

Table 3-5: Iteration of Coupler failures, causes, and solutions

Iteration	Failure	Identified Cause	Solution
1	Coupler spins on motor shaft.	Motor shaft has a smaller diameter and therefore less surface area for clamping, making it the weak link.	Added machined flat to motor shaft and a #6-32 UNC cup-point setscrew to coupler on motor end.
2	Coupler spins up threaded engine shaft	Having fixed the motor end, engine end became the weak link.	Added machined flat to engine shaft and a #8-32 UNC cup-point setscrew.
3	Coupler spins on motor shaft.	Setscrew vibrated loose. Large enough gap exists that the setscrew point is severely damaged and allows shaft rotation.	Mild-strength thread locking compound is applied to setscrews during every assembly.
4	Coupler C-clamp clamping screw snaps, coupler spins with set screw on motor shaft. Galls motor shaft.	The clamping screws on the coupler were not being torqued to the proper limit. Screws were over torqued, fatigued, and fractured at the screw head.	Torqueing sequence developed to ensure bolts operated within their designed limits. See 0.
5	Cracks appear around added setscrews on both coupler ends after extended testing. See Figure 3-5.	Added setscrews were placed unintentionally in the thinnest piece of the coupler C-clamp. Minimal material led to excessive stress in coupler.	New coupler produced with #8-32 UNC cup-point setscrews on both ends, but placed on side of C-clamp with most material.
6	Electric motor shaft snaps in shear at location of machined flat.	Stress concentrations formed around the sharp corner of the unnecessarily deep flat on motor shaft.	The depth of the shaft flat was reduced to 1/2 of its previous value and a 1/16" ball-end mill was used to provide rounded corners.

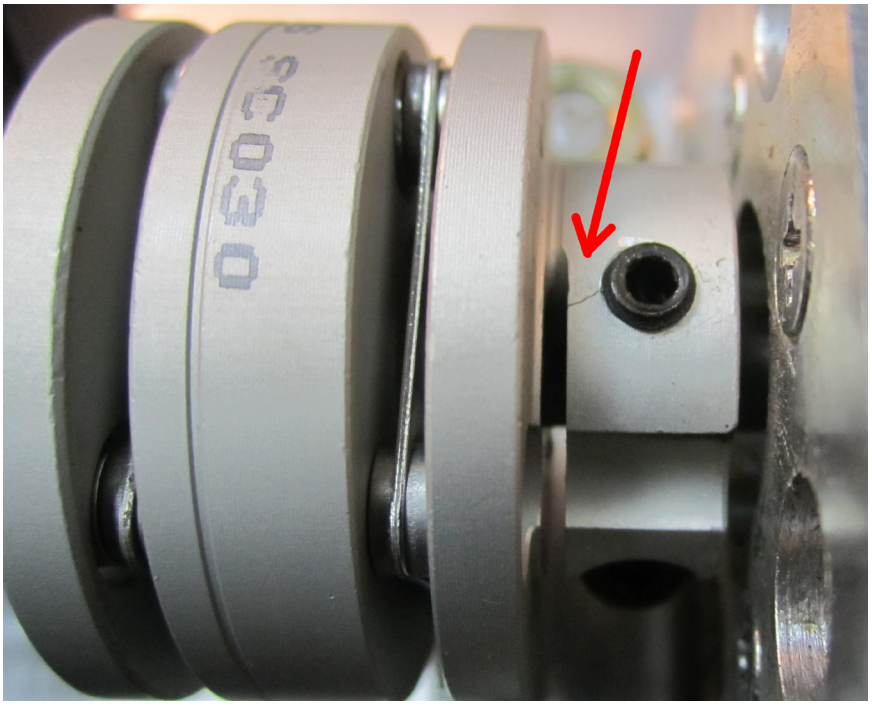

Figure 3-5: Coupler at iteration 5, motor end shown. Note stress fracture to left of set screw.

Another coupler was integrated into the system instead of the SC030R between iterations 4 and 5. This alternate coupler was a Lovejoy Inc. model GS-14. The GS-14 is a small, locking-jaw type coupler. It was incorporated into the system, but was abandoned shortly afterward. The urethane spider between the two aluminum jaws could not withstand the strong torque pulses and catastrophically failed within 5 minutes of operation. With this failure, Kevin Wells at Zero-Max, Inc. was contacted and the issue was discussed; he recommended simply relocating the setscrews to a more robust location (completed in iteration 5).

To date, the iteration 6 design has proven sufficiently durable and robust. With proper torqueing, thread locking, and setscrew location, the flexible disc style coupling appears to be a good choice. The steel discs appear capable of absorbing the strong torque pulses that damaged urethane spider type couplers. It is recommended that the coupler be rebuilt with fresh disc packs regularly and that the clamping and setscrew torques as well as the coupler be inspected regularly for fatigue or other damage. Installation instructions can be found in 0.

3.2.3 Instrumentation

(1) Overview

Having selected a COTS engine and designed the power system architecture, instrumentation could be selected to monitor the engine's status and performance. The instrumentation that was necessary to document the engine's behavior before and after the conversion to JP-8 was discussed and based on the engine parameters important to the conversion process. Identified engine parameters of interest to the project included:

- Fuel mass flow rate – For documentation of fuel consumption and calculation of air-to-fuel mass ratio (AFR), indicated fuel conversion efficiency (comparing fuel energy input to indicated energy output) and mechanical efficiency (comparing fuel energy in to electrical power out)
- Air mass flow rate – For documentation of air mass flow rate and calculation of AFR
- Engine Speed and Crankshaft Position – For testing consistency, engine behavior documentation, and combustion analysis
- Surface and gas temperatures – For documentation and engine monitoring
- Exhaust pressure – For monitoring exhaust pressure and ensuring facility exhaust did not change engine performance
- In-cylinder pressure – For documentation of combustion changes and durability monitoring. Also, for calculating indicated mean effective pressure (IMEP), coefficient of variance of IMEP (COV), indicated fuel conversion efficiency, and various combustion parameters.

Having identified the parameters of interest, the specific types of necessary instrumentation were identified for each parameter; there were some challenging constraints for all of the instrumentation selections, however. One of the clearest challenges was the size of the instrumentation in relation to the engine. For example, encoder models commonly used in automotive engine testing were roughly as large as the crankcase of the O.S. 70SZ-H, making them difficult, if not impossible, to incorporate into the instrumentation system. Another significant issue was simply the measurement range needed for the instrumentation. The fuel mass flow measurement, for example, ranged two orders of magnitude within a measurement range that could be considered error for commonly used fuel mass flow measurement devices. The most difficult constraint was instrumentation cost, though. The Micro JP-8 Burn project budget for material was relatively small compared to other university research budgets. This essentially

meant that compact, high precision instrumentation was needed at an extremely economical price. Ultimately, many of the instrumentation systems were custom designed to provide accurate data at minimal cost.

(2) Air Mass Flow Rate [25]

Numerous methods exist for measuring air flow rates, including positive-displacement flowmeters, flow obstruction flowmeters, viscous flow airmeter, hot-wire anemometers, thermal mass flowmeters, and others [26] [27]. The challenge presented by the micro engine test stand was finding a flowmeter capable of measuring the proper air flow range at an acceptable cost.

Neither the current research nor previous experience provided sufficient background to estimate the expected air mass flow of the O.S. 70SZ-H micro engine. Therefore, the expected air mass flow rate into the engine was uncertain. The only way to estimate the air mass flow was a basic calculation. This calculation was made based on the assumptions that the engine could possibly run from 2,000-10,000 RPM for the desired 250 W electrical power output and that the delivery ratio of the two-stroke engine would range from 10% at 2,000 RPM to 100% at 10,000 RPM. While this range was quite broad, it was necessary to account for all possible measurements inside of the 10,000 RPM test stand limit. The engine speed, total displaced volume per revolution, and delivery ratio were used to calculate an approximate air volumetric flow rate, which was then converted to mass flow rate using an ideal gas approximation. These calculations can be seen in Appendix B.

In addition to looking at transducers capable of the expected volumetric/mass flow, a few additional considerations needed to be made when selecting an air flow transducer. First, two-stroke engines are very susceptible to performance changes due to intake restriction. Because the air flow instrumentation would likely not be a permanent addition to the engine in a final application, it was crucial that the pressure drop was minimized through the intake system to the engine. Another important consideration for this particular project was the cost of the system. High accuracy air flow meters are typically expensive, which was prohibitive with the budget. Using the calculated air mass flow rate, looking at options that produced minimal intake restriction, considering automation capability, and taking cost into consideration, only two flowmeter types were plausible: a hot-wire anemometer or a thermal mass flowmeter. After comparing cost, a hot-wire anemometer was chosen as the final option and was fitted into a custom airflow measurement system.

The hot-wire anemometer transducer chosen was a Kanomax brand 6332 model with a 0965-04 probe. This setup outputs a conditioned 0-5 VDC signal at 2 Hz linearly proportional to the selected range up to 25 m/s with accuracy of 0.1 m/s. The 0965-04 probe was chosen for its small diameter (3mm) and because it is bent 90° to fit into tight locations. This probe is typically used to measure ventilation in applications such as electronics.

A simple venturi was designed in order to match the velocity range of the anemometer probe to the expected volumetric flow rate of the engine. This was done by using a simplified calculation to size the cross-section area of the venturi system. A uniform velocity and no fluid effects in the tube were assumed and the cross sectional area at the measurement location was calculated. This area was adjusted to allow most of the transducer range to be utilized while leaving some measurement overhead. Ultimately, a diameter of 12.7 mm (0.5”) was chosen, corresponding to an expected anemometer velocity range of 0.3-15.1 m/s. This diameter was also favorable as it was nearly the same diameter as the carburetor inlet, suggesting minimal restriction would occur. The venturi also incorporated a tapered air inlet to reduce restriction, an outside diameter of 35 mm to accommodate a paper air filter element (originally designed for motorcycles with 35 mm carburetors), and a unique clamping mechanism to hold the anemometer probe. A cross section from the solid model of this measurement system is shown in Figure 3-6.

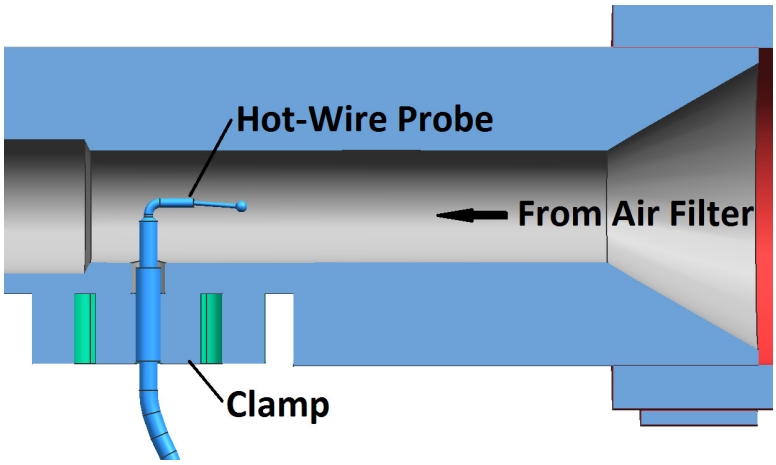

Figure 3-6: Cross section of air intake assembly solid model; shows hot-wire anemometer probe orientation and venturi shape [25]

To calibrate the air intake assembly mass flow measurement, a set of standards originally for vacuum cleaner testing was employed. These standards are ASTM F558, “Standard Test Method for Measuring Air Performance Characteristics of Vacuum Cleaners” and ASTM F431,

"Specification for Air Performance Measurement Plenum Chamber for Vacuum Cleaners." These standards outline the methods and equipment necessary to make steady-state volumetric flow measurements. A plenum box and calibrated orifice plates were used to calculate air volumetric flow rate; this volumetric flow rate was then converted into a mass flow rate using the atmospheric conditions. The calibration was then incorporated as a second order polynomial to calculate air mass flow rate real-time in LabVIEW. This calibration method was chosen because it was the only method of calibration identified and available based on cost and the low flow rates that needed to be measured; a better calibration method likely exists.

Note that after using the anemometer-based mass flow system, it is recommended that other options are pursued in the future. The system works sufficiently, but there are many uncertainties associated with the custom design that would warrant spending more money for a pre-made unit, possibly even a thermal mass flow meter. Evidence of fluid effects within the venturi, such as laminar-turbulent transition during calibration was observed within the desired measurement range. This was evident in significant pressure fluctuations during steady-state suction. Also, the calibration is very difficult to confirm without expensive testing equipment. The probe itself is also fragile and has a limited temperature range (5-80°C). In fact, in early intake air heating experiments, the adhesive that held the probe's internal components together was melted and the sensor failed. If another micro engine test stand is built, it is highly recommended that budgeting more for a pre-built, pre-calibrated mass flow meter be considered. A thermal mass flow meter from a company such as Brooks Instrument, Sierra Instrument, or Bronkhorst would likely be sufficient.

Another note on the intake system is that the relative humidity and atmospheric pressure were recorded for all the tests. These would allow corrections to the air density and, therefore, air mass flow rate. However, the humidity measurement was never actually implemented to correct for the atmospheric humidity; all calculations were performed using 0% humidity. Basic calculations suggest that this only results in a 3.4% error in density from 0 to 100% humidity, justifying its lack of inclusion [28].

(3) Fuel Mass Flow Rate [25]

Similar to the air mass flow measurement, the fuel mass flow measurement challenge came in finding a device capable of the appropriate measurement range at a reasonable cost. The fuel mass flow was especially crucial to the project to enable tuning of the engine and for reporting the fuel consumption rate during the production of electrical power.

Again, with minimal experience in micro engines it was difficult to determine an appropriate fuel mass flow rate. The engine manufacturer claims approximately 0.5 g/s at full load for hobby applications, but as this project was only running the engine to a fraction of this load, a reasonable estimate of fuel mass flow was not available. Instead, fuel mass flow was calculated based on the air mass flow calculations. The stoichiometric AFR of kerosene type fuels such as JP-8 was found to be approximately 14.8 [29]. The stoichiometric AFR of nitromethane-methanol blends was calculated using combustion stoichiometry to be between 4 and 6, based on a range of linear combinations of the two neat fuels. Based on these AFR values and taking the highest value from the nitromethane-methanol blend fuel and lowest value from the kerosene type fuel, the estimated fuel flow rate was 0.003-0.7 g/s. Realizing the lower flow rate was not reasonable from a cost and measurement stability perspective, a target measurement range of 0.05-1 g/s was set.

Choosing a method to measure mass flow rate presented some difficulty. Numerous methods exist to measure fuel flow rate, but few commercial methods exist for such a low mass flow rate. Additionally, nitromethane is corrosive and could damage some sensitive flow meters. Cost was also a consideration for the mass flow meter. Options including level measurement, in-line optical methods, and rotary meters were all considered, but ultimately a fuel scale was determined to be the simplest, lowest cost option to measure mass flow.

There were issues using a scale for mass flow, however, that limited the use of commercially available choices. In order to measure a reasonable fuel mass differential real-time, a high accuracy scale (0.05 g resolution) would be necessary. Commercially available scales with this resolution are expensive and generally do not have the capability to output data real-time to a data acquisition system (some systems do output digital signals that would require manipulation).

To solve this issue, a custom fuel scale was designed and built. An Omega LCAE load cell was identified as the best load cell for the fuel scale due to its low range (1 kg) and its high accuracy/repeatability (0.06% combined error). A platform and base were machined from aluminum stock and the load cell was fitted in-between. Four rubber isolation feet were also added to the system and a 24 fluid ounce hobby fuel tank was placed on the load cell platform. A picture of this fuel scale setup can be seen in Figure 3-7. The LCAE load cell and the machined components together cost ~60% less than buying a commercially available scale.

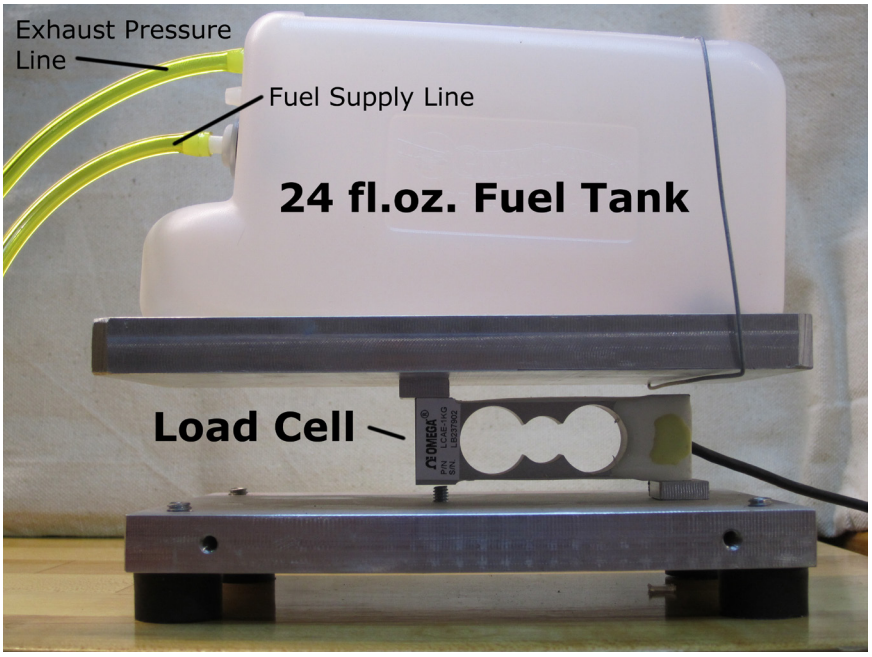

Figure 3-7: Fuel Scale Assembly

The 0.06% error of the load cell would limit accuracy to about 0.6 grams, so additional software and signal processing measures were taken to ensure scale accuracy. First, a switching power supply was used to maintain a constant excitation voltage. Next, by normalizing the load cell output voltage by the excitation input voltage in the acquisition system and taking a 10-sample running average of that quotient, a fairly stable and consistent output signal was obtained. Finally, a set of calibrated weights spanning the mass range of interest were applied and the corresponding voltage quotient recorded. This data was used to determine the best function to estimate the conversion to mass from the voltage quotient. Not surprisingly, a linear fit was able to predict the mass over numerous tests with a coefficient of determination greater than 0.9999 with a 95% confidence interval. With these accuracy enhancements, it was possible to experimentally predict mass to within 0.05 grams.

Once incorporated into the test stand, some additional safeguards were applied to improve the scale's accuracy. The scale was situated on a bench that was isolated from the engine bench to avoid the vibration of the engine. The fuel lines were also fixed to the isolated bench to keep vibrations from the engine from reaching the load cell. These actions greatly reduced the variability of the fuel mass flow rate.

The final output of the fuel scale was read as grams, but the running average was also differentiated with respect to time in LabVIEW to estimate real-time fuel mass flow rate.

(4) Engine Speed and Crankshaft Position

Measuring engine speed and crankshaft position are crucial in engine testing. Engine speed is often the primary variable in documenting engine behavior. Crankshaft position is important when understanding measurements on a crankshaft angle basis, specifically cylinder pressure. These two measurements are collected using an encoder.

Due to the small size, low inertial mass and high speed of the engine, care was needed in choosing an encoder. Additionally, the simplest signal processing possible was desired so that the encoder could be easily implemented. These considerations essentially eliminated a magnetic encoder and demanded an optical encoder. Optical encoders can be compact, have minimal inertial mass, are capable of high speed, and generally output a 5 VDC transistor-transistor logic (TTL) signal which is easily processed.

Optical encoders are commonly used in engine testing. However, these engines usually operate slower and have more available space than a micro engine. This meant that no commonly used encoder provided the necessary parameters for testing the micro engine. This was especially true when looking for an encoder to fit within the available axial length on the crankshaft. In order to find an optical encoder that had all the necessary parameters, smaller encoders used for other applications besides engine testing had to be considered.

The final solution identified was a US Digital EM1 encoding module with a 2” HUBDISK. Pictures of this module and encoding disk can be seen in Figure 3-8. US digital produces a range of encoders that include a module, sensing disk, and housing. None of the models with housings were sufficiently short along the disk axis to fit on the engine crankshaft, however. To solve this issue, the separate module/disk combination was chosen. By separating the disk and encoding module, only 0.310 inches of shaft length was required versus approximately 0.6 inches for the next housed encoder. Specifications of the EM1 module and 2” HUBDISK can be seen in Table 3-6.

Table 3-6: US Digital EM1 and 2" HUBDISK specifications [30] [31]

EM1-2-1800-I	Type	Incremental, two channel quadrature output with index
	Count Frequency	300 kHz
	Operating Temperature	-55 to 125 °C
HUBDISK-2-1800-375-IE	Outside Diameter	2.00 inches
	Bore	0.375 inches
	Operating Temperature	-40 to 100 °C
	Counts per Revolution (CPR)	1800

Figure 3-8: US Digital EM1 module (lower) [30] and 2" HUBDISK (upper) [31]

The 1800 CPR was chosen to provide the ample resolution in crankshaft position for cylinder pressure acquisition. Additionally, the 300 kHz limitation of the EM1 module meant that with 1800 CPR it could accurately measure crankshaft position up to 10,000 RPM, which was the designed maximum test stand speed. The EM1 module output was also used with the AVL IndiModul system for pressure transducer crank-angle-based measurements.

(5) Surface and Gas Temperatures

Temperature measurement was crucial for successfully documenting the engine's behavior both before and after the fuel conversion. The exhaust, intake, cylinder head, and case temperature were all used regularly to document engine cooling and thermal stability. All of the thermocouples used were K-type and were read with a National Instruments (NI) CompactDAQ 9213 acquisition card. The built-in cold-junction compensation of the 9213 card was used for all measurements. Surface temperature measurements were made by using exposed, welded-bead thermocouples that were fixed to the measured surface using commonly available fast-setting

epoxy. Ungrounded probe type thermocouples were used for the exhaust and cylinder head temperature while an exposed bead probe was used for the intake temperature measurement. Both the intake and exhaust thermocouple probe were situated in the center of the gas flow. The cylinder head thermocouple was placed so that the thermocouple measurement junction was on the same plane as the glow plug sealing surface.

(6) Exhaust Pressure

Two-stroke engines can be very sensitive to changes in exhaust pressure and commonly use tuned pipes to improve performance [32]. In order to test indoors, however, a facility exhaust system was needed to remove exhaust fumes. Therefore, in order to avoid creating any suction on the engine exhaust, an Omega PX219 pressure transducer was incorporated into the exhaust system. The PX219 model is a low speed pressure transducer with a range of 0 to 30 psia. The pressure measurement location was taken directly above the exhaust temperature measurement. A stainless steel tube was routed away from the exhaust and the pressure line was then converted to a Teflon tube. The stainless steel tube was used to ensure the pressure line did not overheat while the Teflon tube was used to allow flexibility during stand setup.

(7) In-cylinder Pressure

Early in the project, it was decided that crank-angle-based cylinder pressure analysis was going to be essential when understanding both the operation of the two-stroke, micro engine and also the fuel conversion. The cylinder pressure analysis provided two strong pieces of information.

First, it allowed the calculation of multiple efficiencies. Specifically, the conversion of fuel energy to indicated power allowed us to understand the role the fuel played in lubricating and cooling the engine. Also, the cylinder pressure was used to calculate indicated power to electrical power conversion efficiency, which characterizes the efficiency of the engine- electric machine system.

Second, the cylinder pressure measurement was used to calculate the coefficient of variation of indicated mean effective pressure (COV of IMEP), which would allow tuning of the engine based on quantitative, rather than qualitative, comparison. Usually, micro engines are tuned “by feel” in the field in their application. Because the electric power generation application is not a typical application, it would prove difficult to tune the system “by feel” only. By looking at the temperatures and COV of IMEP, however, a robust operating point could be selected for the engine’s steady-state operation.

A typical in-cylinder pressure acquisition system consists of four basic components: a pressure transducer, a charge amplifier, an acquisition system, and a software package. For simplicity, a complete AVL IndiModul system was used as it was available and easily configured with industry standard settings. The charge amplifier, acquisition system, and software all integrate together to provide fast setup and confident results. Originally, a custom combustion analysis system was considered, but this proved to be ineffective from a scheduling standpoint.

The pressure transducer was the only specific component that had to be selected for the micro engine application. Based on product familiarity, AVL was chosen as the supplier of the pressure transducer. However, because the engine's operating characteristics were not fully known, it was difficult to select a specific transducer. Based on the fuels, operating speed, and size constraints, AVL recommended the GH14D piezoelectric pressure transducer. This transducer provided a pressure range of 0-250 bar and was also among the most compact transducers available.

Even though the GH14D transducer was one of the most compact transducers available, there was still not sufficient material in the stock cylinder head to mount the transducer. The GH14D has an M5x0.5 thread and requires 7 mm of thread engagement. The stock head, however, was only 5-8mm thick at its thickest location, which would not be sufficient for installing the GH14D. In order to address this issue, a custom cylinder head was fabricated.

The primary concern with designing the custom head was developing the same clearance volume and combustion chamber shape as the stock head. Two steps were taken to ensure that the combustion chamber was properly replicated. First, the stock head geometry was measured and a solid model of the combustion chamber shape was created to calculate clearance volume. Next, the solid model volume was verified by measuring the physical volume of the stock head. This was accomplished by placing a small acrylic sheet over the sealing surface of the combustion chamber and filling the volume with automatic transmission fluid using a 25 microliter syringe. The solid model volume and the measured volume of the stock head agreed within 1% after accounting for the glow plug volume, confirming the combustion chamber geometry measurements.

A new cylinder head design was then developed. The same sealing surface, bolt patterns, and glow plug location were used to enable a form-fit-function replacement of the stock head. For the first custom cylinder head, the only change to the combustion chamber was a 30 cubic millimeter (approximately 4% of the clearance volume) volume reduction to account for the volume addition caused by the port needed for the pressure transducer. The major difference between the custom

and stock head was an increased head thickness to allow room for mounting the pressure transducer and an estimated 20-30% increase in surface area to account for the extra thermal mass. Cooling fins were cut radially for machining simplicity. A cross section drawing of the first custom head showing the pressure transducer port geometry and combustion chamber geometry is shown in Figure 3-9. Additionally, pictures showing the stock cylinder head and first custom cylinder head side-by-side are shown in Figure 3-10.

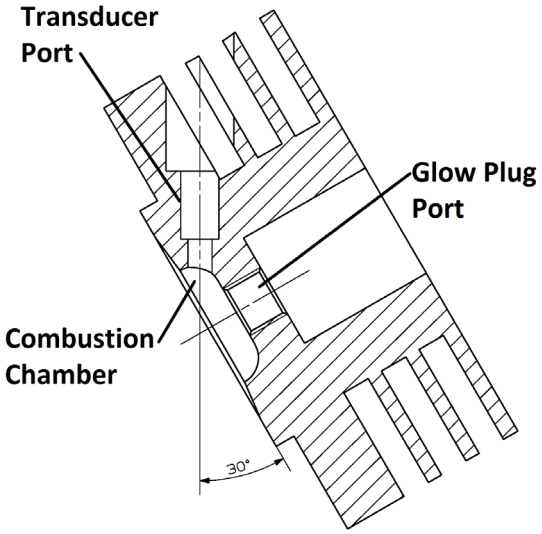

Figure 3-9: Cross section of custom cylinder head, oriented with pressure transducer power vertical [25]

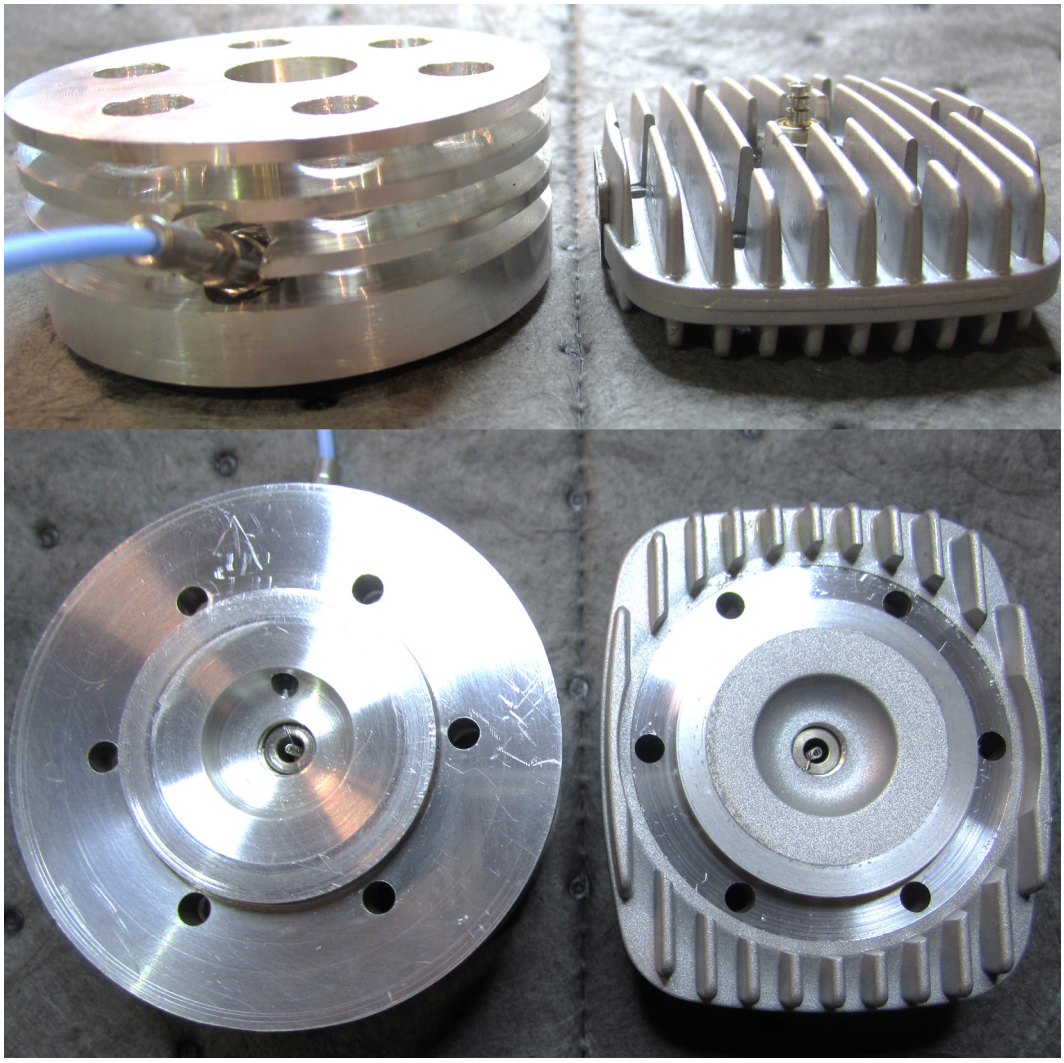

Figure 3-10: Custom cylinder head (left) compared to stock cylinder head (right). Upper: Side view. Lower: Combustion chamber view. Note pressure transducer installed on custom head. [25]

3.2.4 Software

(1) LabVIEW [25]

In an effort to accommodate an aggressive project schedule and to minimize project costs, a National Instruments (NI) CompacDAQ data acquisition system (model cDAQ-9178) was used with NI LabVIEW and NI DAQmx drivers to acquire and display all measurements, with the exception of the cylinder pressure. This system allowed for rapid configuration and a custom acquisition/control interface that could be developed specifically for the project's custom

instrumentation. Data, calculations, and controls were all acquired or executed real-time through a master virtual instrument (VI).

The micro engine test stand had numerous inputs and outputs which included both digital and analog signals. Additionally, those signals could be interpreted into the LabVIEW VIs in different ways. A summary of each type of signal, the NI module and the VI channel type used are shown below.

- Pulse Width Modulation (PMW) Output – an NI9401 digital input/output module was used with a "Counter Output-Pulse Frequency" DAQmx VI to output two different PWM signals. One of the signals controls a hobby servo for the engine throttle and the other signal went to the BLDC motor controller to control the motoring speed.
- Digital Boolean Output – another NI9401 module was used with a "Digital Output" VI to output a 5VDC on/off voltage to the relay used to route power to the BLDC motor. A second NI9401 module was needed because all of the hardware on the first module was reserved for the PWM output tasks.
- Digital Counter Input – an NI9402 module was used with a "Counter Input Pulse Frequency" VI to measure RPM. In order to acquire RPM with the same sample clock as the analog signals, state machine architecture was developed to check for missing samples when the index pulse frequency of the encoder was slower than the analog sampling frequency. This piece of the test software was important because there was not a reliable way to synchronize the RPM measurements with the analog measurements. By measuring the RPM at the same sample frequency as the analog measurements and by ignoring the encoder pulses between analog measurements, RPM could be acquired at the same frequency as the analog inputs.
- Analog Voltage Input – an NI9219 module was used with "Analog Input Voltage" VIs to measure the voltages input from the fuel scale load cell, the load cell excitation voltage, the anemometer transducer, and the exhaust pressure transducer. Once acquired, a running average was started to eliminate the random error associated with these analog measurements. The desired outputs (fuel mass, air velocity, exhaust pressure, AFR, fuel flow rate, and air flow rate) were then calculated real-time in the VI.
- Thermocouple Input – an NI9213 module was used with an "Analog Input Thermocouple" VI to acquire temperature. This VI was set to auto-zero for every sample, used high resolution analog to digital conversion and used the module's built-in cold-junction-compensation.

- DC Load Control Output/Input – using manufacturer-supported drivers and a USB-to-serial convertor, the programmable DC load was fully controlled through LabVIEW. This included setting the test mode, setting ranges, setting commanded power, measuring current/voltage/power, and turning the unit on and off. This allowed for dynamic changes in the commanded power while visualizing the electrical power produced.

In addition to measuring data, calculating parameters, displaying data, and outputting control signals, the developed VI was made to log the measured data and control commands through the LabVIEW TDMS file structure. This allowed for full documentation of all the measured, calculated, and commanded values for later use.

The wiring diagram and a screen shot of the graphical user interface for the master VI is shown in Appendix C.

(2) AVL IndiCom

AVL IndiCom software was used as an interface with the AVL IndiModul system and was used to compute a number of engine combustion parameters. Each of these calculated parameters are briefly explained below.

- Indicated mean effective pressure (IMEP) is the ratio of the work done per combustion cycle divided by the displaced volume. It is a normalized method of documenting engine output and has units of pressure [7].
- Coefficient of variation of IMEP (COV of IMEP) is a measure of the combustion quality. It is defined as the standard deviation of IMEP divided by the mean IMEP for a given number of cycles. As the standard deviation decreases, the combustion quality improves, and the COV of IMEP decreases [7].
- The value and crankshaft angle location of the maximum pressure were also calculated. These are commonly used to assess engine component durability. However, their analysis is not presented in this thesis because minimal differences were observed and durability analysis is outside the thesis scope.
- The location of 50% mass fraction burned (50% MFB) was recorded. This is calculated by the combustion analysis software and is the location where half of the fuel energy is burned in the combustion process [7].
- The duration of the combustion event from 10-90% mass burned (D10-90%) is a measure of combustion event duration in crankshaft angle degrees (CAD). The 10% and

90% mass burned locations are chosen as they are more readily observed from the combustion process [7].

- Rate of heat release (ROHR) is a measure of how fast fuel energy is being released into the cylinder and is calculated by the software using a combustion model and the pressure trace [7].
- Integrated heat release is calculated by the combustion analysis software. It is the finite integral of the ROHR [7].
- The pressure trace was also collected. This is the raw pressure values at each measured crankshaft position and is used to calculate all of the parameters above. For the micro engine testing, 1800 measurements were taken per cycle, equating to an angle resolution of 0.2 CAD.

For additional clarification on these engine combustion calculations, reference any internal combustion engine text.

The IndiCom software was configured to acquire 300 combustion cycles and average the pressure, ROHR, and indicated heat release traces at the end of those measured cycles. This resulted in 300 cycle-based measurements and single pressure, ROHR, and indicated heat release measurements. Values reported in this thesis are the average values of the 300 measured cycles.

Another note on the IndiCom software setup is that the combustion analysis needs engine hardware dimensions and the ratio of specific heats of the in-cylinder gases. The dimensions were updated accordingly for each engine configuration, but the ratio of specific heats required an assumption to be made. Because the micro engine is a homogenous charge engine with poor fuel vaporization, it is difficult to assign a single ratio of specific heats value. The ratio of specific heats was assumed to be 1.32 for all combustion analysis acquisitions. This is a typical value chosen for gasoline engine testing and was the best available approximation. Further research is likely needed to identify if this value is a good approximation for both NM and JP-8 fuels in the micro engine.

3.3 Steady-State Testing of the Nitromethane-methanol-fueled Engine

Having completed the micro engine test stand, testing on the micro engine could begin. However, before converting the engine to JP-8, a series of baseline tests were conducted to evaluate the performance of the unmodified engine with nitromethane-methanol blend fuel. The

purpose of testing the engine in its stock form was to document the performance of the custom cylinder head as compared to the stock cylinder head and to understand the basic behavior of the micro engine.

There was minimal information available on the micro engine before it was tested, so a number of assumptions were made and test methods developed. These included assumptions about the fuel and glow plug choice, the operating speeds, carburetor tuning, and operating temperatures.

The first assumptions that needed to be made were about fuel and glow plug selection. Multiple blends of nitromethane-methanol fuels (henceforth “NM” fuels) are available in the hobby industry and appear to be chosen on operator preference and application. Generally speaking, helicopter engines like the O.S. 70SZ-H are run with higher percentages of nitromethane while fixed-wing aircraft engines run lower amounts of nitromethane. Fuels are available ranging from 0% to over 30% nitromethane, but the O.S. 70SZ-H manual suggests operating with no more than 30% nitromethane. Without any previous experience in fuel selection, a 15% nitromethane blend was chosen simply because it was the nominal nitromethane content. With glow-ignition engines, the fuel selection is often matched to a glow plug selection. O.S. Engines sells four different plugs, designated by a number. These are the #6, #7, #8, and #10 glow plugs, which range from “hot” to “cold” respectively. By personal observation, the difference between these glow plugs is that as the glow plug number increases, the diameter of the glow plug filament spiral increases in size. For example, a #6 plug has a tight filament spiral, while the #10 plug has an open filament spiral. Again, with no experience, the nominal #8 plug was chosen; this is also the glow plug referenced in the engine’s manual as the best nominal choice.

Next, the operating speeds needed to be selected. The choice of operating speeds was based on the amount of power produced by the engine and the limitations of the micro engine test stand. The objective of the project was to convert the engine to JP-8 fuel and to produce 250 W of electric power; therefore the engine was tested at 250 W with the NM blend fuel. There was no engine output information before testing began, so a trial and error approach was taken to determine which speeds the engine could produce 250 W. From this process, and while taking into account the 10,000 RPM limitation of the engine test stand, speeds of 10,000, 9,000, and 8,000 engine revolutions per minute (RPM) were selected as the NM-blend-fueled engine test points.

With these selections, the final consideration to be made was engine temperatures and carburetor settings, which are strongly linked because the engine uses the fuel as a primary

cooling source. Once again, no previous information on engine operating temperatures was available. It was assumed that a target head temperatures of around 130-140°C would be acceptable because no other information available. For comparison purposes, this temperature measurement was made approximately 0.38" from the cylinder bore centerline in the same plane as the glow plug seating surface.

Through some basic experimentation, it was determined that temperature increased with speed and load. So, to obtain this temperature, the engine was started and run at 10,000 RPM with 250 W. The carburetor's main needle was then adjusted to maintain a steady-state temperature of approximately 140°C while a squirrel-cage fan moved air at a velocity of approximately 8.0 m/s over the engine. This velocity equates to approximately 80 L/s volumetric flow rate. Note that the carburetor of the 70SZ-H has three adjustments, but the mid-speed and idle adjustments were left at the stock settings. Additionally, note that the fan was oriented so that the direction of the airflow was along the axis of the crankshaft, flowing from the side opposite the crankshaft to the side with the crankshaft protruding. The final settings were 1.5 turns from fully closed on the main jet, 0.5 turns from fully closed on the mid-speed jet, and the stock idle position (centered). This carburetor setting was maintained throughout the NM blend fuel testing for both the stock and the custom head configuration.

Testing was started after the basic engine operating parameters were selected. The engine was run at 10,000, 9,000, and 8,000 RPM and all tests were conducted with 250 W of electrical load. Each of these three speed-load points was run three times for repeatability, totaling 9 tests per configuration. The method for cycling through these speed-load points included:

1. Warm the engine by running between 50-100 W at a moderate speed
2. Increase speed to 10,000 RPM while simultaneously increasing the load to 250 W.
3. Operate at this speed-load until the head temperature did not change more than 2°C per minute. (This criterion for stability was used for all steady-state testing on both the NM blend and JP-8 testing.)
4. Once stable, collect and store data for 60 seconds.
5. Using the throttle position only, decrease the engine speed to 9,000 RPM.
6. Repeat steps 3 and 4.
7. Using the throttle position only, decrease the engine speed to 8,000 RPM.
8. Repeat steps 3 and 4.
9. Return engine to the 10,000 RPM point and repeat steps 3-8.
10. Repeat step 9 twice for a total of 3 samples of each of the 3 speed-load points.

In the event that the fuel tank was depleted, the engine was stopped, refilled as quickly as possible, and restarted. The engine speed and load was then increased to the next operating point, and the test was resumed. With a 14 fluid ounce fuel tank, this happened approximately once every 4 speed-load points.

These 9 speed-load data points were collected with both the stock head and with the custom cylinder head with the cylinder pressure transducer. For the custom cylinder head, combustion analysis data was collected using AVL IndiCom at the end of the 60 seconds of steady-state data. The steady-state speed-load point data and the combustion analysis data was then compiled in Microsoft Excel.

The results of this steady-state testing with 15% NM blend fuel, the O.S. #8 glow plug, and the stock and custom cylinder head are presented here. The first piece of data compared between the stock and custom cylinder head was a speed comparison. This was completed to show that the other data points, such as temperature and fuel flow rate, could be compared. The speed comparison can be seen in Figure 3-11. Note that all three runs are shown with an average value and an error bar showing twice the standard deviation of the three measurement runs for that speed-load point. The same speed-load points for the stock and custom head are placed adjacent to each other.

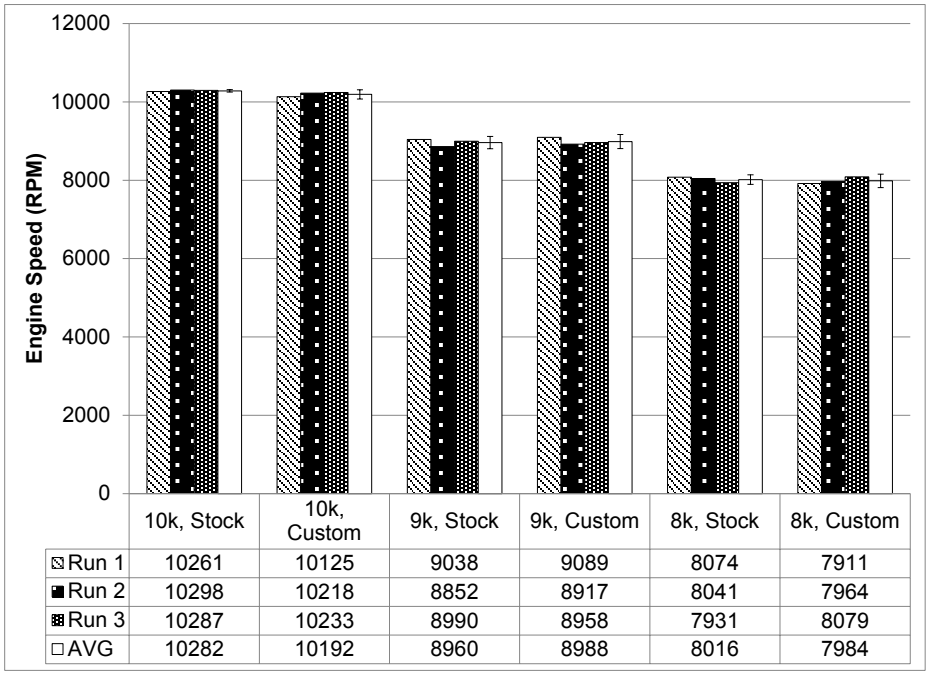

	10k, Stock	10k, Custom	9k, Stock	9k, Custom	8k, Stock	8k, Custom
Run 1	10261	10125	9038	9089	8074	7911
Run 2	10298	10218	8852	8917	8041	7964
Run 3	10287	10233	8990	8958	7931	8079
AVG	10282	10192	8960	8988	8016	7984

Figure 3-11: NM-fueled engine speed comparison of stock and custom cylinder heads

The engine speed comparison shows that the speed was held consistently between the different runs and between the two cylinder head configurations. This confirms that comparison of the other measurements is valid.

The next comparison made was the exhaust gas temperature. This was compared to show that the combustion phasing and heat transfer between the two cylinder heads was similar. If the combustion occurs later in the engine's cycle for a given load, the exhaust temperature could increase. Additionally, if there is less heat transfer out of the cylinder head, the energy in the exhaust gas would likely increase. The exhaust temperature comparison is shown in the same format as the engine speed in Figure 3-12.

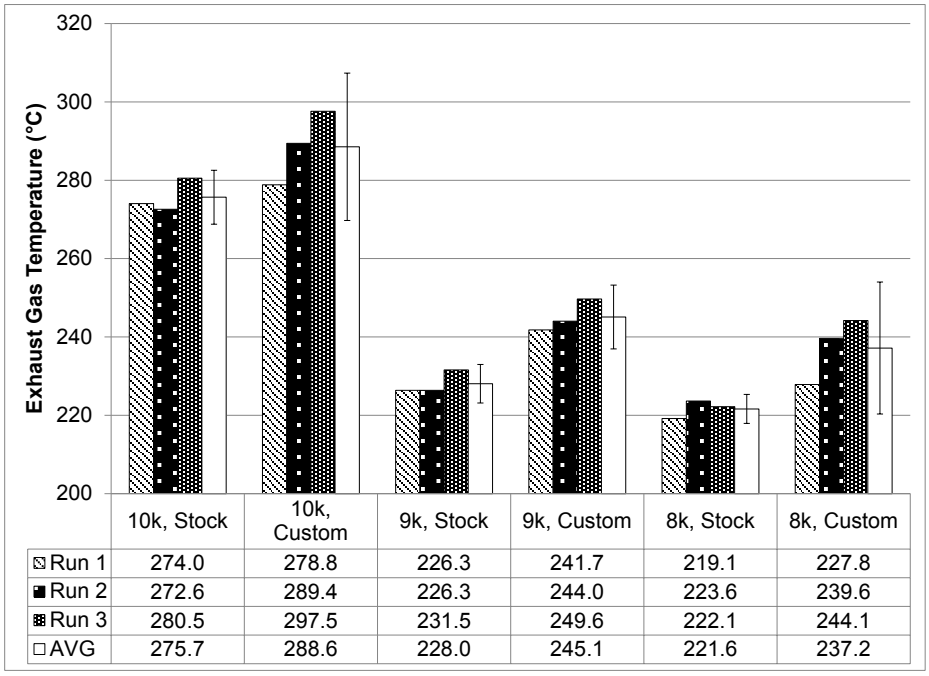

	10k, Stock	10k, Custom	9k, Stock	9k, Custom	8k, Stock	8k, Custom
Run 1	274.0	278.8	226.3	241.7	219.1	227.8
Run 2	272.6	289.4	226.3	244.0	223.6	239.6
Run 3	280.5	297.5	231.5	249.6	222.1	244.1
AVG	275.7	288.6	228.0	245.1	221.6	237.2

Figure 3-12: NM-fueled engine exhaust gas temperature comparison of stock and custom cylinder heads

From the exhaust gas temperature comparison, it does appear that there was a slight temperature increase at each operating point with the custom cylinder head. Without combustion analysis, the reason for this trend is unclear. However, this increase is fairly small compared to the measurement, and in the case of the 10,000 and 8,000 RPM measurement it appears to fall within the range of twice the standard deviation. This suggests that it may be an insignificant error.

The cylinder head temperature also needed to be compared. This temperature was used as a gauge for engine durability, so the values between the stock and custom cylinder head were desired to be very close together. The cylinder head temperatures can be seen in Figure 3-13.

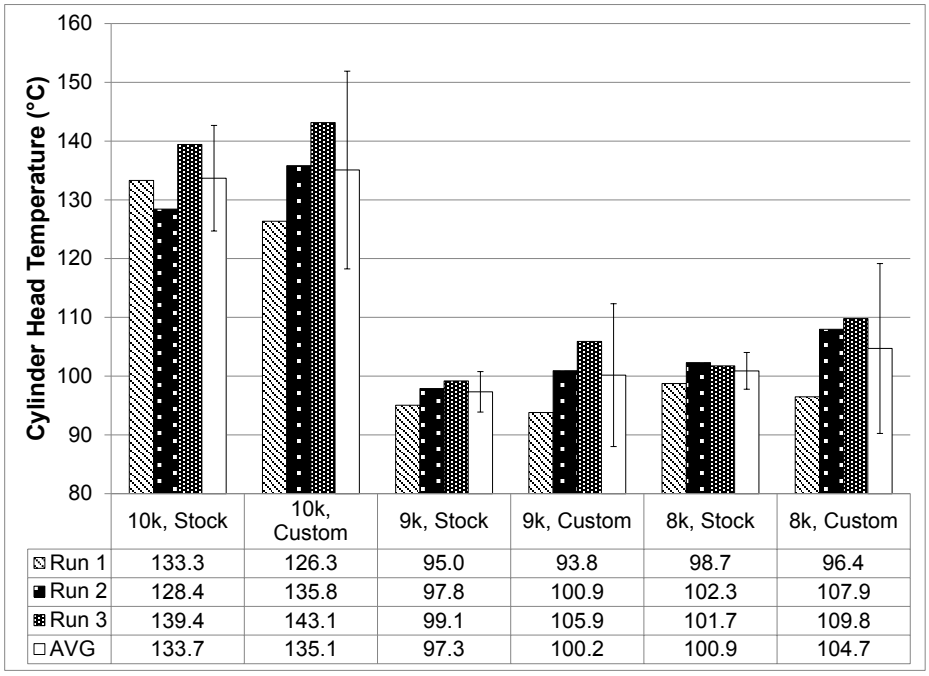

	10k, Stock	10k, Custom	9k, Stock	9k, Custom	8k, Stock	8k, Custom
Run 1	133.3	126.3	95.0	93.8	98.7	96.4
Run 2	128.4	135.8	97.8	100.9	102.3	107.9
Run 3	139.4	143.1	99.1	105.9	101.7	109.8
AVG	133.7	135.1	97.3	100.2	100.9	104.7

Figure 3-13: NM-fueled engine cylinder head temperature comparison of stock and custom cylinder heads

The cylinder head temperatures aligned much more closely than the exhaust temperatures, though the custom cylinder head did have higher standard deviation between the measurements. There was also a trend of increasing temperature through the three runs. This suggests that the engine may not have been fully stabilized. For this testing, however, this was deemed acceptable and the results collected.

The combination of the exhaust and cylinder head temperatures suggest that the custom cylinder head does not exactly match the stock cylinder head. A temperature increase from the stock head to the custom head can be observed in both the exhaust and cylinder head temperatures. The custom head was accepted, though, because the changes are relatively small and the purpose of collecting the NM blend fuel data was simply for comparison purposes later. The important point is that the change between the stock and custom head is not so drastic that the trends observed in the stock head change when the custom head is used instead.

Two additional pieces of data were compared for the stock and custom cylinder head; the fuel mass flow rate and the air-to-fuel mass ratio (AFR). These were not used to compare heads

directly, but rather for documentation for future work. The fuel mass flows can be seen in Figure 3-14 and the AFRs can be seen in Figure 3-15.

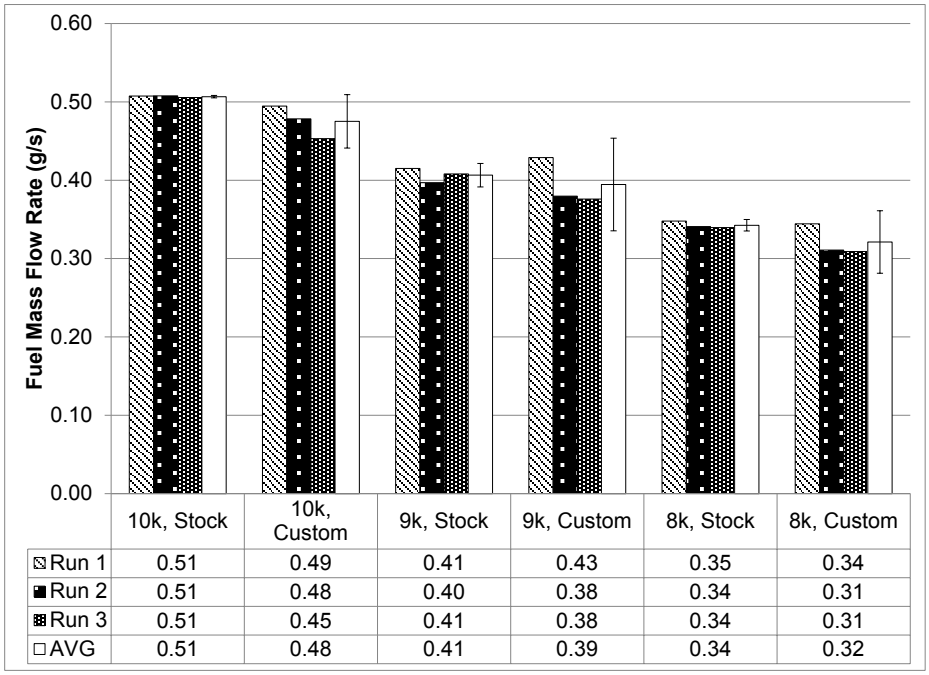

	10k, Stock	10k, Custom	9k, Stock	9k, Custom	8k, Stock	8k, Custom
Run 1	0.51	0.49	0.41	0.43	0.35	0.34
Run 2	0.51	0.48	0.40	0.38	0.34	0.31
Run 3	0.51	0.45	0.41	0.38	0.34	0.31
AVG	0.51	0.48	0.41	0.39	0.34	0.32

Figure 3-14: NM-fueled engine fuel mass flow comparison of stock and custom cylinder heads

For the fuel mass flow comparison, the only clear trend is a slight reduction in fuel consumption at all speeds for the custom cylinder head. This reduction could be tied to the increased temperatures; the fuel flow rate is directly related to how much energy is removed in the micro engine by the evaporative effects of the NM blend fuel. The standard deviation is also higher for the custom cylinder head fuel flow measurements. No clear explanation could be made for this trend.

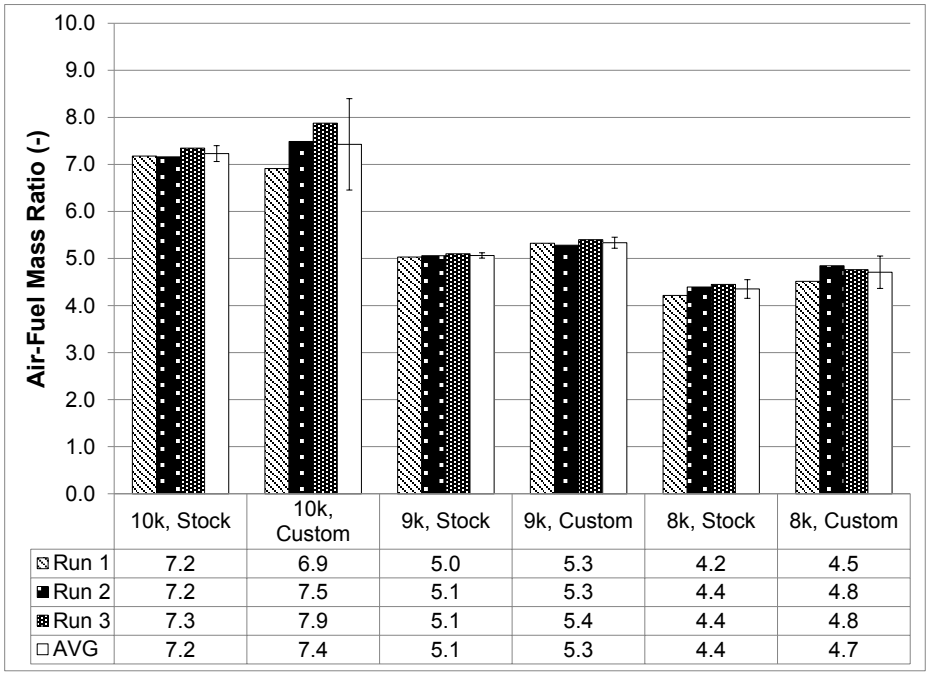

	10k, Stock	10k, Custom	9k, Stock	9k, Custom	8k, Stock	8k, Custom
Run 1	7.2	6.9	5.0	5.3	4.2	4.5
Run 2	7.2	7.5	5.1	5.3	4.4	4.8
Run 3	7.3	7.9	5.1	5.4	4.4	4.8
AVG	7.2	7.4	5.1	5.3	4.4	4.7

Figure 3-15: NM-fueled engine air-fuel mass ratio comparison of stock and custom cylinder heads

The AFR comparison shows, as expected, the reverse trend of the fuel flow rate; the AFR increased at all speeds for the custom cylinder head. Note that the required throttle position to maintain 250 W was identical for the stock and custom heads in the 10,000 and 8,000 RPM cases. The throttle position increased 2% for the 9,000 RPM case with the custom cylinder head. This nonexistent or small change in throttle position confirms that the engine was operating with the same intake restriction.

In summary, the steady-state data revealed that the custom cylinder head did not perfectly replicate the results of the stock cylinder head. There was a slight temperature increase with the custom cylinder head while at the same time a reduction in fuel flow rate. The temperature increase suggests that either combustion was happening slightly later in the engine's cycle or that there was decreased heat transfer through the head. This may have caused the drop in fuel consumption, or it may have been caused by the drop in fuel consumption. It is not clear which of these trends is caused by the other with the data collected. However, this was not a significant concern. The purpose of collecting this data was to simply collect a baseline dataset for the JP-8 conversion, and these small changes do not significantly alter the performance or behavior of the micro engine in its stock configuration.

The purpose of running the custom cylinder head was to obtain in-cylinder pressure data for combustion analysis. No comparison could be made between the stock and custom head as the stock head could not accommodate the pressure transducer, but combustion data was collected with the custom head for the purpose of documentation. Two general trends were observed in this documented data including the engine's behavior at the different operating points and the general combustion behavior of the NM-blend-fueled engine

The first trend observed in the combustion data from the NM-blend-fueled micro engine was the output and combustion quality at the three operating points. During testing, the specific operating points produced very specific sounds. The 10,000 RPM point sounded sharp and it was clear the engine was operating at a point that was well tuned. The 9,000 RPM point, however, sounded as if the engine was struggling to operate. The 8,000 RPM point sounded like the engine was under a heavy load, but the engine did not sound like it was approaching a point where it would stall.

These qualitative observations were reflected in the combustion data with the custom cylinder head. The IMEP and COV of IMEP both showed quantitatively the engine behavior that was audibly observed. First, the IMEP, shown in Figure 3-16, shows that the 10,000 RPM point was producing a high IMEP, which confirms that the engine was not struggling to produce the 250 W of electrical power. The 9,000 and 8,000 RPM points, however, were producing nearly the same IMEP. The expected result is that the 9,000 RPM point would produce IMEP somewhere between the 10,000 and 8,000 RPM point. The lack of this result suggests that the 9,000 RPM point is located in a region of poor operation of the two-stroke engine.

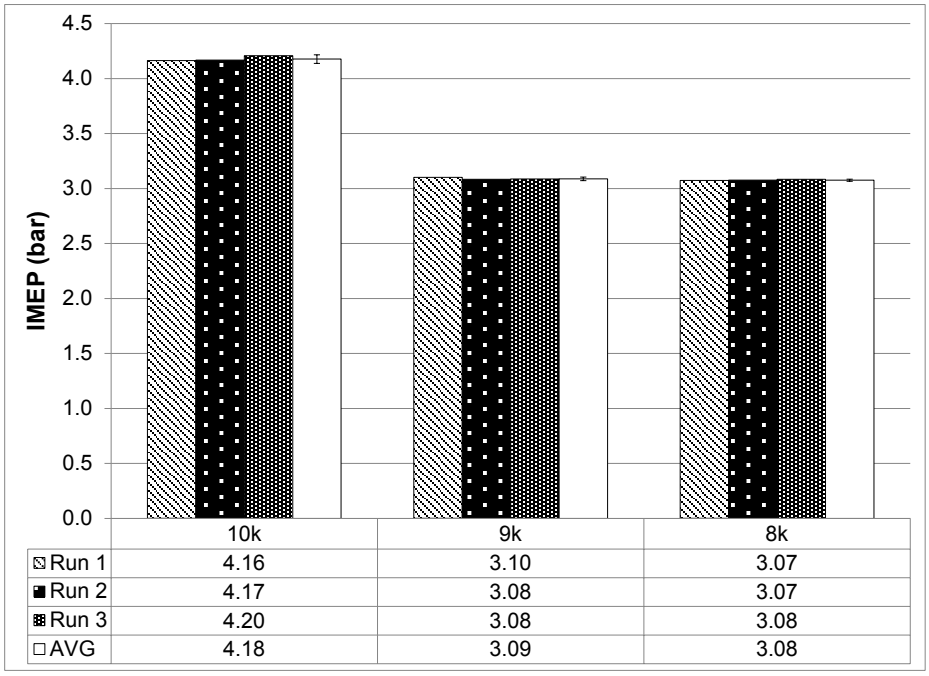

	10k	9k	8k
Run 1	4.16	3.10	3.07
Run 2	4.17	3.08	3.07
Run 3	4.20	3.08	3.08
AVG	4.18	3.09	3.08

Figure 3-16: NM-fueled engine indicated mean effective pressure values at three speeds and 250

This hypothesis was confirmed when examining the COV. The COV is the standard deviation of the IMEP divided by the mean value of the IMEP and is used to determine the quality of the combustion process. Because of the lack of ignition control and the two-stroke operation, the COVs for the micro engine were expected to be quite high. Typical values in automotive engines do not exceed 10%. The COV for the NM-fueled engine testing is shown in Figure 3-17. The behavior observed in the IMEP is confirmed by the COV. The 10,000 RPM point is operating with low COV, which means its combustion was robust and consistent. The 9,000 RPM operating point, however, was running with a COV in excess of 40%, suggesting many misfire cycles. The 8,000 RPM operating point also had high COV values, but not to the extent of the 9,000 RPM operating point.

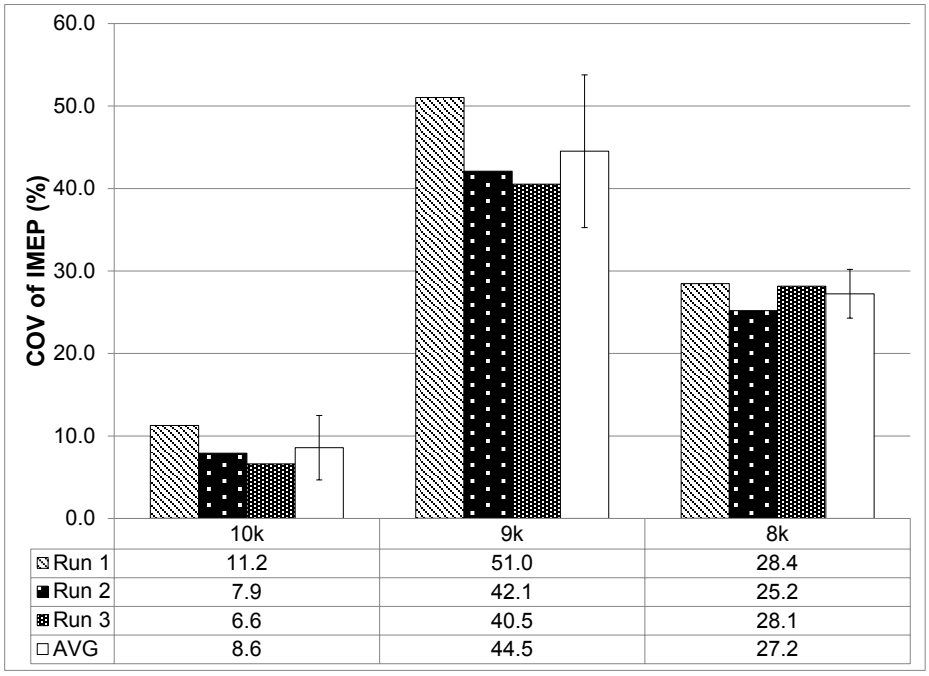

	10k	9k	8k
Run 1	11.2	51.0	28.4
Run 2	7.9	42.1	25.2
Run 3	6.6	40.5	28.1
AVG	8.6	44.5	27.2

Figure 3-17: NM-fueled engine coefficient of variation of IMEP values at three speeds and 250 W

The next general observation about the NM-fueled engine combustion was the location and duration of the fuel's combustion. Spark-ignited engines typically try to burn half of the fuel mass at 7 crank angle degrees (CAD) after top dead center (ATDC) for maximum output. This value is called the 50% mass fraction burn (MFB) location. As seen in Figure 3-18, however, all three of the speeds had a 50% MFB location past 10 CAD ATDC. This is likely by design of the engine; because there is no intelligent control of the start of ignition, the ignition must be sufficiently delayed such that the combustion does not happen early and cause engine damage. This results in reduced engine efficiency, but this is rarely a concern for small hobby engines. The 9,000 RPM point again shows poor combustion characteristics. As the 50% MFB location is delayed further, the efficiency of the engine's cycle decreases. The 9,000 RPM point has a 50% MFB of over 17 CAD ATDC, which is especially late in the engine cycle.

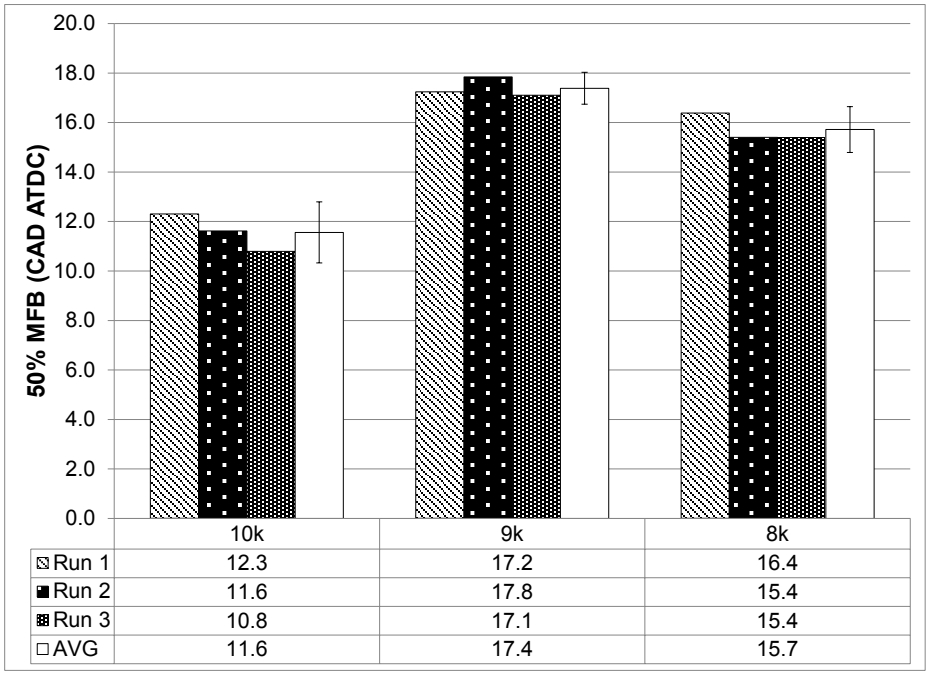

	10k	9k	8k
Run 1	12.3	17.2	16.4
Run 2	11.6	17.8	15.4
Run 3	10.8	17.1	15.4
AVG	11.6	17.4	15.7

Figure 3-18: NM-fueled engine 50% mass fraction burned location at three speeds and 250 W

The final piece of data to be discussed from the combustion analysis is the 10-90% mass burn duration (D10-90%). This value represents the duration that the measurable combustion occurs within the engine cycle. The main trend to note is that the 9,000 RPM point took the longest to combust its fuel. This is a strong indicator of poor fuel-air charge mixing at this speed-load point. Figure 3-19 shows the 10-90% mass burn duration.

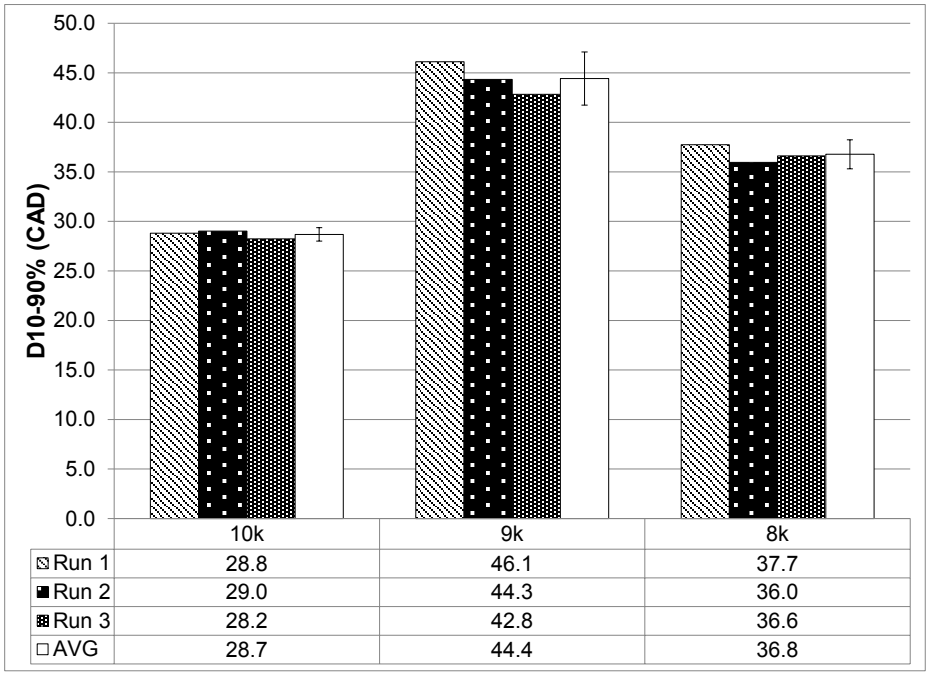

	10k	9k	8k
Run 1	28.8	46.1	37.7
Run 2	29.0	44.3	36.0
Run 3	28.2	42.8	36.6
AVG	28.7	44.4	36.8

Figure 3-19: NM-fueled engine 10-90% fuel mass burn duration at three speeds and 250 W

In summary, the NM-fueled engine combustion analysis provided some insight into the engine's operation. The main observation is that the audibly poor 9,000 RPM operating point was, in fact, a poor operating point. High COV values coupled with late and long burn durations suggest that poor fuel-air charge mixing were occurring at this operating point. The 10,000 RPM operating point showed strong performance and is clearly a point in the engine's operating range that the engine was designed to provide peak performance. The 8,000 RPM operating point, however, is an operating speed that the engine struggles with. While the COV is better than the 9,000 RPM operating point, the later and longer combustion durations also suggest poor gas dynamics at this point. Given the 16,000 RPM rated operating speed of the O.S. 70SZ-H, this is not unexpected.

Chapter 4 Micro JP-8 Burn: Phase 2

The conversion of the micro engine from NM blend fuels to JP-8 involved a stepped approach targeting specific crucial aspects of the conversion. These steps included confirming sufficient fuel lubricity for the two-stroke engine, identifying methods for improved starting, choosing a best method for starting and operation, and completing steady-state testing.

4.1 JP-8 Lubricity Analysis

The O.S. 70SZ-H, like most hobby glow engines, relies on fuel that is premixed with lubricant to provide lubricity to the internal engine components. The O.S. 70SZ-H is a crankcase scavenged two-stroke that uses the crankshaft as a rotary valve to allow a fresh air-fuel charge into the crankcase. This charge moves through the crankshaft into the crankcase, where it is mixed by the motion of the crankshaft and connecting rod. From there, the charge moves into the intake ports and then further into the cylinder, where it is combusted. Through this entire process, the charge is in direct or indirect contact with every moving part in the engine. Additionally, there is no sump of lubricating oil, as there is in larger four-stroke engines. To ensure proper lubrication throughout the engine, the engine has small slots or holes cut into the surfaces that encounter friction. The premixed fuel-lubricant mixture can seep through these slots to lubricate the bearings, bushings, and other interfaces. The vaporized charge also lubricates the piston rings and cylinder walls as it moves through the intake ports to the cylinder.

Because the premixed fuel-oil mixture is so crucial to the engine's durability, special consideration was made to ensure that any JP-8 mixture would have similar, if not better, lubrication than the stock fuel-oil mixture. However, there were two challenges associated with understanding this lubricity. First, there is no published information on the lubricity of most hobby-grade NM blend fuels. Second, the lubricity of JP-8 is known to vary widely. The only way to ensure robust operation was to order lubricity testing of the NM blend and JP-8 fuels.

The first step in the lubricity analysis was to get a firm understanding of the standard hobby fuel lubricity. To do this, a sample of Tower Hobbies, 15% Nitromethane Heli Fuel was tested under the ASTM D6078 (Scuffing Load Ball on Cylinder Lubricity Evaluator, SLBOCLE) and ASTM D6079 (High Frequency Reciprocating Rig, HFRR) standards at Southwest Research Institute (SwRI). These standards are used for diesel-type fuel lubricity testing, but were the best available standards for lubricity testing of premixed fuel-oil mixtures. This Tower Hobbies brand fuel was evaluated as this was the fuel used for the NM-fueled micro engine baseline testing.

The SLBOCLE result for the NM blend fuel was 7,000 grams. This value actually exceeds the accuracy range the SLBOCLE was designed for (6200 g), indicating that the NM fuel-oil blend provides very good tangential friction reduction.

The HFRR result for the NM blend fuel was not as clear as the SLBOCLE test. The HFRR test is an optical method where a prepared steel ball is oscillated 1 mm at 50 Hz for 75 minutes against a prepared plate. The ball is then examined under a microscope and the major and minor axes of the typically elliptical wear scar are reported. For the NM blend fuel, the wear scar was reported as 0.62 mm on the major axis and 0.50 on the minor axis, averaging to a 0.56 mm diameter wear scar. This is a relatively high value for the HFRR test, disagreeing with the SLBOCLE test. After discussing the results with Steve Westbrook at SwRI, a copy of the measured wear scar was provided. An image of this wear scar can be seen in Figure 4-1.

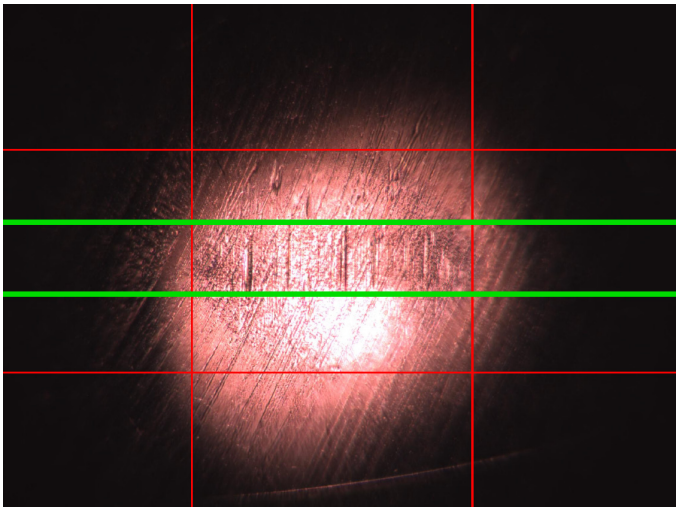

Figure 4-1: Wear scar image result from SwRI NM HFRR test. Red lines show documented scar, green lines show proposed scar

Close examination of the wear scar shows there are two regions of wear. The first is the larger region, shown by the thin, red cursors. This is the area provided in the HFRR results. Discussion with SwRI lead to the hypothesis that this larger scar was more likely attributed to corrosion [33]. It was suggested that the football-shaped scar within the measured scar could possibly be the true scar, shown by the thick, green, horizontal cursors. If this hypothesis was correct, the measured scar would only be 0.375 mm average diameter. This result is a reasonable HFRR result and correlates more closely with the SLBOCLE result. Note, however, that there is no direct correlation between the tests and conditions such as those seen in the HFRR test of the

NM blend fuel are not typical. In fact, Mr. Westbrook had never seen a wear scar like this before, and he had been working in lubricity for many years.

With an estimation of typical fuel lubricity from the SLBOCLE and HFRR tests, a comparison could be made to JP-8. Values for the SLBOCLE and HFRR tests are available for JP-8, but vary widely. Reports provided by Mr. Westbrook and other sources showed SLBOCLE results of approximately 1800 grams and HFRR results near 0.700 mm for JP-8 [34]. These values appear typical in literature review, but can vary like the other properties of JP-8 due to how JP-8 is sourced and stored. Regardless of the true value for any lot of JP-8, it was clear that pure JP-8 would not provide sufficient lubricity and an additional lubricant was necessary.

By examining the commercially available hobby engine industry lubricants, a premix oil was identified that could potentially be compatible with JP-8. In the hobby industry, most fuel is bought premixed and ready for use; only a few lubricants are sold as stand-alone fluids. Of these available lubricants, the Klotz Synthetic Lubricant company lubricants have a good reputation and a wide product line. By contacting Klotz directly, it was confirmed that their “Original Techniplate” lubricant was compatible with kerosene-like fuels, such as JP-8. Original Techniplate is a synthetic-type premix lubricant.

The next step was to identify how much lubricant was necessary to add to the JP-8 mixture to ensure equivalent lubricity of the NM premixed fuel. A 20 volume percent (vol%) mixture (200 mL Original Techniplate, 800 mL JP-8) was selected because most NM blend fuels are advertised with an 18-20% lubricant mixture and no other information was available. This would provide at least one data point that could be built upon with future or qualitative testing. The result of the SLBOCLE test for JP-8 with 20 vol% oil was a load greater than 7,000 grams. The HFRR resulted in a major axis scar of 0.38 mm, a minor axis scar of 0.37 mm, and average scar of 0.38 mm. This means that the JP-8 with 20 vol% oil has approximately equivalent lubricity to a common 15% NM blend fuel.

4.2 Experimentation and Resulting Modifications for Conversion to JP-8

With NM blend fuel baseline testing complete, a solid understanding of the engine’s behavior, and a known JP-8 with lubricant mixture starting point, the JP-8 conversion process could be started. Multiple approaches were considered to identify the best way to convert the micro engine to JP-8. These approaches were at times accidental and theoretical, while other times they were based on

common engine operation. The final solution proved to be a combination of proven and theoretical approaches.

4.2.1 Cylinder Head Heating

The first and most logical step to the conversion was to confirm that a conversion was actually necessary. It seemed plausible that no major modifications would be necessary because of the tight clearances of the O.S. 70SZ-H, the fact that it provided an approximately 11:1 compression ratio, and that there was already a glow plug in the engine. To confirm this, the engine was fueled with JP-8 mixed with a 10 vol% oil mixture. Note that a 10 vol% mixture was used because the results of the lubricity testing were not available yet.

To test the engine, the fuel system was primed to eliminate air bubbles and the carburetor main jet was closed completely. Then, with the glow plug powered by 1.5 VDC, the engine was motored. The main jet was slowly opened to 1.5 turns open, but no ignition was observed. Calling on personal experience, a propane torch was used to heat the cylinder head to 80°C. Again, the main jet was closed completely and then re-opened 0.25 turns. With the engine motoring, there was some unsustainable ignition. The main jet was opened further to 0.5 turns and after a short time, the engine fired and ran. The torch was held on the head to help the engine maintain ignition and was removed after a short amount of time. In the stock configuration, the engine was capable of running on and producing power when fueled by JP-8.

Knowing that the stock configuration could run on JP-8 with additional cylinder head heat, experiments were conducted to identify any other attributes that aided in starting. One experiment was to motor the engine while the cylinder head was being heated with the propane torch. The cylinder head temperature (CHT) was documented when the engine was able to fire and maintain combustion. By varying the glow plugs, it was found that the larger filament spiral glow plug (the O.S. #10 plug) required the lowest cylinder head temperature to start (100°C). The 80°C head temperature was not repeatable. This could be explained because the larger filament spiral diameter results in more surface area on the filament, resulting in the ability to transfer more heat to the compressed charge in the cylinder. Based on this conclusion, the O.S. #10 plug was used for the remainder of the JP-8 conversion.

The cylinder head heating method proved to be a poor method for starting, however. First, it required a large amount of energy to get the head to this relatively high temperature. Second, care had to be taken to avoid heating the engine unevenly and causing the components to warp.

Third, it was relatively unsafe; even when using a 1200 W heat gun instead of the propane torch, the heat required could cause combustion of nearby fuel sources (fuel lines, rags, etc.). Finally, and most importantly, after completing a few cylinder head heating tests, pitting was observed in the cylinder head. This was likely caused by autoignition on the combustion chamber surface, which poses serve durability issues. Therefore, more robust starting solutions were sought out.

4.2.2 Ceramic-Coated Combustion Surfaces

Observing the difference cylinder head heating made suggested that finding a way to increase the temperature in the cylinder could dramatically help starting. There are three ways to increase the in-cylinder temperature. First, apply external heat, as in the cylinder head heating method. Second, increase the compression ratio to let the compression stroke add additional energy to the in-cylinder charge. Finally, reduce the heat transfer out of the cylinder by changing the thermal conductivities of the surfaces in contact with the combustion event.

The first concept solution that was explored was ceramic coatings for the combustion chamber and the piston dome. Ceramic coatings are used in high-performance engines such as drag racing cars and high-output snowmobiles. The theory is that the ceramic coating creates a layer of low thermal conductivity on lightweight components allowing them to be used in extreme output applications without (or, at least, with less) fear of engine failure. In the application of the JP-8-fueled micro engine, the hypothesis was that the coating decreases heat transfer out of the combustion volume and holds more energy in the in-cylinder charge. This would in turn act like a compression ratio increase without the disadvantage of needing additional motoring torque for the higher compression. Additionally, because the clearance volume of the O.S. 70SZ-H engine is so small (approximately 0.700 cc), the thickness of the ceramic coating (0.0015”, nominal) would cause an approximately 1 point increase in the compression ratio. For example, the stock 11:1 compression ratio would increase to 12:1. This small compression change would provide additional energy into the in-cylinder charge with minimal change to the amount of motoring torque necessary.

There are two major suppliers of ceramic-coated components for racing applications, and only Polymer Dynamics, Inc. (commonly PolyDyn) of Houston, Texas, was willing to work with the small components of the O.S. 70SZ-H. PolyDyn’s ceramic coating is an yttrium-zirconia ceramic impregnated in a resin that is painted onto components. This resin is approximately 0.0015” thick. The specific thermal conductivity was not available, according to the company’s owner, Carl Benton. He explained that some research had been done by a local university, but he was

unsure of the results [35]. Investigation did not identify any such research on PolyDyn coatings. However, PolyDyn's influence in the race world influenced the decision to try the ceramic coating. A stock cylinder head and piston were sent out for coating. The combustion chamber of the cylinder head was coated with specific instructions not to coat the sealing surface. The piston dome was also coated with the ceramic coating and a friction reducing, dry-film coating was also applied to the piston skirt.

The ceramic-coated components were reassembled into the engine and tested. Unfortunately, no dramatic results were obtained. At this point in the experimentation, the only benefit of the ceramic coating was a small, perceived improvement in starting time when heating the engine as had previously been done. This small improvement, while helpful, was not a sufficient modification to ensure robust starting on JP-8, so additional starting aides were explored.

4.2.3 External Charge Heating

The next starting method attempted was intake air heating. To do this, a 1200 W heat gun was placed over the intake tube while the engine was motored. The concept of intake air heating is to increase the starting temperature of the fuel-air charge before compression, which results in a much higher in-cylinder temperature at the end of the compression process. Alternately, intake air heating can act to heat the surfaces the fuel-air charge comes in contact with; this keeps fuel from condensing out of the charge as it hits surfaces colder than the charge. The results of the intake air heating experiments can be seen in Table 4-1.

Table 4-1: Results of preliminary intake air heating experiments

Hardware Configuration	Stock	Ceramic-coated Head/Piston	Stock
Approximate Intake Air Temperature	100°C	200°C	300°C
Motoring Time to Start	(No Ignition at 5 min)	3 min, 30 s	2 min, 30 s

Based on these simple and limited results, intake air heating did not seem to provide a robust starting solution. In addition to long start times and a significant power requirement, the intake air heating also proved destructive. The high temperatures in the intake tube melted the hot-wire anemometer's internals and also warped the nearby encoder disk.

The next logical step in attempting to improve starting time was to attempt fuel heating. While this method has the potential to be dangerous, it was explored anyway with the intention of

developing a controlled fuel heater if it was successful. The initial setup was simple. A brass hydraulic tee was placed in the fuel line. The fuel flowed in one side and out the other, while a thermocouple was placed in the remaining tee port to document the true fuel temperature. The fuel was heated as high as 100°C and the engine was motored, but this did not produce any conclusive results. The best observed starting time was over 3 minutes and 30 seconds with a 100°C fuel temperature, which is not only approaching a dangerous temperature, but is also an unimpressive starting result.

The reason behind this unimpressive result is not complicated. The mass of fuel moving into the engine is small in comparison to the amount of air entering the engine; therefore, the amount of additional energy moved into the cylinder is also small. Additionally, the fuel must come in contact with many cold surfaces before it enters the cylinder, so it is unlikely that the fuel will vaporize sufficiently even if it is heated to high temperatures. With this reasoning and the poor results of the fuel heating starting tests, the fuel heating method was abandoned.

4.2.4 Crank-to-Start Testing with Various Hardware Configurations

An interesting observation was made through these experiments, however. When the engine was motored for an extended period of time with JP-8 at a low throttle setting, it eventually fired and ran without external starting aides regardless of the engine hardware. This led to additional “crank-to-start” tests, where a 10% open throttle setting and approximately 0.5 turns out on the main jet was found to yield starting times less than 10 minutes. Additionally, at this time the lubricity testing had been completed, but the 20 vol% oil mixture created longer start times. To compromise between lubricity and starting time, the oil-to-fuel ratio was reduced to 13 vol% (the actual mixing ratio is 15 parts oil to 100 parts fuel, which could be called a 15% fuel-oil mixture. This nomenclature was deemed incorrect later, but the 13 vol% ratio was retained for the remainder of the JP-8 testing).

With this realization, the charge heating tests were paused and experimentation began on engine component configurations. The intention of the crank-to-start testing was to determine which engine component configuration would provide the best base for starting with the intention of adding charge heating aides after identifying this configuration. A number of engine component configurations were iterated through using the crank-to-start tests as feedback on the component design. In total, five cylinder heads were tested with a ceramic-coated piston and three of those cylinder heads were tested without the ceramic-coated piston. The final two heads were only tested with the ceramic piston as it consistently showed an improvement in the starting times.

These cylinder heads and their design intent are explained below. Note that the volume used to calculate the compression ratio was the volume of the cylinder with all of the ports closed, which was 7.42 cc.

- 10.4:1 original aluminum head – The original custom head was designed to have a compression ratio of 11:1. Despite good machining tolerances, the final compression ratio was measured as 10.4:1. This cylinder head was tested to act as the baseline for the other cylinder heads.
- 11.8:1 ceramic-coated stock head – The ceramic-coated head was the stock cylinder head that was first sent to PolyDyn for coating. The addition of the ceramic coating was intended to decrease the thermal conductivity of the combustion chamber and therefore keeping the heat energy in the cylinder.
- 13.4:1 aluminum head – This head was designed to have a compression ratio of 14:1, but machining tolerances reduced that ratio to 13.4:1. This head was used to identify the effects of a compression ratio increase without the addition of the ceramic coating. Note that this value was chosen arbitrarily to balance between increased in-cylinder energy and minimized motoring torque.
- 11.1:1 steel head – A low-carbon steel head was made to identify the effects of decreased thermal conductivity without the use of ceramic coating. It was made from 1020 steel and was designed to be 12:1, but again machining tolerances placed the compression ratio lower.
- 11.5:1 aluminum head with ceramic coating – The final head made was an 11.5:1 head made of 6061 aluminum. The designed compression ratio was 11:1, with the expectation of the ceramic coating increasing this to 12:1. However, only an 11.5:1 compression ratio was realized. (This head design was determined to be the best option through crank-to-start iteration.)

There were three temperature measurements on the engine that were monitored for the crank-to-start tests; the cylinder head temperature, the engine case temperature, and the exhaust temperature. The cylinder head temperature thermocouple was located on the same plane as the glow plug sealing surface, approximately 0.38” from the cylinder bore centerline in the cylinder head. The engine case temperature was recorded by a thermocouple epoxied in direct contact with the surface of the front engine case. Note that this part of the case is the surface that the fuel-air charge comes in direct contact with before entering the intake ports. The exhaust

temperature was recorded by an ungrounded, sheathed thermocouple in the entrance of the muffler. It was placed in the center of the exhaust gas flow.

The crank-to-start tests were simple. First, the engine was cooled to ambient temperatures using a fan and allowed to sit at the ambient temperature until the fan could be shut off and the temperatures did not rise. This was used to confirm that the internal engine components had also returned to ambient temperature. Next, the #10 glow plug was powered using 1.5 VDC supplied by an external power supply (this usually produced a current of approximately 3.9 A). The engine was immediately motored with a fuel supply of JP-8 with 13 vol% oil. A stopwatch was started and the engine temperatures were monitored. On the first instance of sustained ignition, the stop watch was stopped and the cylinder head, engine case, and exhaust gas temperatures were recorded. Then, the fuel supply was removed from the carburetor and the engine was allowed to consume any remaining fuel in the crankcase until it stalled. The glow plug was shut off and the process was repeated.

The crank-to-start test was completed at least three times for each hardware configuration. Additionally, the throttle, carburetor, and motoring speed were held constant for all tests. The throttle was held 10% open. The carburetor was set with the main jet 0.56 turns open, the mid jet 0.50 turns open, and the idle screw in the stock position. The motoring speed was held at 4,000 RPM +/- 80 RPM. Finally, for all tests but the 11.5:1 ceramic-coated aluminum head, the same source of JP-8 and Klotz lubricant was used. The results of this testing can be seen in Table 4-2. Note that one case of the 10.4:1 cylinder head with the ceramic piston did not result in ignition after 20 minutes of cranking. Due to this long test time, it was not repeated. Also, note that the starting times are ranked by color conditioning with red being the longest and white being the shortest. One final note is that these temperatures were recorded manually, so their accuracy is at best +/- 2°C.

Table 4-2: Results of crank-to-start tests with multiple hardware configurations

Cylinder Head	Piston	Cranking Time to First Ignition Event (s)	Cylinder Head Temperature at Ignition (°C)	Engine Case Temperature at Ignition (°C)	Exhaust Gas Temperature at Ignition (°C)
10.4:1 Aluminum Head	Stock	908	78	52	56
		839	78	51	54
		824	78	51	54
10.4:1 Aluminum Head	Ceramic-coated	922	78	52	54
		751	75	50	50
		-	-	-	-
11.8:1 Ceramic-coated Stock Head	Stock	720	80	51	56
		577	77	48	52
		590	78	49	53
11.8:1 Ceramic-coated Stock Head	Ceramic-coated	742	80	51	52
		527	73	47	50
		448	72	46	47
		768	80	52	56
13.4:1 Aluminum Head	Stock	642	84	48	55
		615	83	49	55
		505	79	47	60
13.4:1 Aluminum Head	Ceramic-coated	414	76	47	52
		489	79	48	53
		499	79	48	52
11:1 Steel Head	Ceramic-coated	597	76	48	49
		724	79	50	53
		565	75	48	50
11.5:1 Ceramic-coated Aluminum Head	Ceramic-coated	260	60	36	38
		376	66	39	51
		264	61	37	39
		223	59	36	37

The starting time achieved by any of these results would not be an acceptable starting time for an engine. However, it does provide insight into which configuration provided the best capability for starting. A few key observations were made about the hardware configurations:

1. First, the ceramic-coated piston always improved starting times. This was realized early on and the 11:1 steel head and the 11.5:1 ceramic-coated aluminum head were not tested without the ceramic piston.
2. The stock head produced very long starting times, which is why it was iterated upon.

3. The ceramic-coated stock head with the ceramic piston produced better starting results, but it also had high variability.
4. The 13.4:1 aluminum head produced good results. However, based on some initial observation, it seemed like once the engine was running there were combustion issues. With this head, the engine frequency stalled under load. This suggested that combustion was occurring too soon in the cycle, causing the piston to be stopped before it reached the top of its stroke. No further operating data was collected for fear of catastrophic failure.
5. The 11:1 steel head produced similar results as the 11.8:1 ceramic-coated stock head. This could have been a valid option to pursue, but the aluminum heads were easier to machine, did not rust, and the ceramic coating was easily applied for low cost (about $15 per piece).

Before the testing on the 11.5:1 ceramic-coated cylinder head was commenced, an interesting observation was made. All three of the temperature measurements were consistent throughout the crank-to-start testing, regardless of the hardware configuration. Table 4-3 shows the average, median and standard deviation of the temperatures for all of the tests except the 11.5:1 test.

Table 4-3: Average, median and standard deviation of temperatures for crank-to-start tests (does not include 11.5:1 aluminum head tests)

	Cylinder Head Temperature at Ignition (°C)	Engine Case Temperature at Ignition (°C)	Exhaust Gas Temperature at Ignition (°C)
Average	78.0	49.2	53.0
Median	78.0	49.0	53.0
Standard Deviation	2.8	1.8	2.8

Statistically speaking, the close average and median suggest that the temperature distribution between tests is a normal distribution. Additionally, the low standard deviation suggests a narrow distribution of temperatures. These observations led to the conclusion that the ignition process is not dominated by any resulting behaviors of the engine hardware, but rather by another source.

The engine case temperature was particularly interesting. The case temperature is not directly affected by the head or piston choice and does not vary as much as the exhaust gas temperature. Additionally, the standard deviation of the engine case temperature approaches the

scale of error expected simply from thermocouple accuracy. This suggested that this temperature was a dominant controller of the ignition behavior. Through some basic comparison research, this temperature was believed to correspond closely to the sort of temperature expected for the flash point of JP-8. The flash point is the temperature at which a sample of fuel in atmospheric pressure will form a combustible mixture and is normally used to determine safety considerations in fuel shipment and storage. The flash point of JP-8 is set by the MIL-DTL-83133G standard as a minimum of 38°C. This is 11°C lower than the case temperature. However, the batch of JP-8 being used for testing had been sitting in a 5-gallon can for about 3 months and came from an unknown reserve. The volatility of JP-8 is known to decrease as it ages because of its oxidation when exposed to air. This suggested that the flash point of the JP-8 used in this testing may have been higher than the specified minimum due to long-term storage.

The reason the 11.5:1 head tests were not included in the statistical analysis is that a different batch of JP-8 was used for these tests. This batch of JP-8 came from a supplier to the US Army through the Keweenaw Research Center and was sealed on arrival and mixed fresh for the 11.5:1 head tests. The results of the 11.5:1 ceramic-coated head test are significantly better than any of the other tests, which is surprising as the 11.5:1 head should behave similarly to the 11.8:1 ceramic-coated stock head. The only difference was the change to the fresh JP-8. Note also that the case temperature average was 37°C for the 11.5:1 head crank-to-start tests, which is within measurement error of the 38°C minimum for JP-8 flash point.

This observation led to the major hypothesis behind the JP-8 conversion: improving crankcase charge preparation through crankcase heating. Heating the engine surfaces, specifically the engine case where fuel-air mixing occurs, to a temperature approaching the flash point of JP-8 should theoretically allow a combustible mixture to form in the crankcase. This mixture would then cause more rapid ignition during motoring. This hypothesis was confirmed early on using the 1200 W heat gun to heat the engine case. By heating the entire engine case instead of just the cylinder head, preliminary tests showed the ability to start the engine in less than 60 seconds instead of up to 900 seconds with the worst engine configurations. A new goal of being able to heat the crankcase to approximately 50°C was set to take advantage of this effect.

In addition to developing this hypothesis, the crank-to-start testing illustrated that the best hardware configuration for the JP-8 conversion was the 11.5:1 ceramic-coated aluminum head with the ceramic-coated piston. This configuration provided the best starting times considering machining effort and overall robustness.

4.2.5 Crankcase Heating

The first approach to crankcase heating was to apply a small heater to the engine case in the same location the engine case temperature was recorded. The first heater identified was a model K05711980-M made by the Watlow® Electric Manufacturing Company. This model had a small electric grid layered in a flexible polyimide substrate that was approximately 0.007" thick. It also came with a pressure sensitive adhesive and had an outside diameter of 1" with a maximum output of 5 W [36]. These dimensions and properties should have made the Watlow heater a perfect option for crankcase heating as it required no modifications to the engine and would fit neatly against the surface of the engine case. Figure 4-2 shows a picture of the 1" diameter Watlow heater installed on the front engine case. Note that this part of the case is removable and is shown while being held in a vise. The top of the case in the picture is the location of the start of the front intake port. The location where the Watlow heater is corresponds to the surface opposite the crankshaft and connecting rod.

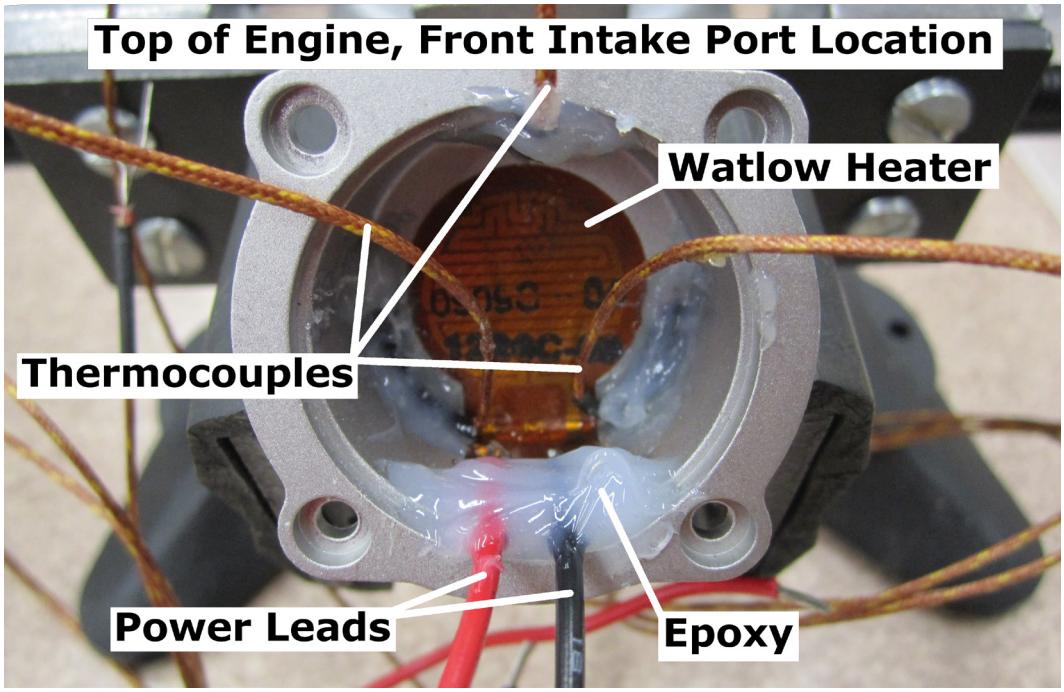

Figure 4-2: Front engine case instrumented with Watlow polyimide heater (shown in bench-top vise)

The instrumented engine case was then reinstalled and the Watlow heater was powered with its maximum voltage of 12 VDC. The expectation was that this heater would create a surface in

excess of 50°C where the fuel-air charge enters the crankcase. However, the heat transfer out of the case was not taken into account and ultimately the Watlow heater could not raise the engine case temperature above 30°C in ambient conditions. A more powerful solution was necessary to achieve the desired 50°C case temperature.

The next most economical solution was to purchase a commercial diesel glow plug, make an adapter, and install this adapter so it was in contact with the same surface as the Watlow heater. A Bosch 80010 Duratherm® glow plug was purchased and a simple aluminum adapter was made that used the bolt pattern of the front engine case. Omega brand OMEGATHERM® thermal contact paste was applied to the adapter and it was bolted into place. Figure 4-3 shows this setup on the engine while on the micro engine test stand.

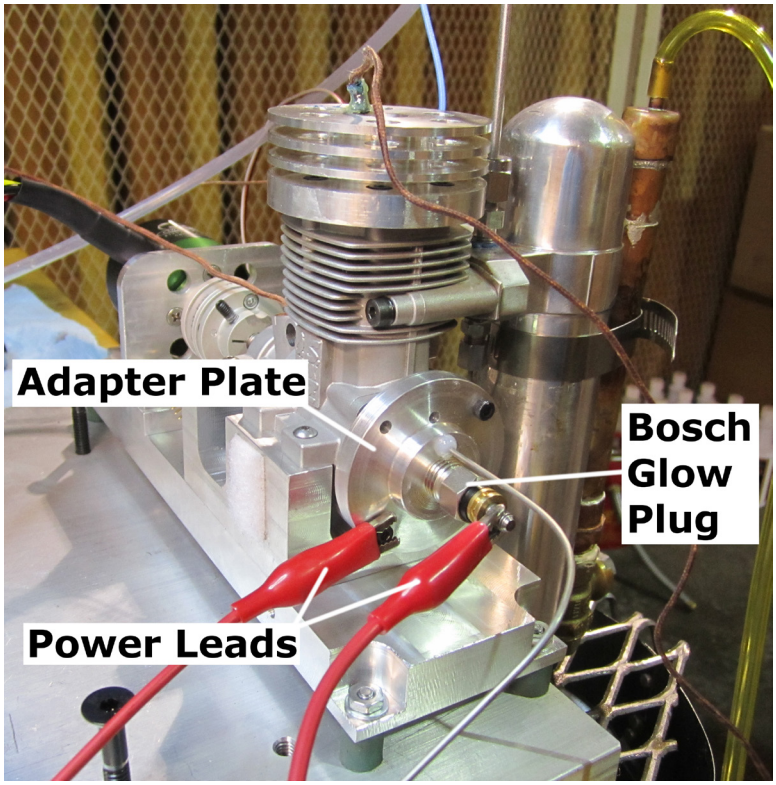

Figure 4-3: Bosch glow plug adapter plate installed on engine fixed to the test stand

Testing with this adapter did not yield acceptable results, however. Three observations were made that led this approach to be abandoned. First, even though the temperature at the engine case could exceed 120°C, the starting times could not be reduced below 90 seconds, which was almost double the time expected from the heat gun crankcase heating tests. Second, the method

for mounting the adaptor was not well designed and led to the case pushing in and making contact with the rotating crankshaft and connecting rod. This contact was minor and not noticeable until after the components were disassembled. Finally, the high temperatures necessary to achieve the best possible starting time were leading to the fuel burning inside of the crankcase. Figure 4-4 shows the front engine case removed from the engine. Note the black soot around the center of the engine case. Note, also, the circular wear marks from the connecting rod and crankshaft interfering with the engine case.

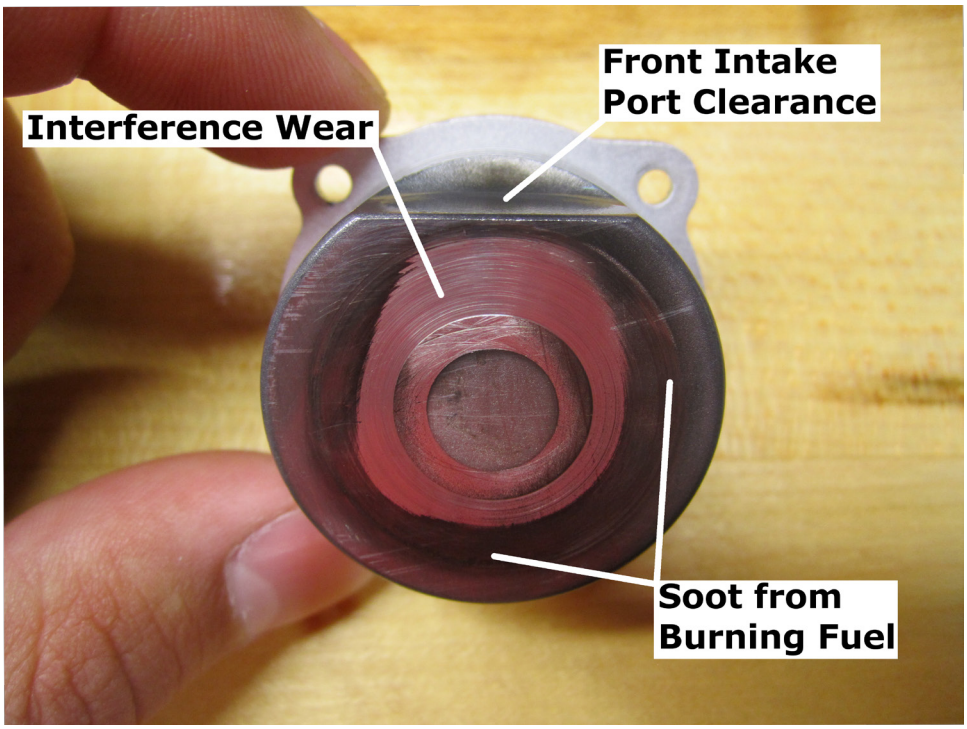

Figure 4-4: Internal side of front engine case after Bosch glow plug adapter testing

Primarily because of the fuel burning in the crankcase, this approach was abandoned.

At this point in the experimentation, it seemed that a localized heat source on the front engine case was not an acceptable solution. More widespread heating seemed necessary; this thought seemed logical based on the hypothesis that fuel coming into contact with a cold surface would not be able to form a combustible mixture. Although the Bosch glow plug adapter created a very high surface temperature, any fuel that vaporized would come in contact with the cold surfaces surrounding that hot surface and would likely re-condense into liquid.

In order to create more widespread heating, the polyimide heater concept was re-explored. Birk Manufacturing, Inc. was identified as another manufacturer of polyimide heaters. Birk's selection of heaters came in more sizes and resistances than Watlow's selection allowing for a more tuned approach to heating the engine crankcase. They were also thin, flexible, and provided with a pressure sensitive adhesive. From Birk's catalog, three heaters were selected. These heaters, their resistances and their intended location can be seen in Table 4-4.

Table 4-4: Selected Birk polyimide heater sizes, resistances and locations [37]

Heater Model Number	Size (in)	Resistance (Ω)	Intended Location
BK-3503-7.2-L12-01	1.0x0.5	7.2	Bottom of Crankcase
BK-3543-7.9-L12-01	0.25x0.5	7.9	Outside of crankcase, over intake ports
BK-3546-6.6-L12-01	0.5x0.5	6.6	Outside of crankcase, over intake ports

The 3503 model heater was chosen so that three of these heaters could be placed on the bottom of the crankcase, centered along the center plane of the cylinder bore. Figure 4-5 shows the engine being instrumented with these heaters (engine shown upside down in vise).

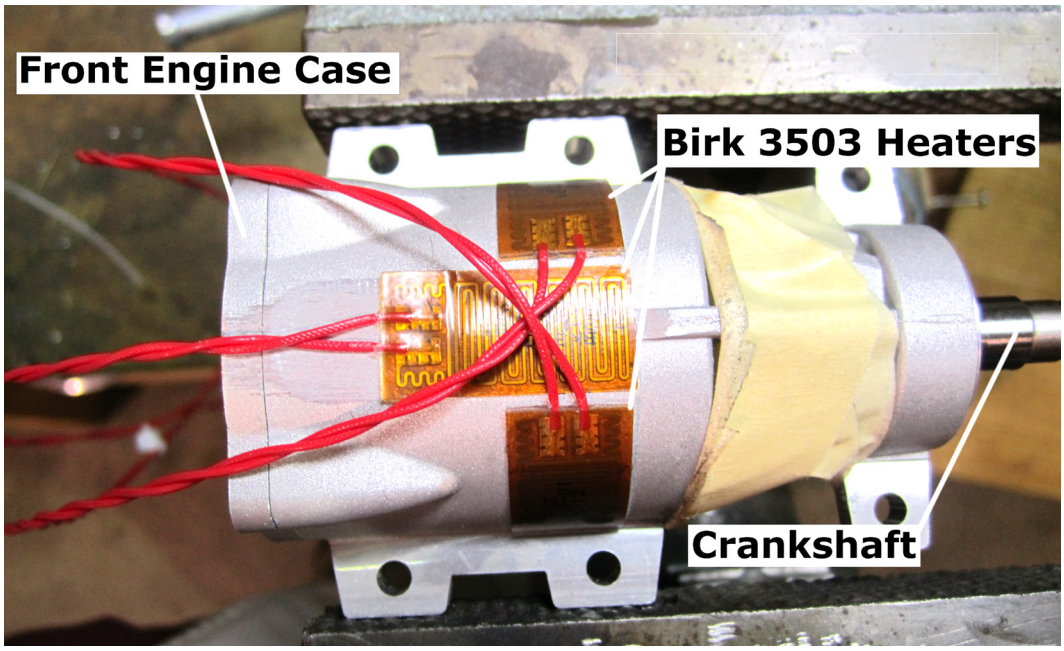

Figure 4-5: Birk 3503 heater installation on engine crankcase

The 3543 and 3546 model heaters were installed over the intake ports on the outside of the engine case. However, these heaters were selected with too low of a resistance which caused an excessive power density over the area of the heater given the constant voltage source available. This caused these smaller heaters to melt their polyimide substrates and short to the engine case, rendering them useless. Additionally, tests done with these additional intake port heaters did not yield appreciably better results compared to the three 3503 heaters while they were still functional. Note that further testing could be explored in the future with heaters that have the proper power densities for the given power source, but the installation and application of the 3543 and 3546 heaters will not be discussed here any further.

The connection and method to power the Birk model 3503 heaters was decided based on heater durability and the available power source. First, the heaters were configured to run as three resistances in parallel to provide the maximum power to the engine given the fixed power source of the 12 VDC marine-grade battery powering the rest of the micro engine test stand. Birk recommends, however, that the temperature of the polyimide heaters not exceed 160°C for longer than 4 hours as it leads to a failure of the pressure sensitive adhesive. In order to comply with this recommendation, the power provided to the heaters was pulsed 0.5 seconds on and 0.25 seconds off. This pattern was decided somewhat arbitrarily as it was not possible to document the temperature under the polyimide heaters with the available thermocouple hardware. Long-term usage of this method did not show any degradation to the polyimide substrate or the pressure sensitive adhesive.

In order to test the effectiveness of the crankcase heating method, the crank-to-start testing was modified and applied to the engine with the Birk heaters. The engine was first cooled to ambient conditions. Then, the three Birk 3503 heaters were powered for 30 minutes with the 0.5 seconds on/0.25 seconds off pulse. The O.S. #10 glow plug was also powered for 30 minutes. This “thermal soak time” was decided upon through experimentation and was essential to fast starting times. After 30 minutes had elapsed, the engine was motored while the crankcase heaters remained powered. The time and temperatures at the first sustained ignition event were documented. Once the engine was running, the fuel supply was removed and the engine was allowed to burn the fuel remaining in the crankcase. The results of these crankcase heating, crank-to-start tests can be seen in Table 4-5.

Table 4-5: Final starting tests with (3) Birk 3503 heaters at 23°C and 973 mbar ambient conditions

Attempt Number	Cranking Time to First Ignition Event (s)	Cylinder Head Temperature at Ignition (°C)	Engine Case Temperature at Ignition (°C)	Exhaust Gas Temperature at Ignition (°C)
1	29	54	52	40
2	34	55	55	40
3	33	53	53	41
4	38	54	53	41
Average	**33.5**	**54**	**53.25**	**40.5**

While no written objective for a starting time for the JP-8-fueled demonstration engine, this starting time was deemed acceptable. With the three Birk heaters, this objective appears to be met.

Note that Table 4-5 shows that while the cylinder head and engine case temperatures were elevated above the estimated flash point of the fuel, the exhaust gas temperature was nearly equal to the estimated flash point temperature. Since exhaust temperature was a good indicator of the fuel-air mixture temperature, this temperature should be documented and used to predict when the JP-8-fueled engine will start for future testing with crankcase heating.

The power requirement of the three 3503 Birk heaters were somewhat high. With a measured resistance of 8.1 ohms per heater and an equivalent resistance of 2.7 ohms, the three Birk heaters drew approximately 4.6 A from a 12.4 V source. This meant that there was a power requirement of 57 W with a duty cycle of 67%. For the 30 minutes required to thermally soak the engine, this meant 68,400 J of electrical energy were need to heat the engine. To put this in perspective, this is approximately twice the energy found in a 2600 mA-hr, 3.7 VDC cell phone battery.

The use of polyimide heaters was chosen as a final starting solution. However, this is likely not the best solution for providing crankcase heat. Additional heaters around the engine, insulation around the heaters to channel more energy into the crankcase, or even a heated water jacket around the crankcase would likely provide more efficient methods of transferring energy to the crankcase. However, this was outside the scope of this thesis, and, therefore, the polyimide heaters proved an acceptable solution.

Two final notes on the JP-8 conversion hardware concern the O.S. #10 glow plug: First, when the #10 glow plug was identified as the best glow plug for starting, a brief durability study was completed. The concern with constantly powering the O.S. #10 glow plug was that there may be a possibility that leaving the plug powered for an extended period of time would result in the plug electrically shorting to ground. To test this, variable DC voltage power supply was attached to the glow plug and it was powered; initial testing showed that the glow plug could be powered for at least 30 minutes at 2.2 VDC. Subsequent experimentation confirmed that the #10 glow plug was a robust solution when powered by its nominal 1.5 VDC voltage; no glow plugs were shorted out in any of the JP-8 testing. Second, the O.S. #10 glow plug is that it had to remain powered after the engine was started for low-load conditions. This is contrary to the NM-fueled micro engine where the glow plug is self-sustaining. When under the 250 W load, however, the glow plug power could be removed when the engine was fueled by JP-8. There was notable degradation in the combustion quality when the micro engine was fueled by JP-8 and the glow plug was removed, but for the purpose of comparison to the NM-fueled engine, the glow plug was not powered for any subsequent 250 W steady-state testing.

To reiterate, the final JP-8 conversion hardware consisted of a ceramic-coated cylinder head with an 11.5:1 compression ratio, a ceramic-coated piston with a friction reducing coating on the skirt, and three 1.0” x 0.5” polyimide heaters providing 57 W of electric power during starting. The starting process involved powering the heaters with a 0.5 second on/0.25 second off pulse from a 12.4 VDC source and powering the glow plug with 1.5 VDC for 30 minutes. The polyimide heaters were shut off once the engine was started, but the glow plug had to remain powered until the full 250 W of load were applied.

4.3 Steady-State Testing of the JP-8-fueled Engine

With the final starting method and engine hardware configuration selected, steady-state data could be collected for the JP-8-fueled micro engine. The methods used for the NM-fueled testing were used for the JP-8-fueled testing, but a few additional considerations were also made specific to the JP-8-fueled engine. These included some thermal management considerations and operating speed considerations that needed to be made due to the change in fuel.

The first major change noted as steady-state testing began was the need for additional cooling air flow. JP-8 has a significantly lower latent heat of vaporization than NM blend fuels and a significantly higher air-to-fuel mass ratio, meaning that it cannot remove as much energy from the engine surfaces as it flows through the engine. This explains why the fan setting of 8.0 m/s using

the NM-fueled engine testing could not sufficiently maintain a 140°C cylinder head temperature with any tested carburetor setting when fueled by JP-8. After internal discussion, it was decided that increasing the fan to its maximum speed was an acceptable solution for this demonstration project. For the remainder of the testing, the fan speed was increased to 17.5 m/s. This was the maximum speed of the cooling fan, and equates to approximately 150 L/s volumetric air flow rate.

The next change to be addressed for JP-8 testing was the engine operating speeds. For reasons that are not clear, the JP-8-fueled engine did not sound audibly safe to run at 10,000 RPM. The engine sounded strained and on the verge of damage. Not wanting to damage the engine in the final stages of the project, this operating point was abandoned. Additionally, this operating point was not necessary because further testing revealed that the JP-8-fueled micro engine could produce 250 W of electrical power as low as 7,000 RPM, which was not possible with the NM-fueled engine. Therefore, the selected operating speeds for the JP-8-fueled engine were chosen as 9,000, 8,000, and 7,000 RPM.

With a new fan speed of 17.5 m/s, the carburetor was tuned using the same method as the NM-fueled engine tuning. The engine was run to the highest operating speed (9,000 RPM) and the power increased to 250 W. The carburetor was then tuned to achieve a cylinder head temperature of approximately 140°C. Note that the same thermocouple location was used for the JP-8 and NM-fueled engine testing. Ultimately, a main jet position of 0.47 turns open (1 “click” less than 0.5 turns), a mid-speed jet position of 0.5 turns, and the stock idle position were chosen as the optimal carburetor settings.

Again, the same methods used for testing for the NM-fueled engine were used for the JP-8-fueled engine. See Section 3.3 for the 10 step process of engine testing.

Data from the JP-8-fueled engine steady-state testing is presented here for documentation purposes. The analysis is brief as it is expanded on Section 4.4.

The first data examined from the three runs for each of the three speed-load points was the engine speed. The engine speeds can be seen in Figure 4-6. All of the speeds agreed reasonably, so the data analysis was continued. Note that all three runs are shown with an average value and an error bar showing twice the standard deviation of the three measurement runs for that speed-load point.

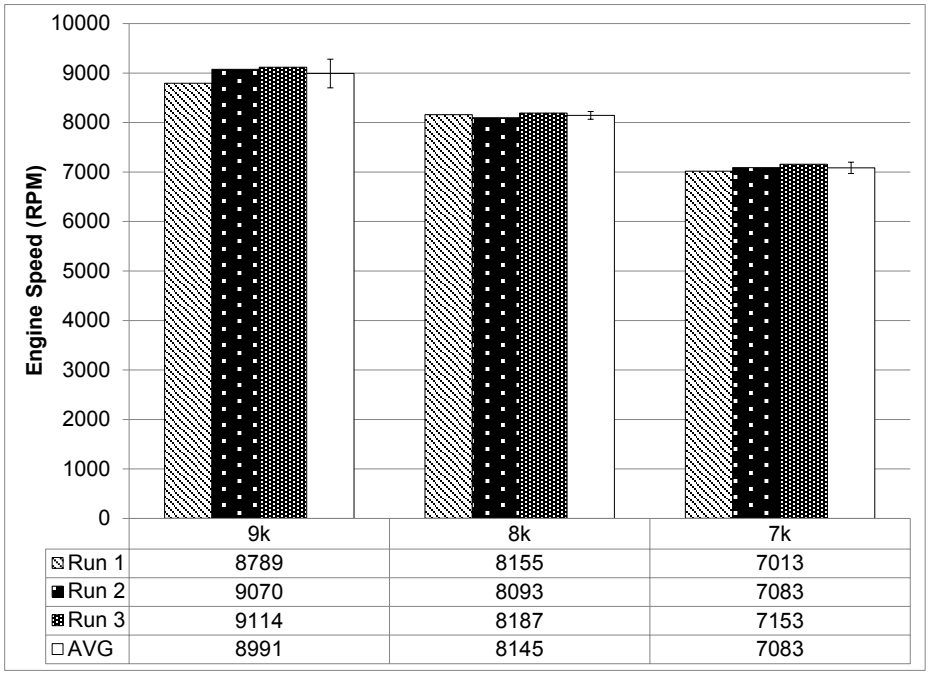

	9k	8k	7k
Run 1	8789	8155	7013
Run 2	9070	8093	7083
Run 3	9114	8187	7153
AVG	8991	8145	7083

Figure 4-6: JP-8-fueled engine speed comparison

Next, the exhaust gas and cylinder head temperatures were examined to ensure the tests were stable and consistent. Figure 4-7 shows the exhaust gas temperature while Figure 4-8 shows the cylinder head temperature. Both of these measurements showed good stability for the three runs at each speed-load point. Note the considerable higher exhaust temperature and the more consistent head temperature compared to the NM-fueled engine tests, seen in Figure 3-12 and Figure 3-13, respectively.

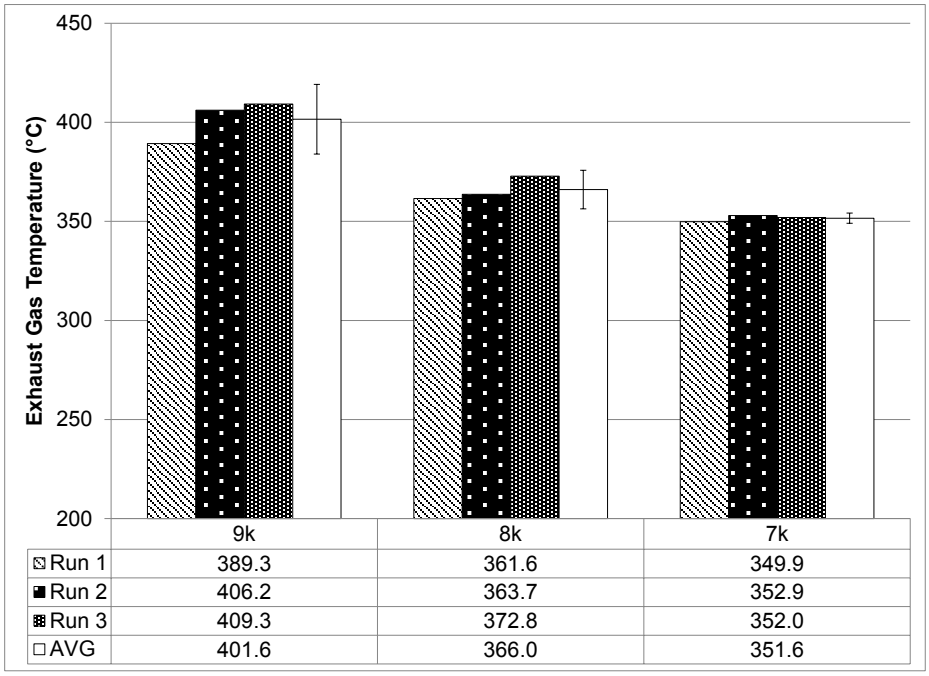

	9k	8k	7k
Run 1	389.3	361.6	349.9
Run 2	406.2	363.7	352.9
Run 3	409.3	372.8	352.0
AVG	401.6	366.0	351.6

Figure 4-7: JP-8-fueled engine exhaust gas temperature comparison

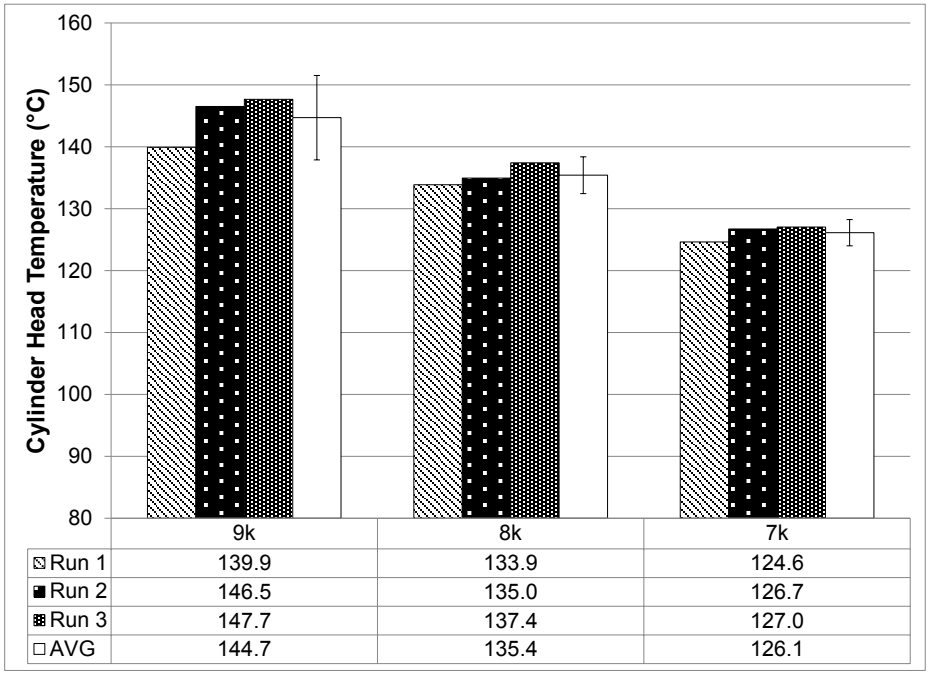

	9k	8k	7k
Run 1	139.9	133.9	124.6
Run 2	146.5	135.0	126.7
Run 3	147.7	137.4	127.0
AVG	144.7	135.4	126.1

Figure 4-8: JP-8-fueled engine cylinder head temperature comparison

The next and most interesting data examined was the fuel flow rate and the air-to-fuel mass ratio (AFR). The fuel flow rates can be seen in Figure 4-9. JP-8 is a more energy dense fuel than the NM blend fuel, so a drop in fuel flow rate was expected. Additionally, this drop in fuel flow rate should be expected because of JP-8's higher stoichiometric AFR.

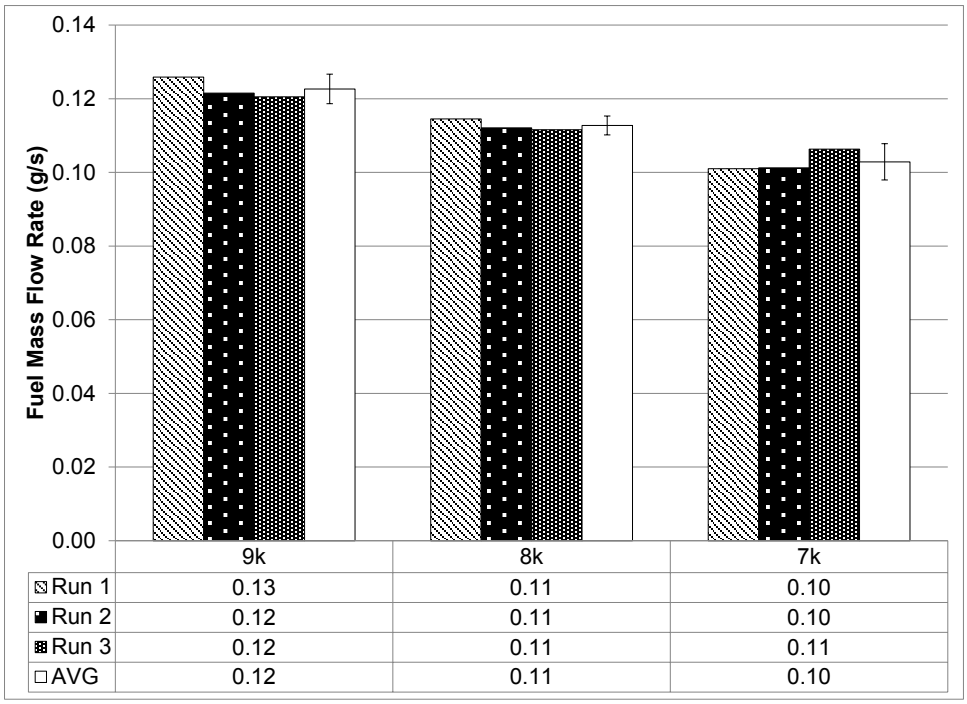

	9k	8k	7k
Run 1	0.13	0.11	0.10
Run 2	0.12	0.11	0.10
Run 3	0.12	0.11	0.11
AVG	0.12	0.11	0.10

Figure 4-9: JP-8-fueled engine fuel mass flow rate comparison

The AFRs provide additional insight into the use of fuel in the engine. Figure 4-10 shows the AFRs for the different engine speed-load points. First, notice that the AFR is significantly higher than the stoichiometric AFR of 14.8. This fuel lean condition was expected due to the narrow window of flammability of JP-8 in comparison to NM blend fuel. NM-fueled engines can run excessively fuel rich because the fuel is highly volatile and oxygenated. JP-8, being kerosene based, cannot run excessively rich because it has low volatility. Another interesting observation is that the AFR for the 8,000 and 7,000 RPM points is nearly identical, yet the 8,000 RPM point has a slightly higher fuel flow rate. Qualitatively, the 8,000 RPM point was similar to the 9,000 RPM point with the NM-fueled engine in that it did not give the feeling of a robust operating point. This higher fuel flow rate with lower AFR could suggest poor gas exchange.

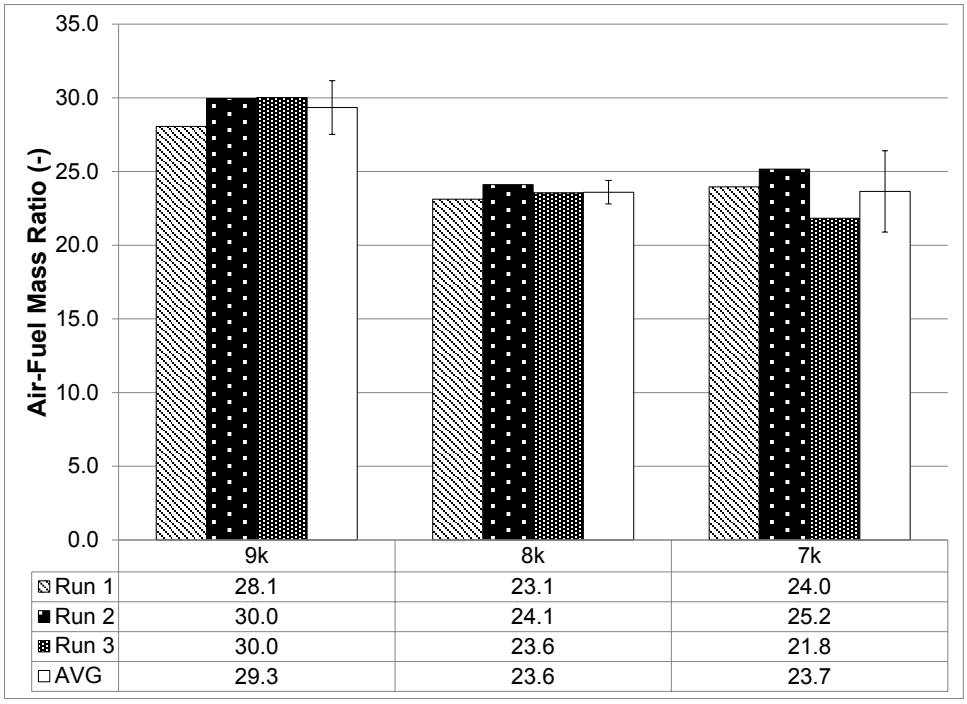

	9k	8k	7k
Run 1	28.1	23.1	24.0
Run 2	30.0	24.1	25.2
Run 3	30.0	23.6	21.8
AVG	29.3	23.6	23.7

Figure 4-10: JP-8-fueled engine air-to-fuel mass ratio comparison

Next, the combustion analysis data could be evaluated. The IMEP was the first calculation to be examined. The IMEP values, seen in Figure 4-11, showed significant variability from run to run and between the speed load points. The values for the COV, shown in Figure 4-12, reflected this high variability. The COV values for the JP-8-fueled micro engine were also quite high and no specific operating point showed drastically reduced COV. This variability and high COV is due to high rates of misfire in the JP-8-fueled engine.

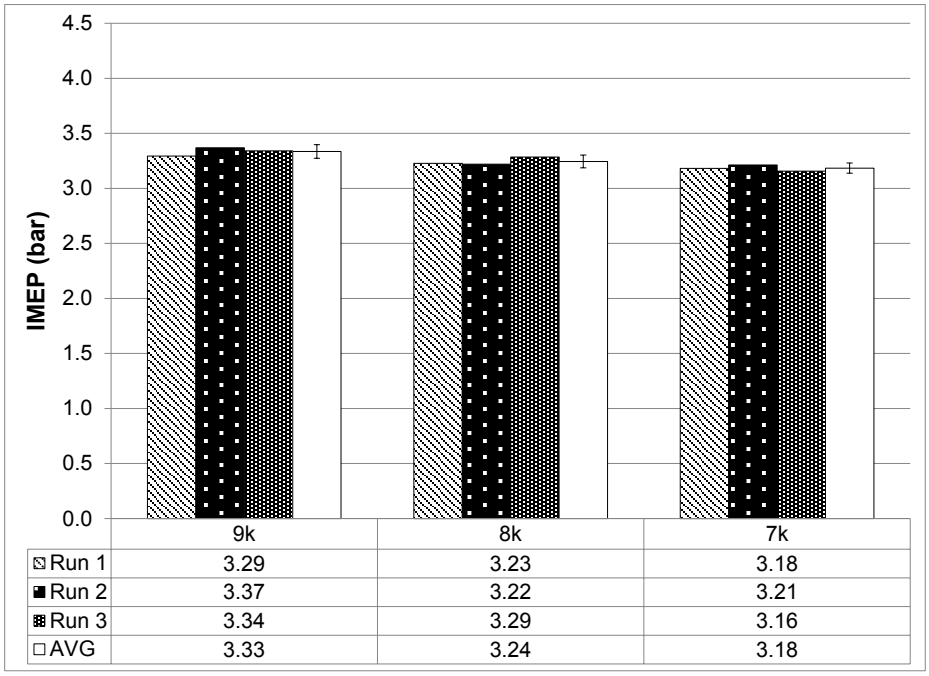

	9k	8k	7k
Run 1	3.29	3.23	3.18
Run 2	3.37	3.22	3.21
Run 3	3.34	3.29	3.16
AVG	3.33	3.24	3.18

Figure 4-11: JP-8-fueled engine indicated mean effective pressure comparison

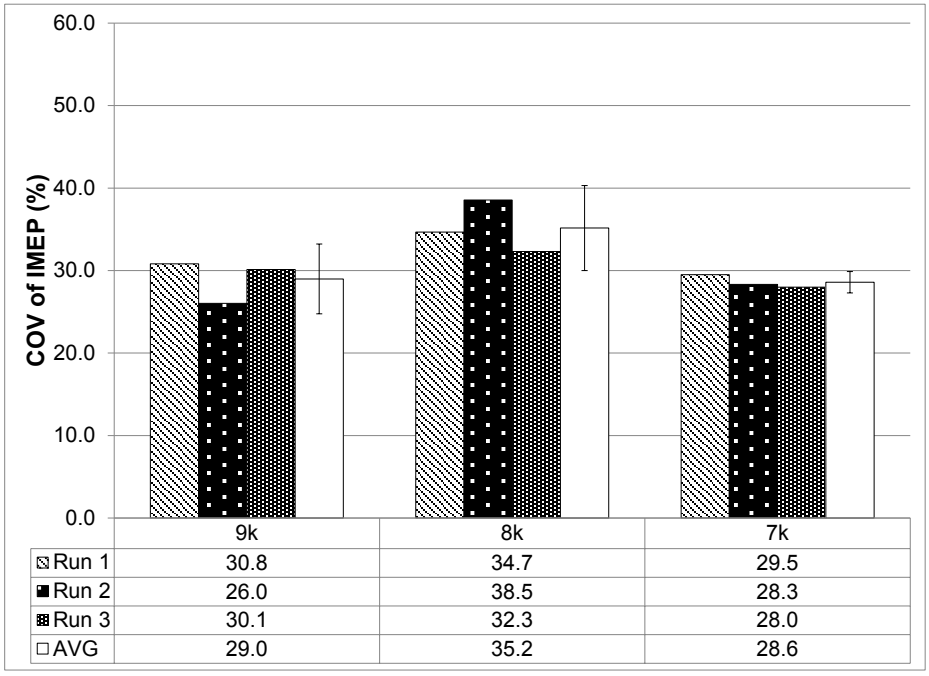

	9k	8k	7k
Run 1	30.8	34.7	29.5
Run 2	26.0	38.5	28.3
Run 3	30.1	32.3	28.0
AVG	29.0	35.2	28.6

Figure 4-12: JP-8-fueled engine coefficient of variation of IMEP comparison

The final data compared was the 50% MFB and D10-90% burn duration; these calculations can be seen in Figure 4-13 and Figure 4-14, respectively. The location of the 50% MFB is extremely late in the cycle, suggesting poor mixing and low efficiency. In a gasoline SI engine, the 50% MFB location is located approximately 7 CAD ATDC, but all of the JP-8-fueled engines values are in excess of 24 CAD ATDC. The D10-90% burn duration is also long and shows combustion happens through most of the expansion stroke. This is an inefficient form of combustion and is likely due to poor fuel vaporization or potentially poor fuel-air charge mixing.

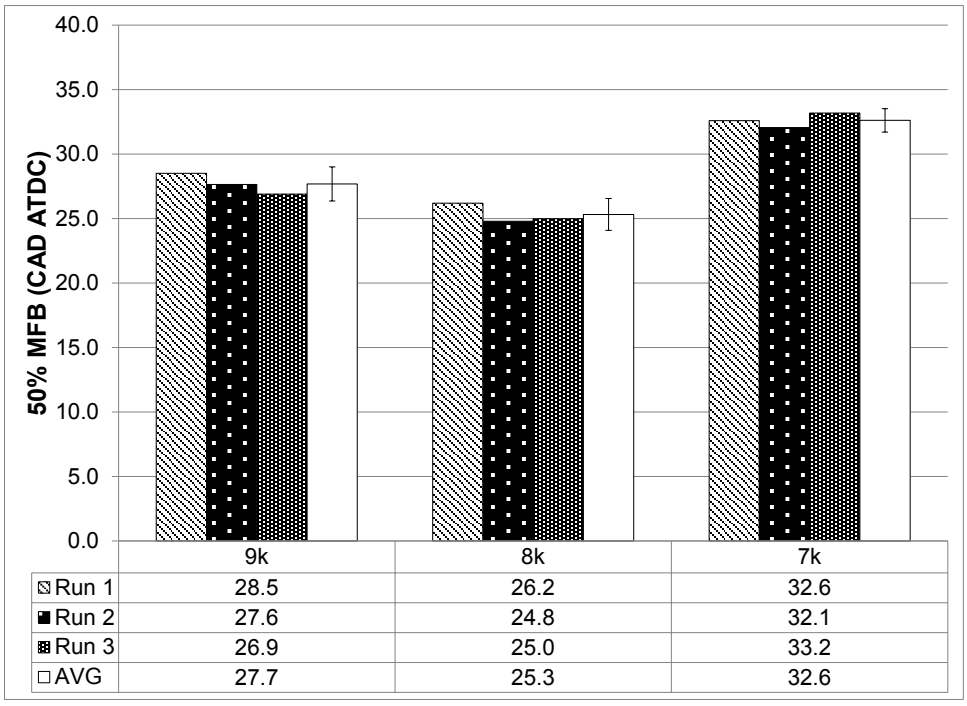

	9k	8k	7k
Run 1	28.5	26.2	32.6
Run 2	27.6	24.8	32.1
Run 3	26.9	25.0	33.2
AVG	27.7	25.3	32.6

Figure 4-13: JP-8-fueled engine 50% mass fraction burned location comparison

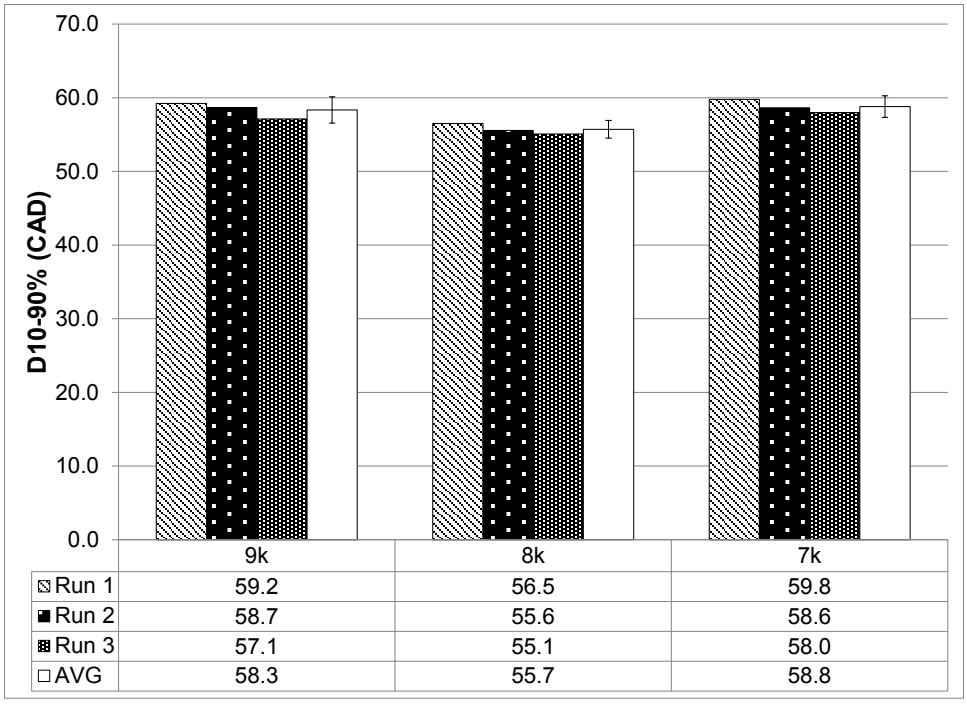

	9k	8k	7k
Run 1	59.2	56.5	59.8
Run 2	58.7	55.6	58.6
Run 3	57.1	55.1	58.0
AVG	58.3	55.7	58.8

Figure 4-14: JP-8-fueled engine 10-90% fuel mass burn duration comparison

A general analysis of the behavior of the JP-8-fueled micro engine is that it does provide increased fuel efficiency over the NM-fueled engine, but there is high variability and the run quality is poor. The behavior of JP-8-fueled engine is to combust late in the cycle with a long duration. However, this poor combustion behavior is offset by the increased energy in the fuel, leading to comparable output with lower fuel consumption.

4.4 Comparison of the JP-8-fueled Engine to the Nitromethane-methanol-fueled Engine

The final step in the micro engine JP-8 conversion was to compare the results of the JP-8 and NM-fueled engine to show how the conversion affected the engine performance and operation. Comparison of the steady-state data, combustion analysis data, and calculated efficiencies showed that the JP-8 conversion created multiple changes in the engines behavior. These differences could be explained using the steady-state data and show the benefits and weakness of the JP-8-fueled micro engine.

Note that because of the operating characteristics of the engine running on NM blend and JP-8 fuel, only two speed-load points were common of the three runs for each fuel. These were the

9,000 and 8,000 RPM speeds with 250 W of electrical power generation. All results discussed here were under a 250 W electric power generation load.

4.4.1 Calculation of Efficiencies

The discussion surrounding the comparison of the NM blend and JP-8-fueled engines is best approached by first considering the efficiencies associated with the engine and test stand. These efficiencies include the mechanical, indicated fuel conversion, and system efficiency, and provide a way to examine the final result of the many changes created by the micro engine conversion. Before comparisons are made, however, explanation of the definition of the calculated properties and efficiencies is necessary.

A crucial parameter used to calculate the efficiencies was the indicated power. The indicated power was calculated using the AVL IndiCom combustion analysis software and is defined as:

$$Indicated\ Power\ (W) = \frac{IMEP\ (Pa) * Volume\ Displaced\ per\ Power\ Cycle\ \left(\frac{m^3}{revolution}\right)}{Engine\ Speed\ \left(\frac{revolution}{second}\right)}$$

This value was calculated on a cycle-by-cycle basis for each of the 300 cycles measured with the combustion analysis software and then averaged into a single value for each of the measured steady-state points. The displaced volume used was the 11.5 cc swept volume of the engine. The indicated power can be interpreted as the rate at which work is done on the piston. It does not include any friction effects past the interaction of the piston with the cylinder wall and does include heat transfer, piston-cylinder interface friction, and piston blow-by. Essentially, the indicated power is the amount of power available in the combustion volume before any interaction with the other engine components, the test stand coupler, or the test stand generator electronics. For this reason, it was chosen as the main comparison parameter for the efficiency calculations.

The first efficiency evaluated is the mechanical efficiency. The mechanical efficiency was defined as the ratio of the demanded electrical power by the indicated power, or

$$Mechanical\ Efficiency\ (\%) = \frac{Demanded\ Electrical\ Power\ (W)}{Indicated\ Power\ (W)} * 100$$

This efficiency is a measure of how much of the indicated power from the combustion volume made it through the engine, coupler, generator electronics, and finally into the DC load bank. For all of the steady-state tests, the demanded electrical power was 250 W; this nominal value was

used for all of the calculations. A drop in the mechanical efficiency is the result of increased friction effects in the engine, misalignment losses, and efficiency of the generator motor and conversion electronics. However, because the test stand remained the same for both the NM blend and JP-8-fueled engine tests, this efficiency is primarily an indicator of the friction at a given speed.

The next efficiency considered was the indicated fuel conversion efficiency. This was defined as the ratio of the indicated power produced divided by the rate at which fuel energy was delivered to the engine, or

$$Indicated\ Fuel\ Conversion\ Efficiency\ (\%) = \frac{Indicated\ Power\ (W)}{Rate\ of\ Fuel\ Energy\ Delivered\ (W)} * 100$$

$$= \frac{Indicated\ Power\ (W)}{Fuel\ Mass\ Flow\ Rate\ \left(\frac{g}{s}\right) * Net\ Heat\ of\ Combustion\left(\frac{J}{g}\right)} * 100$$

The amount of fuel energy delivered is the fuel mass multiplied by the energy per unit mass, which was taken as the net heat of combustion for the fuel, using the fuel properties in Section 2.2.2. The indicated fuel conversion efficiency is a measure of how well the fuel energy is converted into work in the cylinder. A high value for the indicated fuel conversion efficiency means more of the fuel energy was captured in the cylinder and converted to work.

Indicated fuel conversion efficiency is often calculated for automotive engines using the indicated heat release and the mass of fuel delivered per power cycle. This approach is done because the amount of fuel delivered by the fuel injection system per cycle is known. For the micro engine, however, fuel is delivered using the carburetor and the fuel is not delivered directly into the cylinder, but rather into the crankcase. This means that the amount of fuel delivered per power cycle cannot be known exactly. Therefore, it is more appropriate to use the rate at which the fuel is delivered and the indicated power rather than the indicated heat release.

The final efficiency that was calculated was the overall system efficiency. This efficiency is defined as the demanded electrical power divided by the rate at which fuel energy was delivered to the engine. In other words, the system efficiency is the mechanical efficiency multiplied by the indicated fuel conversion efficiency. Trends from the system efficiency were not explored as trends are better explained in the mechanical or indicated fuel conversion efficiency. The system

efficiency is provided for the purpose of understanding how well a micro engine-generator converts the chemical energy in the fuel into electrical power.

Having explained the three efficiency calculations and their meaning, they can be presented. Figure 4-15 shows the mechanical, indicated fuel conversion, and system efficiency for the 9,000 and 8,000 RPM points for both the stock, NM-fueled engine and the modified, JP-8-fueled engine. Note that the mechanical efficiency is placed on a separate axis to allow for better visual fidelity.

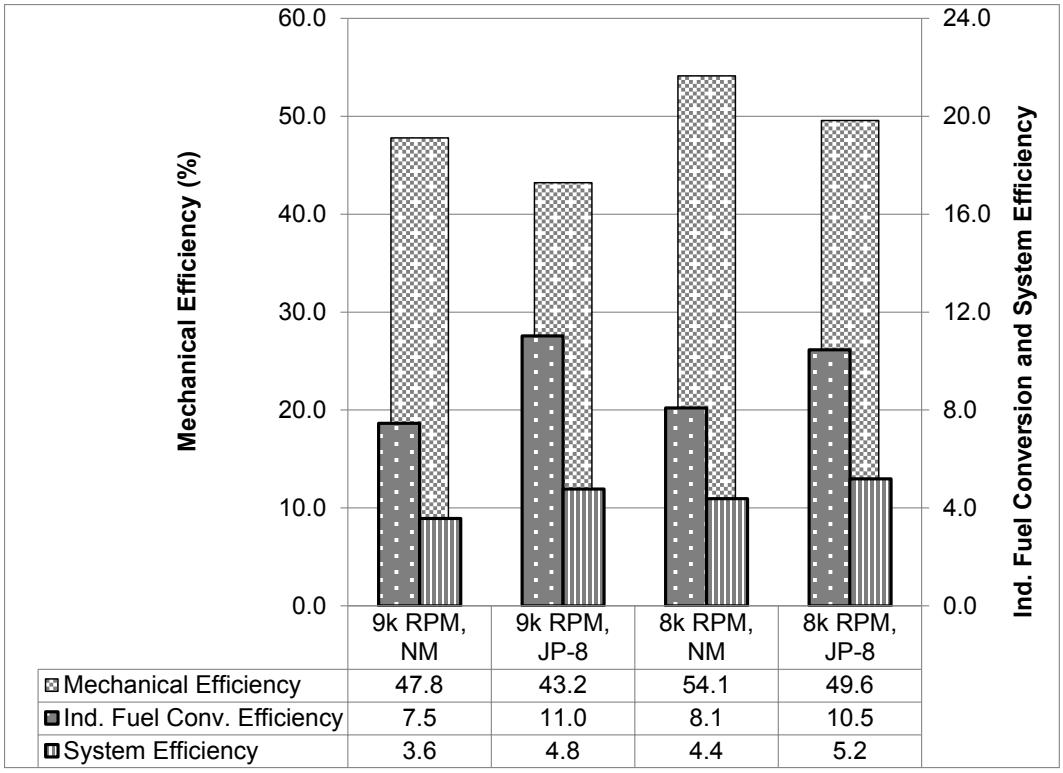

Figure 4-15: NM vs. JP-8 mechanical, indicated fuel conversion, and system efficiencies comparison

Trends in the efficiencies can be observed both between speeds and between fuels. Friction effects from speed and fuel lubricity can be observed from the mechanical efficiency values. Indicated fuel conversion efficiencies increased when the engine was switched from NM blend fuel to JP-8 fuel. Finally, the system efficiency was increased for both speeds with the JP-8-fueled engine.

4.4.2 Mechanical Efficiency

First, consider the effects of friction with engine speed. As engine speed increases, the fluid effects between the interfacing engine component surfaces will produce more hydrodynamic drag. Therefore, for a given load, more work has to be done on the piston to produce the same amount of output work. This trend can be seen when comparing either of the fuels at the two speed points. Consider the NM-fueled engine at 9,000 RPM versus the 8,000 RPM case. The mechanical efficiency decreased from 54.1% to 47.8% as the speed increased to 9,000 RPM while the load was held constant at 250 W. This demonstrates that as the engine speed increases, the efficiency of the mechanical system decreases.

Next, consider the change in mechanical efficiency for a given speed when the fuel is switched from NM blend to JP-8. For both speed-load points, the mechanical efficiency decreased when the fuel was switched to JP-8. For example, the mechanical efficiency decreased from 47.8% to 43.2% when the fuel was switched to JP-8 at the 9,000 RPM speed-load point. This suggests that there was increased friction in the engine modified for JP-8 and is not totally unexpected. Recall that from the lubricity testing, a 20 vol% amount of oil was determined necessary to achieve the same lubricity properties as the NM fuel-oil blend. However, for starting purposes, the amount of oil in the JP-8 fuel-oil blend was reduced to 13 vol% and a dry-film lubricant was applied to the piston skirt. This seems to have decreased the mechanical efficiency as more indicated power is need to overcome the friction effects in the engine.

The increased friction in the JP-8-fueled micro engine can be seen in multiple measurements. First, the throttle position was increased 17% and 26% above the NM-fueled engine throttle position for the 9,000 and 8,000 RPM cases, respectively. This throttle increase translated into higher indicated work and improved gas dynamics in the two-stroke micro engine. This is shown in the increased IMEP and the decreased COV for the JP-8-fueled engine compared to the NM-fueled engine. The values of the IMEP and COV are shown in Figure 4-16.

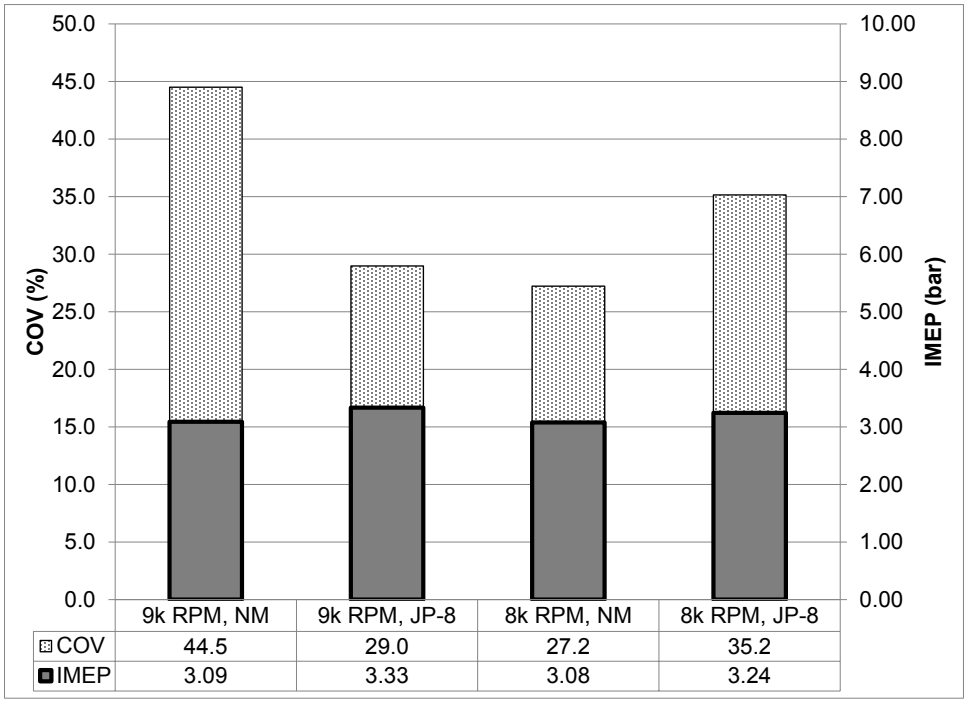

Figure 4-16: NM vs. JP-8 IMEP and COV of IMEP comparison

Opening the throttle further in the JP-8-fueled engine changed the scavenging behavior of the engine, greatly improving the 9,000 RPM operating point for the JP-8-fueled engine as compared to the NM-fueled engine. For the NM-fueled engine, the 9,000 RPM operating point had poor combustion characteristics, reflected in the 44.5% average COV. When the engine was converted to JP-8 at 9,000 RPM, however, the COV was reduced to 29%. Notice that this effect was not reflected in the 8,000 RPM operating point, however. The exact reason for this behavior is not understood; however, an argument can be made that the increased throttle opening for the JP-8-fueled engine testing altered the gas dynamics in the engine, changing the operating behavior though engine speed did not change. The throttle position for the 8,000 RPM JP-8 operating point was only 4% greater than the throttle position at the 9,000 RPM operating point on NM blend fuel. Therefore, the 8,000 RPM operating point may be falling into the same poor engine operating range that affected the 9,000 RPM operating point for the NM-fueled engine. This low combustion quality operation is likely due to poor scavenging or poor air-fuel charge mixing behavior at this throttle setting. Conversely, the 9,000 RPM JP-8-fueled engine throttle position was 8% greater than the 9,000 RPM NM-fueled engine throttle position, which again moved the operating away from this poor operating point.

4.4.3 Indicated fuel conversion Efficiency

The next observation from the efficiency calculations was the increased indicated fuel conversion efficiency for the JP-8-fueled engine. Recall from the definition of the indicated fuel conversion efficiency that the numerator of the efficiency is the power generated in the cylinder while the denominator is the rate of fuel energy delivered. If the JP-8 and NM-fueled engines combustion process was similar, the indicated fuel conversion efficiency could be expected to remain the same. If this was the case, then the fuel energy delivered would have to increase by the same amount that the work required (i.e. IMEP) increased. However, this is not the case.

The reason for this improved indicated fuel conversion efficiency lies in the reduced fuel energy consumption of the JP-8-fueled engine. Reduced JP-8 mass flow was expected to be consumed because the net heat of combustion for JP-8 is 2.4 times the estimated net heat of combustion for NM blend fuel; theoretically, this means that only 41.7% (i.e. 1/2.4) of the NM blend fuel flow rate should be required for the JP-8-fueled engine to deliver the same amount of fuel energy to the engine. Figure 4-17 shows the measured fuel flow rates and measured AFR divided by the stoichiometric AFR for each specific fuel. The fuel flow rate shows that the JP-8 fuel flow rate is 31.1% of the NM fuel flow rate for the 9,000 RPM case and 35.2% for the 8,000 RPM case. This means that not only was the fuel consumption less, but the fuel energy consumed for the JP-8-fueled engine was lower for both of the speed-load points. This results in higher indicated fuel conversion efficiency.

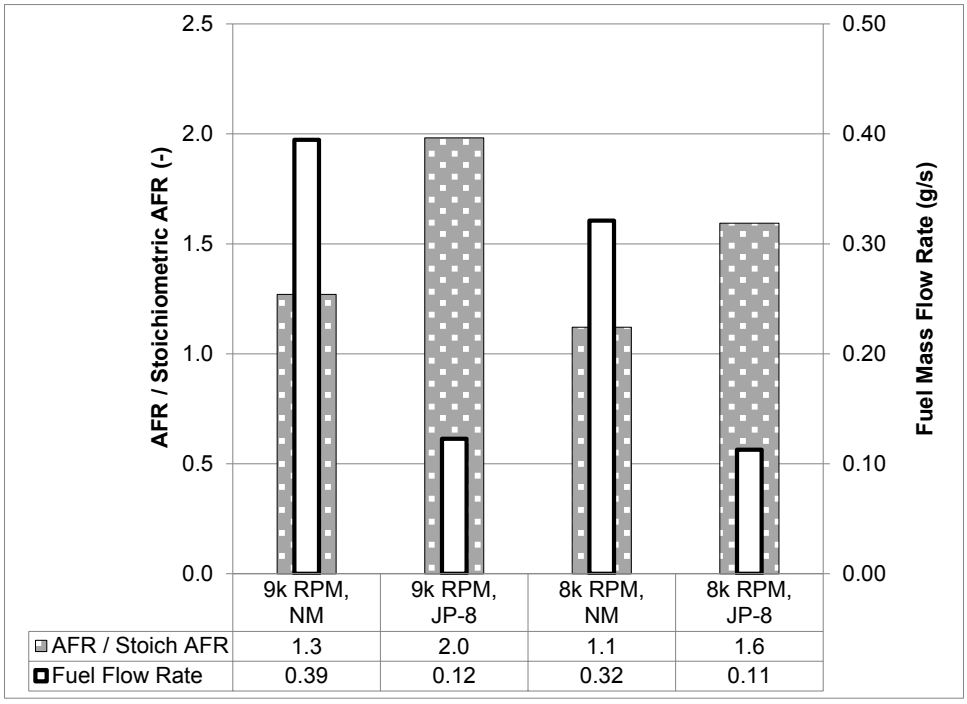

Figure 4-17: NM vs. JP-8 fuel mass flow rate and AFR/stoichiometric AFR comparison

The reason for this reduced fuel energy consumption lies in the operating principles of the micro engine with JP-8 instead of NM blend fuel. Figure 4-17 shows that the AFR divided by AFR_s for both operating points with NM blend fuel were fuel-lean of their stoichiometric conditions. Ideally, this would mean that all of the fuel could be combusted. However, fuel was always observed exiting the engine through the exhaust when fueled by the NM blend. This is because the NM blend fuel has a high latent heat of vaporization which is used in the engine design to cool the engine; this high latent heat of vaporization also results in only a fraction of the fuel being vaporized and combusted in the engine. Because the fuel energy is not converted to work and is lost through the exhaust as liquid fuel, the indicated fuel conversion efficiency of the NM-fueled engine is quite low.

The micro engine operates in a different way when fueled by JP-8. JP-8 and other heavy fuels operate best in global fuel-lean conditions; most automotive diesels, for example, never come close to operating at their global stoichiometric AFR. This is because the long, non-oxygenated hydrocarbon chains in heavy fuels require longer durations to burn completely. This is not needed for oxygenated, short hydrocarbon chains like NM blend fuels because the small molecules readily interact with gaseous oxygen molecules or the oxygen components attached to

the fuel molecules (methanol and nitromethane both have oxygen molecules bonded to the hydrocarbon chain). The result of this fuel behavior is that the micro engine must be run significantly fuel-lean when fueled by JP-8, even when compared to the lean conditions with NM fuel. This is illustrated by the AFR/stoichiometric AFR measurement; the JP-8-fueled engine runs approximately 50% leaner than the NM-fueled engine

This fuel-lean condition for JP-8 has implications in the fuel conversion efficiency and in the engine operation. Because the JP-8-fueled engine runs so much leaner, more of the fuel can be combusted and less fuel is lost through the exhaust. The result of this is higher indicated fuel conversion efficiency compared to the NM-fueled engine, which is a welcome improvement.

4.4.4 Temperature Comparison

This excessive fuel-lean condition is not the designed intent of the JP-8-fueled micro engine, however; in fact, this is detrimental to both the friction and thermal management in the engine. As shown in the IMEP measurement, there is likely more friction in the JP-8-fueled engine. This could be a result of the reduced oil content in the oil-fuel mixture, but it could also be simply due to less fuel moving through the engine. In either case, the increased friction in the micro engine is likely detrimental to the engines durability and useable lifetime compared to the NM-fueled engine.

Thermally, there is a significant issue with running JP-8 as a fuel in the micro engine. Recall that the micro engine relies on the fuel to remove energy from the combustion surfaces, thus cooling the engine. The JP-8-fueled engine, however, not only moves less fuel mass through the engine, but the JP-8 also has a lower latent heat of vaporization. This means that a dramatically lower amount of heat energy is removed from the engine. This is reflected in the exhaust and cylinder head temperatures, which are shown in Figure 4-18. Note also that this temperature is a best case scenario because additional cooling air was required for the JP-8-fueled engine; the cooling fan was run at 17.5 m/s for the JP-8-fueled engine and only 8.0 m/s for the NM-fueled engine. Without this additional cooling air, the JP-8-fueled engine would not have been operational for more than a few seconds before the engine surface temperatures moved into destructive ranges.

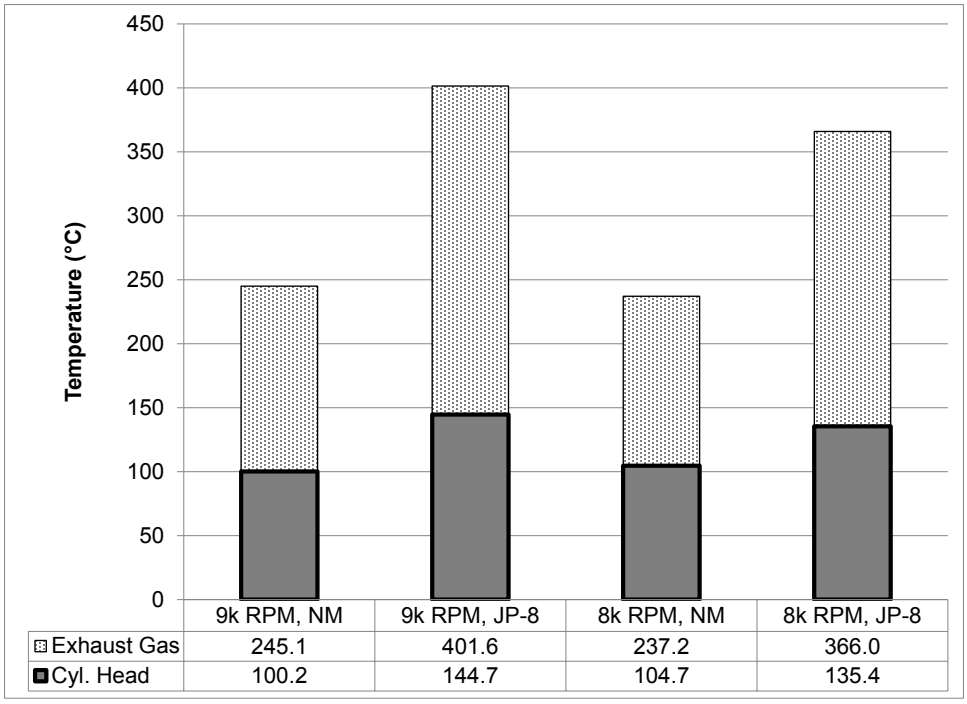

Figure 4-18 NM vs. JP-8 exhaust gas and cylinder head temperature comparison

The temperature comparison moves the discussion into the combustion behavior of the JP-8-fueled engine. Notice from Figure 4-18 that the exhaust temperatures are considerably higher than their comparable NM-fueled speed-load points. This is a strong indicator of delayed combustion phasing. Essentially, the fuel is still burning as the exhaust port opens and this burning fuel heats the exhaust thermocouple. This difference may be slightly exaggerated, however, because of the liquid NM blend fuel in the exhaust. The high latent heat of vaporization of the NM blend and the presence of liquid fuel in the exhaust may have caused the exhaust gas temperature of the NM-fueled engine to be lower than its true value as fuel vaporized on the thermocouple probe. This can be compared to the same phenomenon that makes a wet-bulb temperature lower than a dry-bulb temperature with thermometers. Therefore, the exhaust gas cannot completely confirm the late combustion phasing.

4.4.5 Combustion Analysis

The combustion phasing can be confirmed, however, by examining the location of the 50% mass fraction burned and 10-90% burn duration. The 50% mass fraction burned is the crankshaft angle degree (CAD) after top dead center (ATDC) where 50% of the fuel burned in the

combustion event is consumed; it is abbreviated 50% MFB. Note that top dead center (TDC) is the location where the piston has reached the top of its stroke. The 10-90% burn duration is the span of crankshaft angle degrees required to burn 10% to 90% of the fuel mass combusted in the cycle; it is abbreviated D10-90%. The 50% MFB and D10-90% can be seen in Figure 4-19.

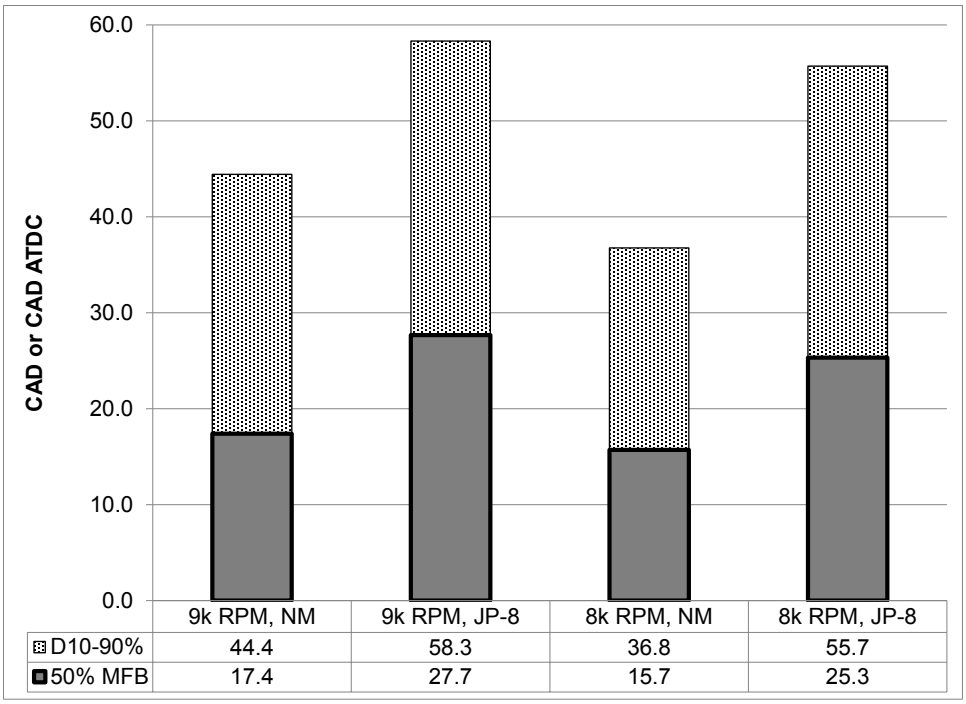

	9k RPM, NM	9k RPM, JP-8	8k RPM, NM	8k RPM, JP-8
D10-90%	44.4	58.3	36.8	55.7
50% MFB	17.4	27.7	15.7	25.3

Figure 4-19: NM vs. JP-8 50% MFB and D10-90% comparison

The location of 50% MFB and the D10-90% value show that the JP-8 combustion phasing was indeed later than the NM-fueled micro engine combustion. In fact, it was significantly later, which confirms that fuel was likely still burning in the exhaust port, causing the high exhaust temperature. Based on ideal-cycle internal engine thermodynamics, the cycle with the highest efficiency is a cycle where all of the fuel combusts immediately and instantly after top dead center. With the late combustion phasing, shown by the late 50% MFB and long D10-90%, the JP-8-fueled engine is likely less thermodynamically efficient than the NM-fueled engine. Note, however, that the NM-fueled engine also combusts relatively late in its cycle and has a long combustion duration.

Another interesting trend from the D10-90% values is that as the speed increases, the burn duration also increases. While speculative, this could be an indicator of insufficient fuel-air

charge mixing as the engine speed increases. The fuel in both cases may not have sufficient time and turbulence to mix with oxygen and burn completely, resulting in longer crank-angle domain burn times.

Comparison of the 50% MFB and D10-90% values may show late combustion phasing, but the rate of heat release (ROHR) shows how the combustion was actually happening in the crankshaft angle domain. The rate of heat release was calculated by AVL IndiCom using a function of the cylinder pressure; it shows the rate at which fuel energy is being released through combustion into the combustion volume. The ROHR can be seen in Figure 4-20. This is the average ROHR for the three runs at each speed-load operating point.

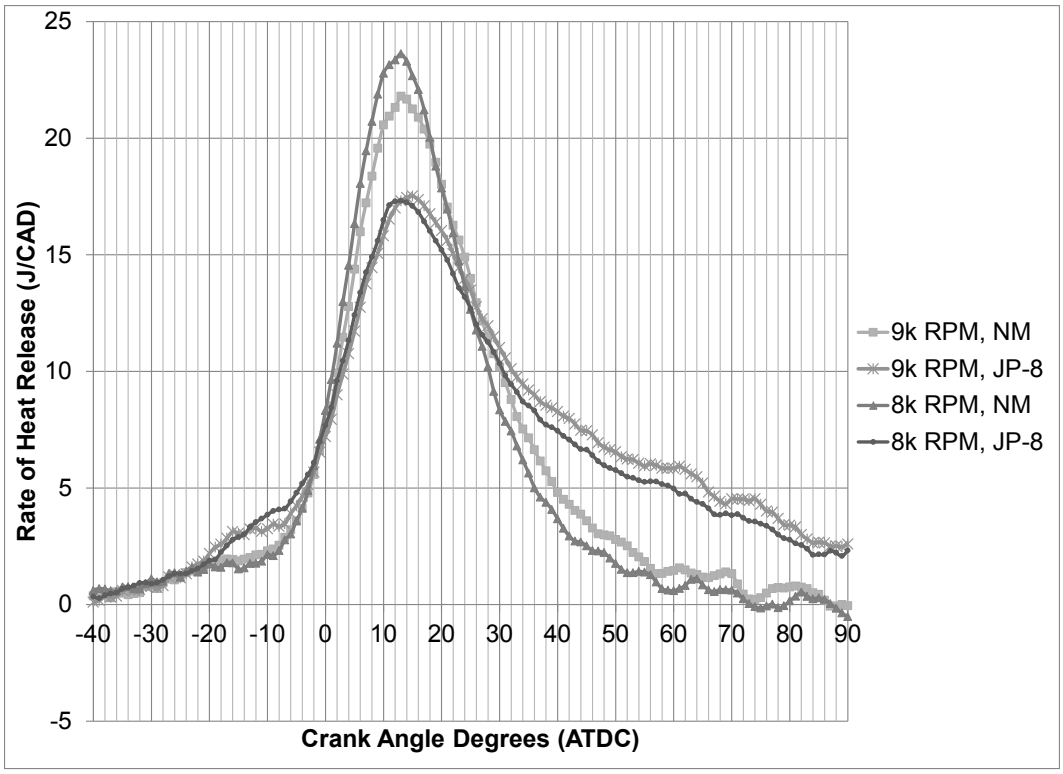

Figure 4-20: NM vs. JP-8-fueled engine rate of heat release comparison

Figure 4-20 shows that the NM blend fuel is combusting in a uniform and relatively symmetric fashion. This is a typical pattern of heat release and compares on a qualitative level to gasoline combustion. The JP-8 combustion is much less uniform, however. First, notice the small hump of combustion located around -20 CAD ATDC. This indicates the possibility of some sort of fuel pre-ignition early in the compression stroke. The exact cause of this hump is unclear because

this ROHR curve was taken as an average from three hundred combustion cycles acquired and three tests. Next, notice that the ROHR does not achieve the same amplitude for the JP-8-fueled engine compared to the NM-fueled engine. This indicates slower combustion. This slow combustion is also longer combustion, which is shown in the increased JP-8 ROHR from about 25 CAD ATDC to the end of the measurement. To summarize, the JP-8 ROHR shows a longer, slower combustion process. It also has evidence of possible early combustion events, which could be detrimental to engine performance and durability.

The final piece of data that is pertinent to the micro engine fuel conversion project is the actual pressure trace. Interestingly, the pressure traces between the NM blend and JP-8-fueled engine and even the 9,000 and 8,000 RPM runs are quite similar. The pressure traces averaged from the three runs for each condition can be seen in Figure 4-21. A motored pressure trace (i.e. no combustion) is shown for reference,

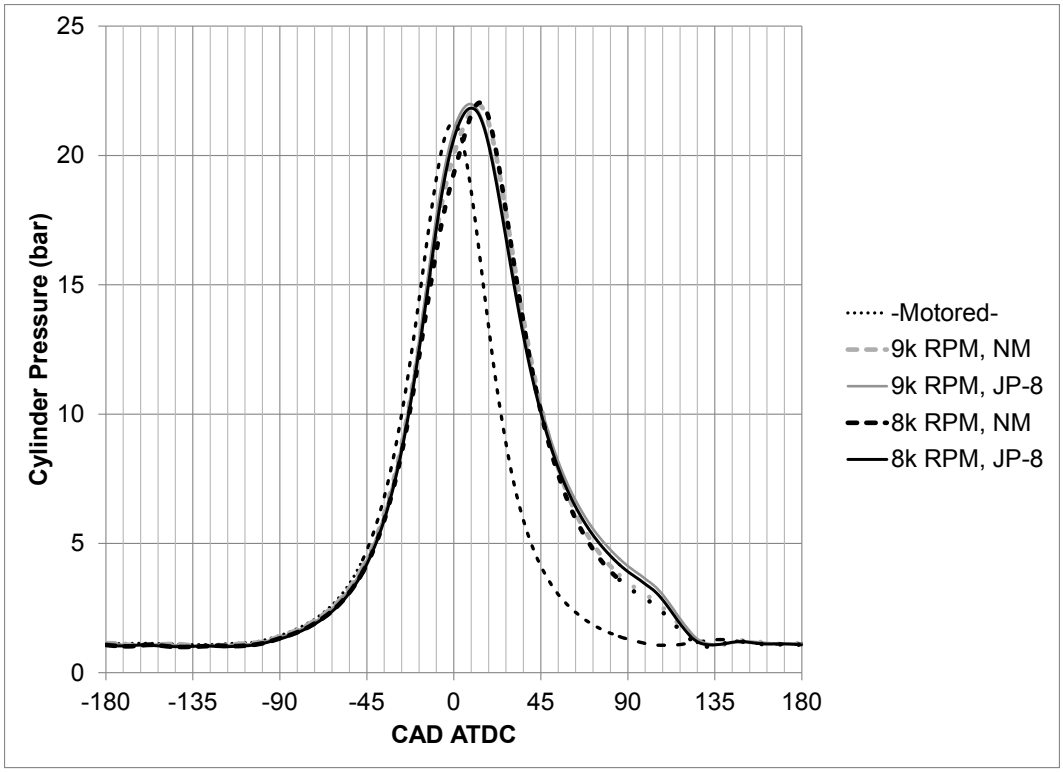

Figure 4-21: NM vs. JP-8-fueled engine in-cylinder pressure traces

The averaged pressure traces shows that although the run characteristics of the JP-8 and NM-fueled micro engine varied greatly, the end result is a similar pressure profile in the cylinder,

translating into a similar power output. The JP-8 burns slower and longer, meaning the pressure trace peaks slightly earlier than the NM-fueled engine and stays elevated above the NM-fueled engine pressure trace late in the combustion process. An interesting point is that the location of the exhaust port opening can be seen in Figure 4-21 at approximately 105 CAD ATDC; it is evident in the rapid change in pressure slope. The JP-8 pressure traces are higher at 105 CAD ATDC than the NM-fueled engine pressure traces indicating that, while both fuels are still burning at 105 CAD ATDC, the JP-8 is releasing more energy into the cylinder than the NM-fueled case. This confirms that the higher exhaust temperatures for JP-8 were an indication of late combustion phasing.

4.4.6 Summary

A summary of the steady-state data points is presented in Table 4-6. The 9,000 RPM and 8,000 RPM operating points are shown as well as the 10,000 RPM NM blend and 7,000 RPM JP-8 operating points. Each speed-load point also has a “Ratio” column which shows the quotient of the NM blend data divided by the JP-8 data. In Table 4-6, the fuel flow rate is also normalized into the typical brake-specific fuel consumption. This is the fuel flow rate normalized by the power output. For the micro engine this value is reported as “eBSFC,” or electric brake-specific fuel consumption, as the documented power was the electric power of 250 W. This is shown mainly for comparison to more frequently published fuel consumption values.

Table 4-6: Steady-state testing data summary of NM vs. JP-8-fueled engine

		9,000 RPM			8,000 RPM			10,000 RPM	7,000 RPM
Property	Units	NM	JP-8	Ratio	NM	JP-8	Ratio	NM	JP-8
Exhaust Temperature	°C	245	402	1.64	237	366	1.54	289	352
Cylinder Head Temperature	°C	100	145	1.44	105	135	1.29	135	126
Fuel Flow	g/s	0.395	0.123	0.31	0.321	0.113	0.35	0.475	0.103
eBSFC	g/(kW-hr)	5682	1766	0.31	4624	1624	0.35	6842	1481
Air-Fuel Mass Ratio	-	5.3	29.3	5.50	4.7	23.6	5.01	7.4	23.7
Throttle Position	%	44.3	52.0	1.17	38.3	48.3	1.26	51.0	45.7
IMEP	bar	3.09	3.33	1.08	3.08	3.24	1.05	4.18	3.18
COV	%	44.5	29.0	0.65	27.2	35.2	1.29	8.6	28.6
50% Fuel Mass Burned	CAD ATDC	17.4	27.7	1.59	15.7	25.3	1.61	11.6	32.6
10-90% Fuel Mass Burned	CAD	44.4	58.3	1.31	36.8	55.7	1.52	28.7	58.8
Ind. Fuel Conversion Efficiency	%	7.5	11.0	1.48	8.1	10.5	1.29	9.5	9.8
Mechanical Efficiency	%	47.8	43.2	0.90	54.1	49.6	0.92	31.3	58.1
System Efficiency	%	3.6	4.8	1.34	4.4	5.2	1.18	3.0	5.7

In summary, the micro engine conversion from NM blend fuels to JP-8 showed both advantages and disadvantages. The primary advantage is that through all of the modifications to the engine's behavior, the end result is that the overall engine-generator system efficiency is improved when operating on JP-8 versus NM blend fuel. This improvement is dominated by the improvement in indicated fuel conversion efficiency, which is caused by reduced fuel consumption. Unfortunately, the reduced fuel consumption and lower latent heat of vaporization demand additional cooling for

the JP-8 engine, negating some of the advantage of the JP-8-fueled engine's improved indicated fuel conversion efficiency. The JP-8 engine also showed a strong likelihood of increased mechanical friction, which could have been due either to reduced fuel-oil mass flow, reduced lubricity of the fuel, or a combination of the two effects. Finally, the combustion phasing of the engine changed considerably with the JP-8-fueled micro engine, but the end result is a roughly similar pressure trace and power output.

Chapter 5 Project Summary and Observations

Micro engines offer many advantages that make them plausible for compact applications. However, the use of nitromethane-methanol blend fuel in these applications could be problematic because this fuel is highly flammable, corrosive, expensive, and not always readily available. The alternate fuel of JP-8 was selected to convert a micro engine to in order to combat these disadvantages and make micro engine applications more feasible. Additionally, JP-8 was necessary to comply with the US military's "Single Fuel Forward" initiative. This led to the Micro JP-8 Burn project, which had a primary objective of demonstrating the ability to generate 250 W of power out of a small engine while fueled by JP-8.

The project was broken into two phases. Phase 1 included selecting an engine for the conversion, developing a micro engine test stand, and performing baseline tests to evaluate the stock engine performance. Phase 2 included experimentation to determine how to convert the engine from its stock nitromethane-methanol blend fuel to JP-8, to perform steady-state operating testing at multiple operating points, and to compare the performance of the nitromethane-methanol-fueled engine to the engine converted to run on JP-8.

After examining multiple options, the O.S. brand 70SZ-H engine was selected for the conversion from its stock nitromethane-methanol blend fuel to JP-8. The 70SZ-H is an 11.5 cc, glow-ignition, crankcase scavenged, two-stroke engine used to power remote controlled hobby helicopters. With a rated output of 1842 W, the engine was oversized to allow for lower-speed operation.

To fully understand and document the conversion process, a micro engine test stand was developed. This test stand was designed to generate electrical power, rather than measuring torque, using an electric system consisting of a BLDC motor, a motor controller, and a DC load bank. Great care was taken when creating the test stand to avoid transmitting vibration to the surroundings and to ensure good engine-motor alignment. Instrumentation specific to the micro engine was developed to acquire the parameters deemed necessary to document the conversion. These measurement instruments included a custom built fuel scale, a custom built air flow meter, a small optical encoder, a cylinder pressure transducer, various thermocouple measurements, and a low-speed exhaust pressure transducer. The micro engine test stand provided all the necessary measurements to understand the engine's behavior and provided consistent test conditions.

Once the test stand was developed, the nitromethane-methanol-fueled stock O.S. 70SZ-H was tested at three, steady-state conditions. These test points included 10,000 RPM, 9,000 RPM, and 8,000 RPM engine speeds while generating a constant 250 W of electrical power. From the measured data, there was a trend of increasing temperatures, increasing fuel flow rate, and increasing air-to-fuel mass ratio (i.e. more fuel-lean) with increased engine speed. An additional observation was that the 9,000 RPM operating point showed poor combustion quality which may have been caused by poor internal gas dynamics in the two-stroke engine. Combustion analysis was also completed on the nitromethane-methanol-fueled engine, which showed relatively late combustion events and long combustion durations. This is likely by design due to the lack of intelligent ignition control in the glow-ignition engine.

The completion of the nitromethane-methanol-fueled engine testing completed Phase 1 of the Micro JP-8 Burn project and transitioned the project into Phase 2. The first step of Phase 2 was to develop the appropriate modifications to convert the 70SZ-H engine to run on JP-8. This was completed by identifying the appropriate fuel lubricity, developing methods to improve starting time, collecting steady-state data, and finally by comparing the results of the JP-8 steady-state testing to the results of the nitromethane-methanol based testing.

A series of experiments were conducted to identify how to operate the micro engine on JP-8 and to understand how this operation occurs. Traditional methods such as cylinder head, intake, and fuel heating were initially explored with poor results. Then, a number of hardware configurations, including compression ratio, material, and coatings changes, were tested without starting aids to identify the fastest starting time. In this experimentation, a strong correlation between the engine case temperature and the flash point of JP-8 was observed. Eventually, the use of small polyimide heaters on the engine case was identified as a robust method for starting the engine on JP-8. The hypothesis behind this operation was that as the internal engine surfaces are heated beyond the flash point of JP-8, flammable mixtures can develop in the engine, leading to improved cold-starting. The hardware experimentation also led to the selection of a ceramic coating on the combustion chamber and the piston dome as the best hardware to improve cold starting with minimal engine modifications.

The final hardware configuration for the 70SZ-H engine was tested under steady-state conditions while fueled with JP-8. This data was then compared with the baseline nitromethane-methanol-fueled engine data. Evidence of increased friction, better conversion of fuel to electric power, and higher temperatures were observed with the JP-8-fueled micro engine. All of these behaviors appear linked to a decreased fuel flow rate through the engine; as the fuel flow rate is reduced,

lubricant flow into the engine is reduced, less fuel is lost through the scavenging process, and less heat is removed by the fuel vaporizing on the engine components. The net effect of the JP-8 fuel conversion is improved overall efficiency at the expense of more difficult thermal and lubrication management.

Chapter 6 Recommendations for Future Work

The Micro JP-8 Burn project was successful in that demonstration of a JP-8-fueled micro engine was accomplished. However, throughout the project a number of areas surfaced that deserve further consideration. Issues with the micro engine test stand and the JP-8-fueled engine, specifically, need more attention.

While the micro engine test stand provided many capabilities, it does have room for improvement. This is especially true for the coupler, the loading system, and the air flow measurement.

First, the coupler is not sufficiently durable and should be reinvestigated. The Zero-Max SC030R is a great product, but this is not its designed application. The high torque pulsations from the micro engine demand that the coupler be replaced or reconditioned frequently; the reoccurring fatigue failures suggest the coupler is being operated too close to its designed limits. Also, the practice of using a set screw to limit shaft rotation in the coupler is not particularly well suited to the high speeds and high vibration of the micro engine application. It is recommended that a more substantial coupler be chosen or fabricated and keyways should be added to the motor and engine shafts. This would have been completed under this thesis, but further modification would have delayed the project.

Second, the use of an electric loading system provided a simple, cost-effective system. However, this system could be improved to provide more information and to be (potentially) less costly. The addition of a reaction cradle and load cell for torque measurement would add a minimal amount of cost to the system and allow the true energy and efficiency calculations for the engine alone, rather than the engine-electronics combination. The cost of the system could possibly be reduced by designing a high-power circuit that integrates the DC load bank, the relay, and the BLDC motor controller into a single unit.

Finally, uncertainty still exists around the air flow measurement. The method of using a custom venturi with a hot-wire anemometer was chosen because it was supposed to cost the least; ultimately it only costs a few hundred dollars less than a pre-built, fully calibrated thermal mass

flow meter. While the cost difference may seem justified, it does not warrant the numerous hours and additional equipment necessary to perform calibration. Another modification that is needed for the air flow measurement is the addition of a plenum. The lack of a plenum was an oversight in the early phases of the project and was not identified as an issue until the end of the project. Two-stroke engines are known for strong backflow of the intake air; if sufficient volume does not exist between the carburetor and the air flow measurement, the air flow measurement may read higher than the true value. The plenum acts as a buffer for this back flow, ensuring an accurate air flow measurement.

The JP-8-fueled micro engine also presented a number of potential areas of research. These included developing a better understanding of the lubricity effects, refining the heated crankcase concept, confirming the micro engine durability, finding methods of improved fuel-air charge mixing, and finally determining the best thermal management solution.

The initial expectation from the JP-8 lubricity was that it would be sufficient for the purposes of the Micro JP-8 Burn project. This proved true. However, there were documented effects of increased friction when the engine was fueled by JP-8. Personal observation shows that the internal engine components do not seem to hold up as well when lubricated by JP-8. For example, the upper connecting rod bushing seemed to wear much faster when fueled by the JP-8 with 13 vol% oil mixture than when fueled by commercial NM blend fuels. The tradeoff between starting and lubricity is a difficult balance which needs to be explored further. It is recommended that a complete a series of ASTM D6078 and D6079 tests on multiple blends of JP-8 and lubricants to determine the minimal lubrication that matches the NM blend fuels.

The next area of research is the refinement of the crankcase heating concept. The use of polyimide heaters worked acceptably for a proof-of-concept. The 30 minutes required for starting, however, would likely be unacceptable in a final application. It is recommended that available heat sources from the system the micro engine is implemented into are used to heat the crankcase constantly. For example, an auxiliary cooling system could be plumbed into a crankcase water-jacket to supply this heat to the engine at all times. Additionally, research should be conducted to determine the exact relation between fuel and starting. The hypothesis of the crankcase exceeding the flash point does have evidence to substantiate it, but this does not fully explain this phenomenon.

One element that was not explored in this thesis was the durability of the JP-8-fueled micro engine. A number of steps would need to be made to analyze the engine's durability. First,

beginning and end of life measurements would need to be conducted on an unmodified, NM-fueled engine. This would determine the baseline durability of the O.S. 70SZ-H or whatever other engine was converted. Next, a high-lubricity JP-8 – oil mixture should be run in the same way to determine if the neat fuel constituent affects the durability of the engine. Finally, a test with minimal or no additional oil should be run to determine a worst case scenario for the JP-8-fueled micro engine. This is only a basic recommendation; many tests could be conducted on the durability of the micro engine.

Initial project discussion mentioned that this demonstration engine could eventually lead to other projects where fuel injection or some other method of enhanced fuel-air mixing was developed. With the crankcase scavenged engine, the use of a port-type fuel injection would probably not be successful as the fuel droplets have to travel a long, indirect path into the combustion chamber. The addition of direct injection, such as those explored in the literature review, may cause durability and lubrication issues. Essentially, more research is required to determine whether use of increased fuel-air mixing methods is effective in such a small engine.

Perhaps the topic in most urgent need of attention on the JP-8-fueled micro engine is the need for improved thermal management. With the lower mass flow rate and lower latent heat of vaporization of JP-8, the primary cooling method for the micro engine has essentially been lost. Without the fuel vaporizing and removing heat from the combustion surfaces, run away temperatures should be fully expected. For the JP-8-fueled micro engine, this was mitigated by moving more cooling air over the engine. In a final application, this would likely not be acceptable. The addition of a liquid-cooled head and liquid-cooled cylinder liner could help remove more heat from the system in strategic locations, allowing fuel to vaporize while not creating excessive temperatures.

Works Cited

[1] U.S.A. Department of Defense, *Directive Number 4140.25,* U.S.A. Department of Defense, 2004.

[2] R. R. Raine and H. Thorwarth, "Performance and Coubstion Characteristics of a Glow-Ignition Two-Stroke Engine," in *SAE World Congress*, Detroit, MI, 2004.

[3] P. I. Lacey and S. R. Westbrook, "Diesel Fuel Lubricity," in *International Congress and Exposition*, Detroit, MI, 1995.

[4] ASTM International, *D6078-04: Standard Test Method for Evaluating Lubricity of Diesel Fuels by the Scuffing Load Ball-on-Cylinder Lubricity Evaluator (SLBOCLE),* 2010.

[5] ASTM International, *D6079-04: Standard Test Method for Evaluating Lubricity of Diesel Fuels by the High-Frequency Reciprocating Rig (HFRR),* 2004.

[6] Y. A. Cengel and M. A. Boles, Thermodynamics, An Engineering Approach (Sixth ed.), New York, NY: McGraw-Hill, 2008.

[7] J. B. Heywood, Internal Combustion Engine Fundamentals, McGraw-Hill, 1988.

[8] ASTM International, *D93-11 Standard Test Methods for Flash Point by Pensky-Martens Closed Cup Tester,* ASTM International, 2011.

[9] ASTM International, *E659-78 Standard Test Method for Autoignition Temperature of Liquid Chemcials,* ASTM International, 2005.

[10] U.S.A Department of Defense, *MIL-DTL-83133H,* 2011.

[11] U.S.A. Environmental Protection Agency, *Methyl Alcohol,* 1999.

[12] U.S.A. Environmental Protection Agency, *Nitromethane,* 1999.

[13] U.S.A. Environmental Protection Agency, *Oils, Fuel: NO. 1,* 1999.

[14] U.S.A. Environmental Protection Agency, *Oils: Diesel,* 1999.

[15] R. R. Raine, K. Moyle, G. Otte and J. Robertson, "Cost-Effective Teaching and Research Dynamometer for Small Engines," *International Journal of Engineering Education,* vol. 18, no. 1, pp. 50-57, 2002.

[16] T. Ogawa and Y. Kawaguchi, "Performance Testing of 5cc Glow-Igntion Four-Stroke Engine," in *ASME-JSME Thermal Engineerign and Summer Heat Transfer Conference*, Vancouver, British Comlumbia, Canada, 2007.

[17] S. K. Menon, "Performance Measurement and Scaling of Small Internal Combustion Engines," University of Maryland, College Park, 2006.

[18] D. Cordon, M. Walker, S. Beyerlein, J. Steciak and M. Cherry, "Catalytically Assisted Combustion of JP-8 in a 1 kW Low-Compression Genset," in *Small Engine Technology Conference and Exhibition*, San Antonio, Texas, 2006.

[19] J. L. M. W. a. D. H. Brian J. Duddy, "Conversion of a Spark-Ignited Aircraft Engine to JP-8 Heavy Fuel for Use in Unmanned Aerial Vehicles," in *SAE International*, 2011.

[20] G. Cathcart, G. Dickson and S. Ahern, "The Application of Air-Assist Direct Injection for Spark-ignited Heavy Fuel 2-Stroke and 4-Stroke Engines," in *SAE International/JSAE*, 2005.

[21] "O.S. Engines .70 SZ-H Ring 3D Heli Engine," O.S. Engines, [Online]. Available: http://www.osengines.com/engines/osmg1972.html. [Accessed 09 November 2012].

[22] "Innov8tive Designs; Cobra C-4130-14 Brushless Motor, Kv=450," Innov8tive Designs, [Online]. Available: http://www.innov8tivedesigns.com/product_info.php?cPath=21_120_12. [Accessed 09 November 2012].

[23] "Model 8510, 600W Programmable DC Electronic Load - B&K Precision," B&K Precision, [Online]. Available: http://www.bkprecision.com/products/dc-electronic-loads/8510-600-w-programmable-dc-electronic-load.html. [Accessed 09 November 2012].

[24] Zero-Max, Inc., "ServoClass Couplings," Zero-Max, 2010.

[25] A. L. Wiegand, S. Miers, J. Blough, D. Kowalski and A. Biske, "Development of a Micro-Engine Testing System," in *SAE Small Engine Technology Conference*, Madison, WI, 2012.

[26] J. Holman and J. Lloyd, Experimental Method for Engineers (Seventh ed.), McGraw-Hill, 2001.

[27] M. Plint and A. Martyr, Engine Testing Theory and Practice (Third ed.), Oxford, U.K.: Butterworth-Heinemann, 1999.

[28] A. L. Sebok, "Simplified Air Density Correction of Vacuum Cleaner Performance Data," *IEEE Transactions on Inductry and General Applications,* vol. 6, no. 1, 1970.

[29] A. Lefebre, Gas Turbine Combustion (Second ed.), Taylor & Francis, 1999.

[30] U.S. Digital, Inc, "US Digital|Products>>EM1 Transmissive Optical Encoder Module," [Online]. Available: http://usdigital.com/products/encoders/incremental/modules/EM1. [Accessed 09 November 2012].

[31] US Digital, "US Digital|Products>>HUBDISK-2 2" Transmissive Rotary Codewheel," [Online]. Available: http://usdigital.com/products/encoders/incremental/rotary/disks/HUBDISK-2.

[Accessed 09 November 2012].

[32] J. B. Heywood and E. Sher, The Two-Stroke Cycle Engine; It's Development, Operation, and Design, Ann Arbor, MI: Braun-Brumfield, 1999.

[33] S. Westbrook, Interviewee, *Discussion of Lubricity Testing History and Testing Results.* [Interview]. 22 May 2012.

[34] E. Frame, G. Bessee and H. J. Marback, "TFLRF Report No. 317: Biodiesel Fuel Technology for Military Appilcation," U.S. Army TARDEC Fuels And Lubricants Research Facility (SwRI), San Antonio, TX, 1997.

[35] C. Benton, Interviewee, *Discussion on PolyDyn Ceramic Coatings; Application and Technology.* [Interview]. 28 June 2012.

[36] Watlow, Inc., "Polyimide Heaters," Watlow, Inc., 2012.

[37] Birk Manufacturing, Inc., "Design and Manufacture of Flexible Heating Elements and Thermal Systems," Birk Manufacturing, Inc., [Online]. Available: http://www.birkmfg.com/stockheaters.html. [Accessed 09 November 2012].

Appendix A Coupler Alignment and Installation

This appendix is included to provide a reference on coupler alignment and installation on the micro engine test stand. It assumes the final coupler configuration presented in Section 3.2.2 is being used.

Table A-1: Coupler Alignment and Installation Instruction

Step	Tasks	Tools
1	With all setscrews and clamping screws loosened, place coupler on electric motor shaft (do not tighten).	N/A
2	Place encoder disk on engine crankshaft and into encoder module slot. Spin threaded crankshaft into coupler while ensure the encoder disk is not flexed. Install 6 screws to hold engine to engine cradle, but do not tighten.	N/A
3	Remove motor end setscrew. Visually align flat on motor shaft with opening from setscrew. Position coupler axially to engage as much of the motor shaft as possible. Apply thread locking compound to setscrew and install. While holding the coupler and gently oscillating the motor +/- 5°, tighten the setscrew finger tight. You will feel the setscrew hit the flat as you oscillate until it is completely tightened and in good contact with the shaft flat. This oscillation ensures the setscrew has good contact with the shaft flat.	Light Source, Mild Thread locking Compound (Blue), 5/64" hex wrench
4	Torque the motor end clamping screw to 0.5, 1.0, and 1.5 Nm in three steps. For the 0.5 and 1.0 Nm steps, torque the clamping screw, loosen the setscrew, and re-tighten the setscrew finger tight. Retightening the setscrew ensures the flat remains properly engaged. For the final 1.5 Nm step, loosen the setscrew ~1/2 turn, torque to 1.5 Nm, and tightened the setscrew fully. No limit has been identified for the setscrew torque.	Torque wrench capable of 0.5-1.5 Nm, 2.5 mm hex socket for torque wrench, 5/64" hex wrench
5	Repeat steps 3 and 4 for the engine side of the coupler.	See steps 3 and 4.

Appendix B Initial Air Mass Flow Estimation Calculations

Assumptions:

1. The O.S. 70SZ-H could produce 250 W of electrical power from 2,000 to 10,000 RPM.
2. The delivery ratio* (assumed to be air mass, only) was 10% at 2,000 RPM and 100% at 10,000 RPM. This allows the absolute extremes to be observed over the desired RPM range.
3. The total displaced volume of the O.S. 70SZ-H would be used as the displaced volume instead of the volume when all of the gas exchange ports of the two-stroke engine were closed.
4. Ideal gas approximations were appropriate.

*Delivery ratio – "Compares the actual scavenging air mass (or mixture mass) to that required in an ideal charging process"

$$\Lambda = \frac{mass\ of\ delivered\ air\ per\ revolution}{displaced\ volume * ambient\ air\ density}$$

Calculations:

1. Displaced volume calculation:

$$V_d = \left(\frac{\pi}{4}\right) * B^2 * S$$

$$where:$$

$$V_d = Displaced\ volume\ (m)$$

$$B = Cylinder\ bore\ (m)$$

$$S = Engine\ stroke\ (m)$$

   For the O.S. 70SZ-H,

$$V_d = \left(\frac{\pi}{4}\right) * 0.0258^2 * 0.0220 = 11.5014 * 10^{-4}\ m^3$$

2. Volumetric flow rate calculations:

$$\dot{V} = N * V_d * \left(\frac{1}{n}\right) * \Lambda$$

$$where:$$

$$\dot{V} = Volumetric\ flow\ rate\ \left(\frac{m^3}{s}\right)$$

$$N = Engine\ Rotational\ Speed\ \left(\frac{rev}{s}\right)$$

$$n = Revolutions\ per\ cycle$$

$$\Lambda = Delivery\ ratio\ (-)$$

For the O.S. 70SZ-H at 2,000 RPM and 10% delivery ratio,

$$\dot{V_{low}} = \left(\frac{2{,}000\left(\frac{rev}{min}\right)}{60\left(\frac{s}{min}\right)}\right) * 11.5014 * 10^{-4}\ m^3 * \left(\frac{1}{1}\right) * 0.10 = 3.8338 * 10^{-5}\left(\frac{m^3}{s}\right)$$

For the O.S. 70SZ-H at 10,000 RPM and 100% delivery ratio,

$$\dot{V_{high}} = \left(\frac{10{,}000\left(\frac{rev}{min}\right)}{60\left(\frac{s}{min}\right)}\right) * 11.5014 * 10^{-4}\ m^3 * \left(\frac{1}{1}\right) * 1.00 = 1.9169 * 10^{-3}\left(\frac{m^3}{s}\right)$$

3. Estimate air mass flow using ideal gas approximation at normal temperature and pressure.

$$\rho = \frac{P}{R * T}$$

$where$:

$\rho = Density\ \left(\frac{kg}{m^3}\right)$

$P = Pressure\ (Pa)$

$R = Specific\ gas\ constant\ \left(\frac{J}{kg * K}\right)$

$T = Temperature\ (K)$

At 101, 325 Pa and 293 K for air ($R = \frac{8314.41\frac{J}{kg\ mol*K}}{28.95\left(\frac{kg}{kmol}\right)} = 287.20\ \left(\frac{J}{kg_{air}*K}\right)$),

$$\rho = \frac{101{,}325\ (Pa)}{287.20\ \left(\frac{J}{kg_{air} * K}\right) * 293\ K} = 1.20\frac{kg}{m^3}$$

Find mass flows:

$$m_{low} = V_{low}\left(\frac{\dot{m^3}}{s}\right)\dot{} * \rho\ \left(\frac{kg}{m^3}\right) = 3.8338 * 10^{-5}\left(\frac{m^3}{s}\right) * 1.20\left(\frac{kg}{m^3}\right) = 4.6000 * 10^{-5}\left(\frac{kg}{s}\right)$$

$$m_{high} = V_{high}\left(\frac{\dot{m^3}}{s}\right)\dot{} * \rho\ \left(\frac{kg}{m^3}\right) = 1.9169 * 10^{-3}\left(\frac{m^3}{s}\right) * 1.20\left(\frac{kg}{m^3}\right) = 2.3003 * 10^{-3}\left(\frac{kg}{s}\right)$$

Appendix C LabVIEW Virtual Instrument GUIs and Wiring Diagrams

This appendix includes the graphical user interfaces (GUI) and wiring diagrams for the LabVIEW virtual instruments (VI) necessary to control and acquire data from the micro engine test stand. It is provided to preserve the program in the event it is lost or accidentally modified.

The airflow VI was used to interpolate measured voltage into airflow and was incorporated into the micro engine test stand VI as a sub-VI. The fuel flow VI was used to interpolate measured voltages into fuel mass and fuel mass flow and was incorporated into the micro engine test stand VI as a sub-VI. The throttle interpolation VI was used to interpolate commanded throttle positions into a duty cycle for a pulse output and was incorporated into the micro engine test stand VI as a sub-VI. The N-point running average VI was taken from the National Instruments user forum and was written by Nic Linely. It was used to filter the fuel and airflow measurements and was implemented into the micro engine test stand VI as a sub-VI.

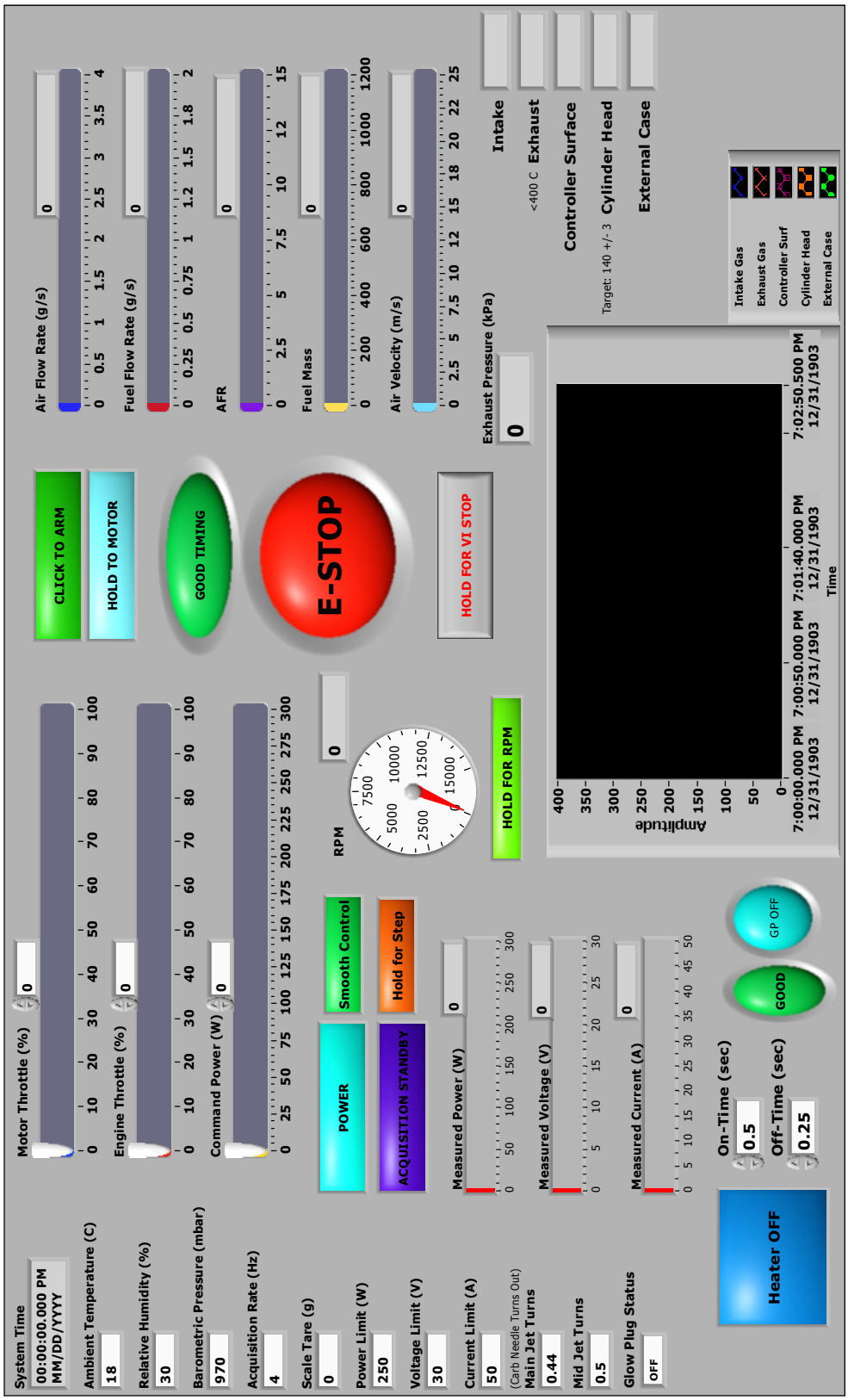
System Time
00:00:00.000 PM
MM/DD/YYYY
Ambient Temperature (C)
18
Relative Humidity (%)
30
Barometric Pressure (mbar)
970
Acquisition Rate (Hz)
4
Scale Tare (g)
0
Power Limit (W)
250
Voltage Limit (V)
30
Current Limit (A)
50
(Carb Needle Turns Out)
Main Jet Turns
0.44
Mid Jet Turns
0.5
Glow Plug Status
OFF
Heater OFF
Motor Throttle (%)
Engine Throttle (%)
Command Power (W)
POWER
ACQUISITION STANDBY
Smooth Control
Hold for Step
Measured Power (W)
Measured Voltage (V)
Measured Current (A)
On-Time (sec)
0.5
Off-Time (sec)
0.25
GOOD
GP OFF
RPM
HOLD FOR RPM
CLICK TO ARM
HOLD TO MOTOR
GOOD TIMING
E-STOP
HOLD FOR VI STOP
Air Flow Rate (g/s)
Fuel Flow Rate (g/s)
AFR
Fuel Mass
Air Velocity (m/s)
Exhaust Pressure (kPa)
Intake
<400 C Exhaust
Controller Surface
Target: 140 +/- 3 Cylinder Head
External Case
Amplitude
Time
7:00:00.000 PM 12/31/1903
7:00:50.000 PM 12/31/1903
7:01:40.000 PM 12/31/1903
7:02:50.500 PM 12/31/1903
Intake Gas
Exhaust Gas
Controller Surf
Cylinder Head
External Case

Figure C-1

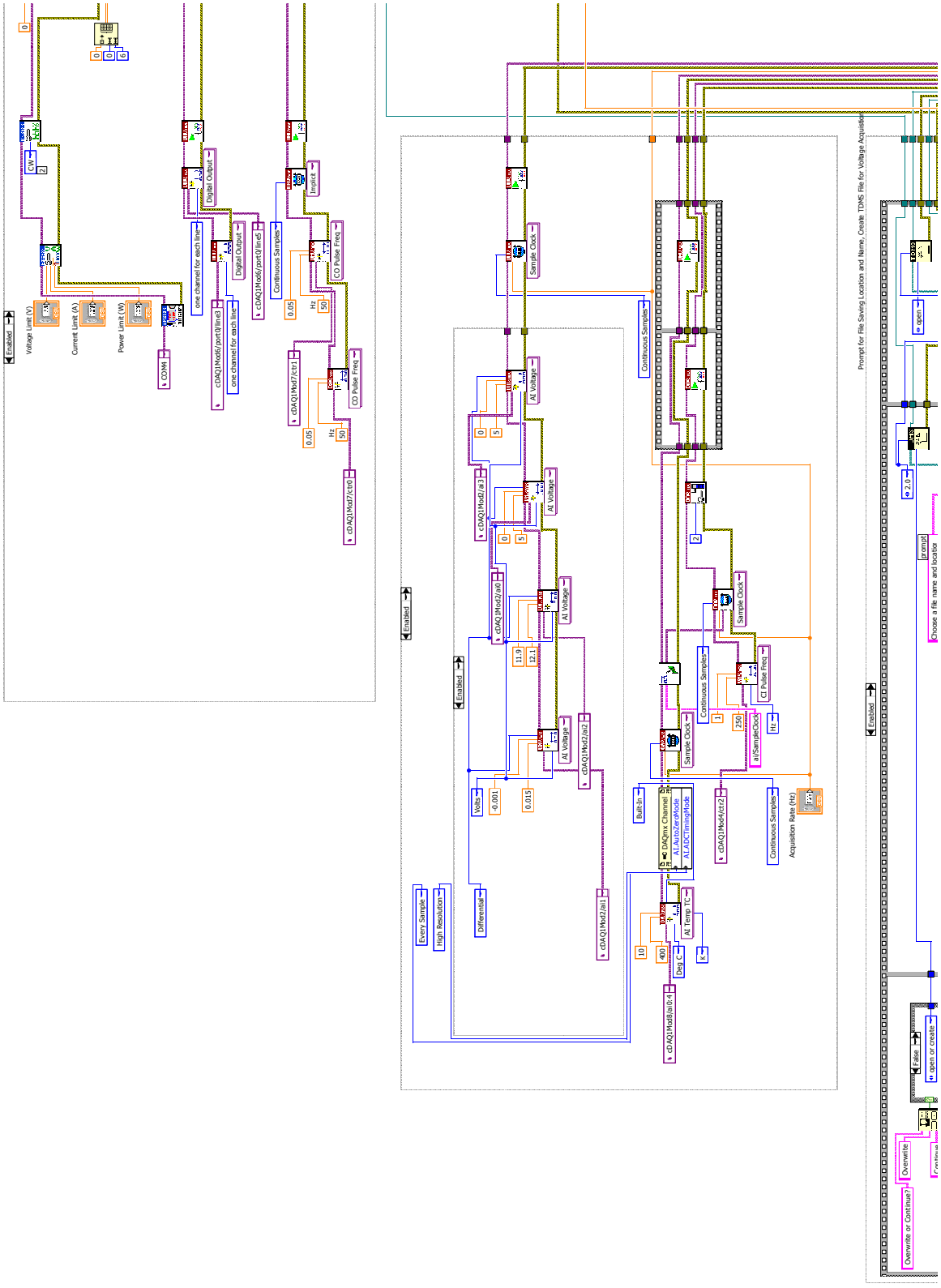
Enabled
Voltage Limit (V)
Current Limit (A)
Power Limit (W)
COM4
one channel for each line
Digital Output
cDAQ1Mod6/port0/line3
cDAQ1Mod6/port0/line5
Continuous Samples
0.05
Hz
50
CO Pulse Freq
cDAQ1Mod7/ctr1
cDAQ1Mod7/ctr0
Sample Clock
AI Voltage
cDAQ1Mod2/ai3
cDAQ1Mod2/ai0
cDAQ1Mod2/ai2
cDAQ1Mod2/ai1
Volts
-0.001
0.015
11.9
12.1
Every Sample
High Resolution
Differential
Built-In
DAQmx Channel
AI.AutoZeroMode
AI.ADCTimingMode
AI Temp TC
cDAQ1Mod8/ai0:4
Deg C
K
10
400
cDAQ1Mod4/ctr2
Continuous Samples
Acquisition Rate (Hz)
CI Pulse Freq
ai/SampleClock
Prompt for File Saving Location and Name, Create TDMS File for Voltage Acquisition
open
2.0
prompt
Choose a file name and locatio
False
open or create
Overwrite
Overwrite or Continue?

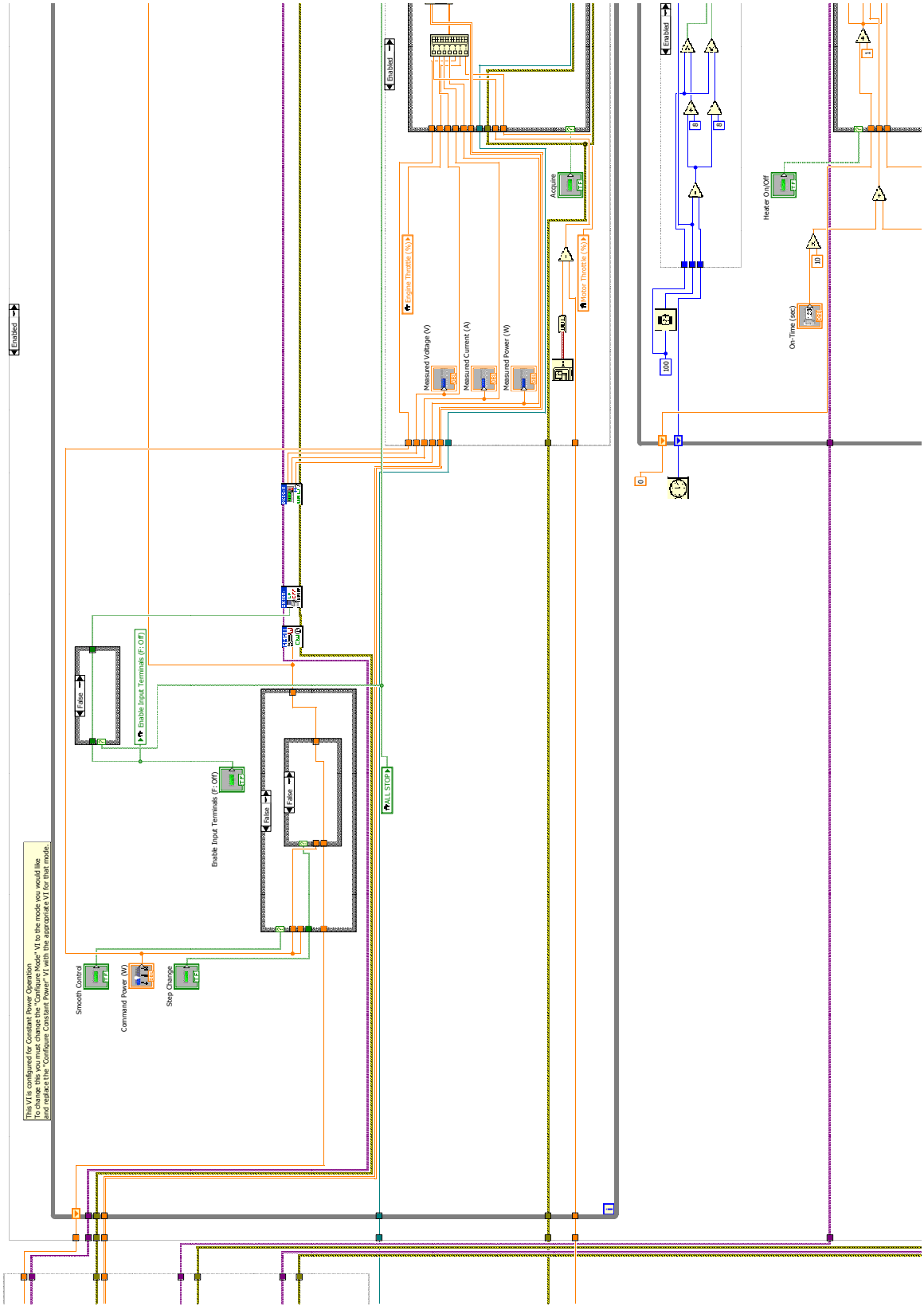
Enabled
Acquire
Measured Voltage (V)
Measured Current (A)
Measured Power (W)
Engine Throttle (%)
Motor Throttle (%)
Heater On/Off
On-Time (sec)
Enable Input Terminals (F: Off)
ALL STOP
Smooth Control
Command Power (W)
Step Change
This VI is configured for Constant Power Operation
To change this you must change the "Configure Mode" VI to the mode you would like
and replace the "Configure Constant Power" VI with the appropriate VI for that mode.

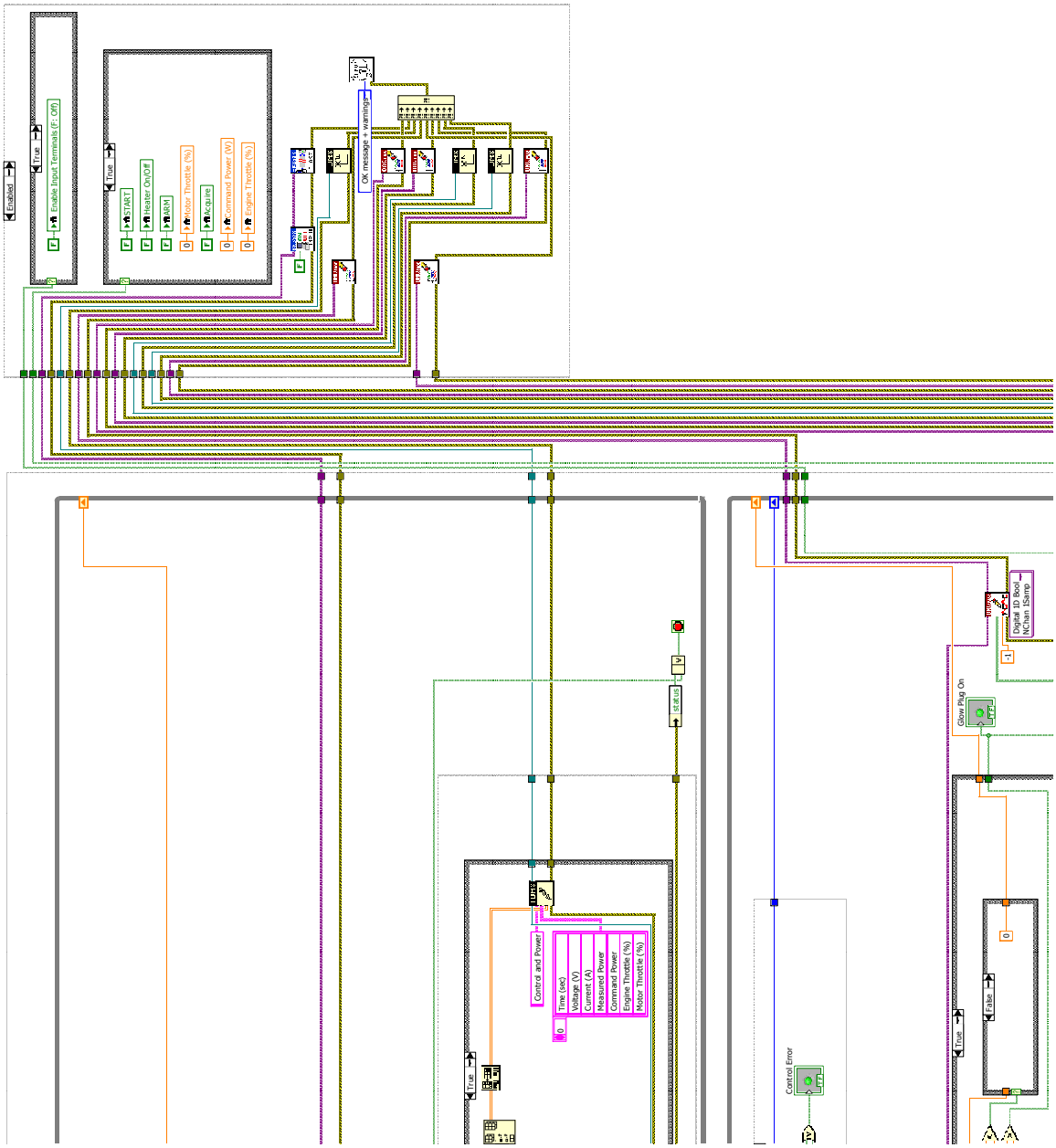
Enabled
True
Enable Input Terminals (F: Off)
True
START
Heater On/Off
ARM
Motor Throttle (%)
Acquire
Command Power (W)
Engine Throttle (%)
OK message
Warnings
status
Control and Power
Time (sec)
Voltage (V)
Current (A)
Measured Power
Command Power
Engine Throttle (%)
Motor Throttle (%)
Glow Plug On
Control Error
Enable
True

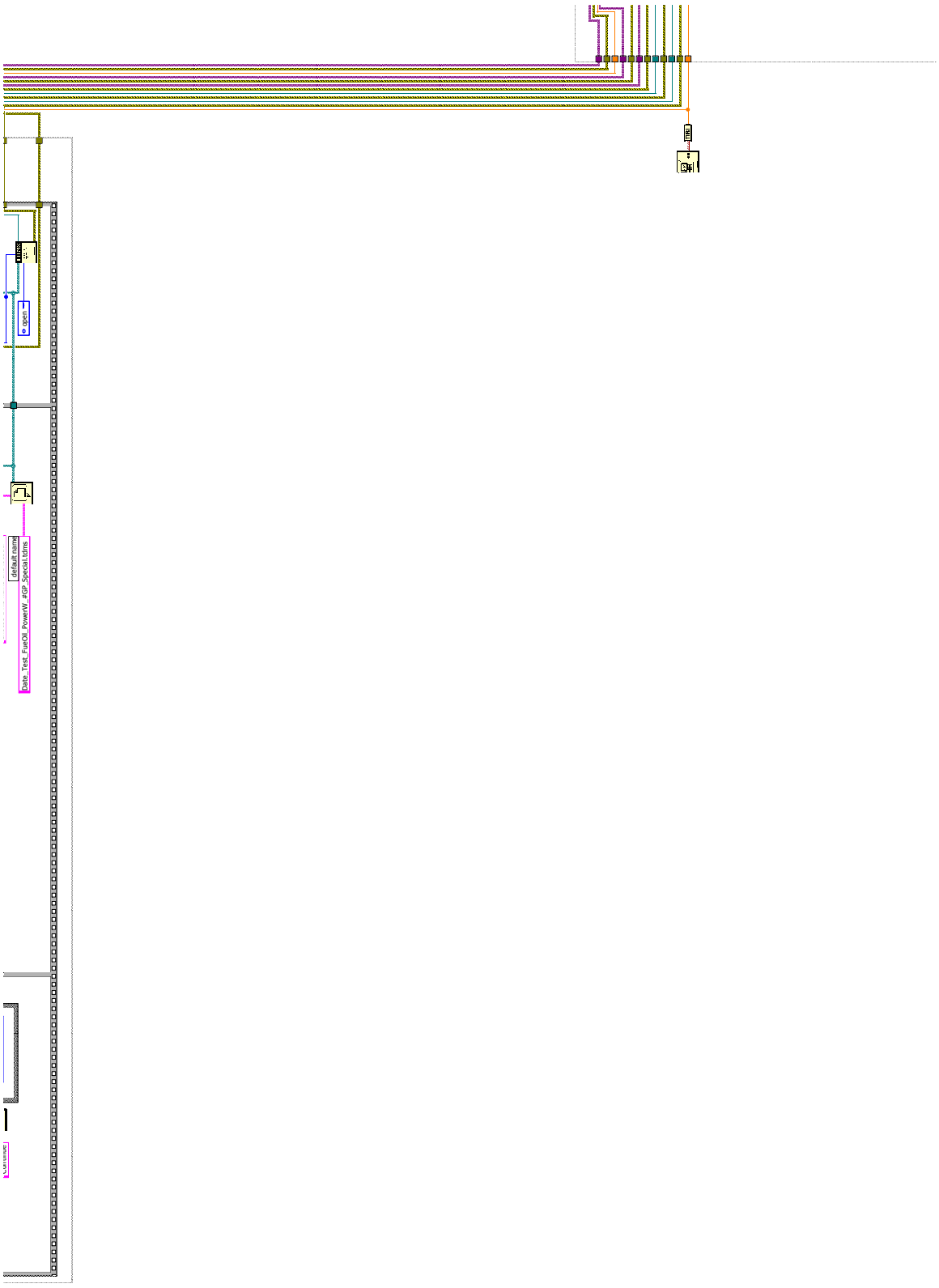
open
default name
Date_Test_Fue09_PowerW_#GP_Special.tdms

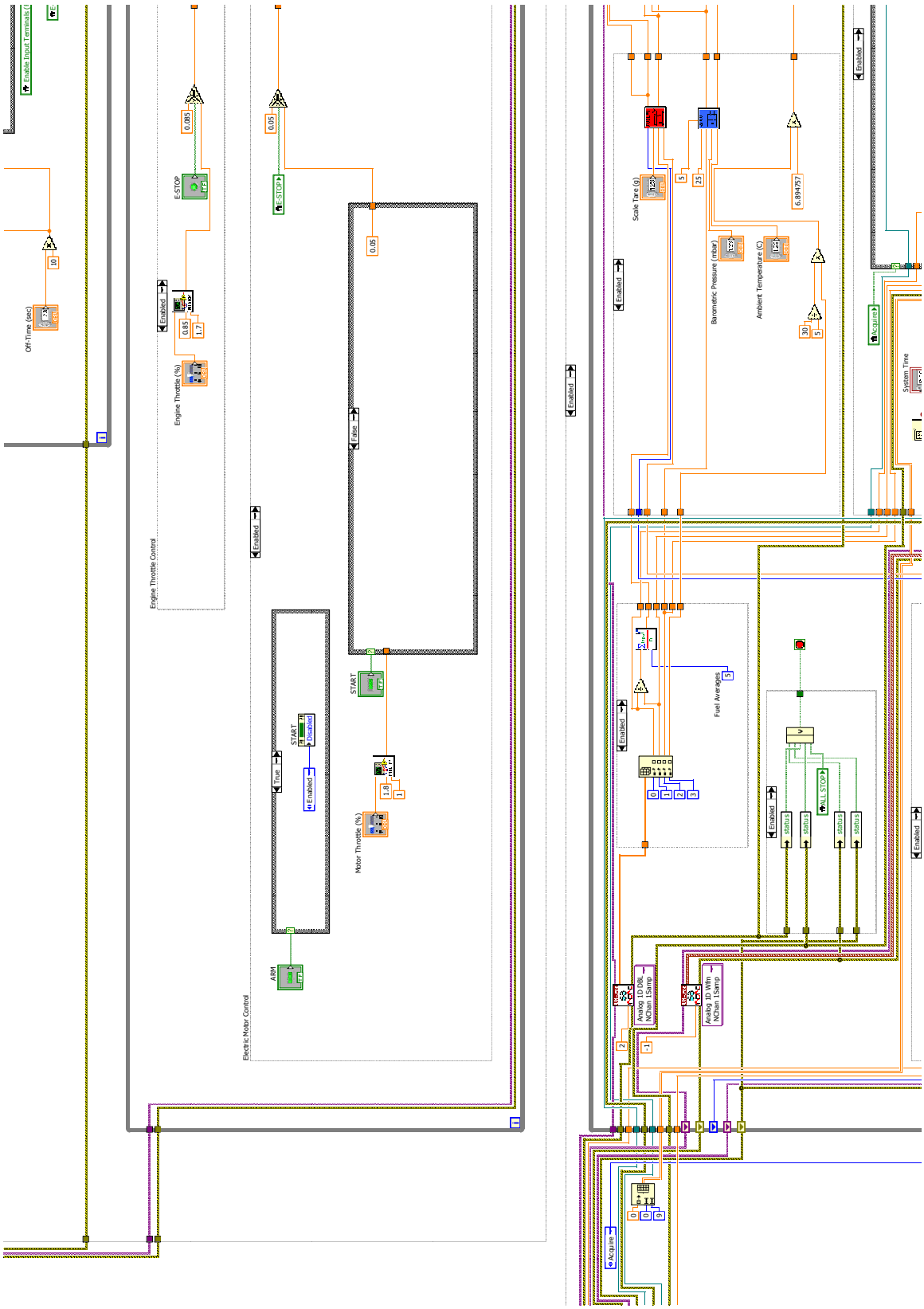
Enable Input Terminals
Off-Time (sec)
E-STOP
Engine Throttle (%)
Engine Throttle Control
Electric Motor Control
START
ARM
Motor Throttle (%)
Scale Tare (g)
Barometric Pressure (mbar)
Ambient Temperature (C)
Fuel Averages
ALL STOP
Analog 1D DBL NChan 1Samp
Analog 1D Wfm NChan 1Samp
System Time

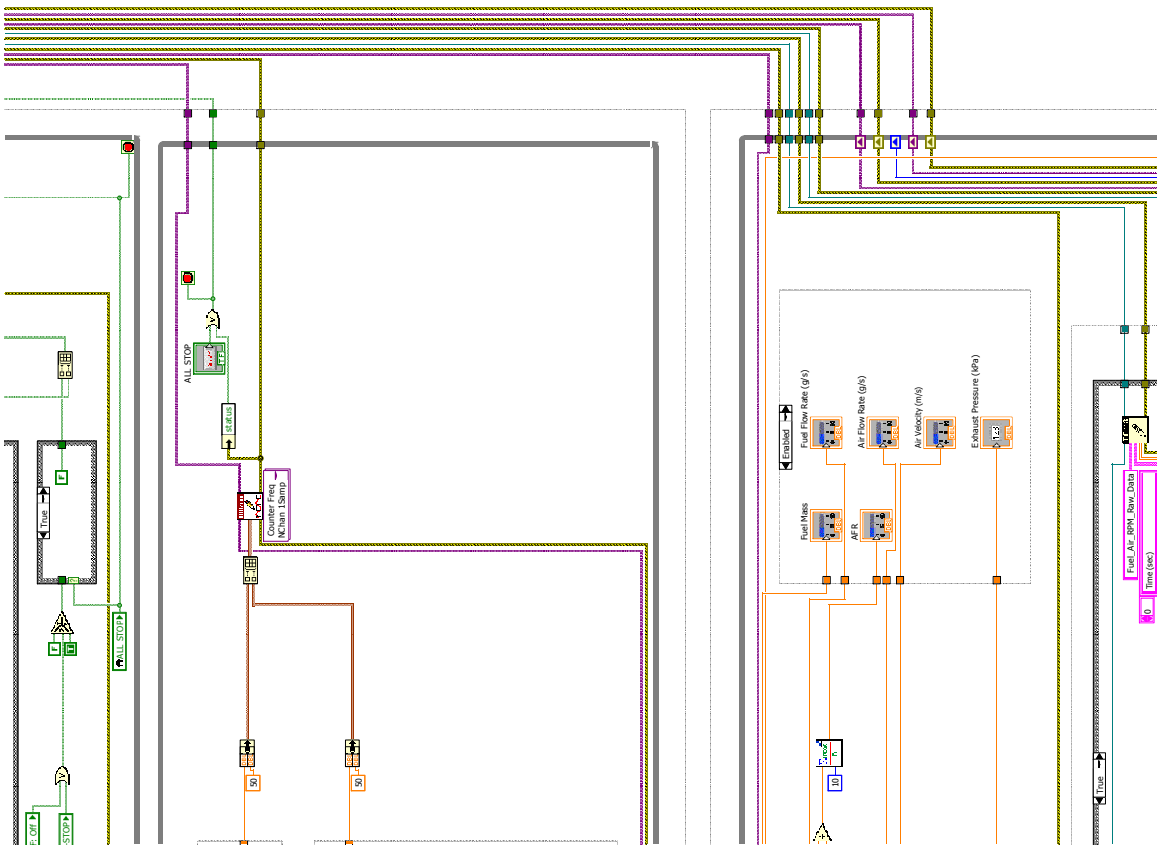
ALL STOP
Status
Counter Freq
NChan 1Samp
Enabled
Fuel Flow Rate (g/s)
Air Flow Rate (g/s)
Air Velocity (m/s)
Exhaust Pressure (kPa)
Fuel Mass
AFR
Fuel_Air_RPM_Raw_Data
Time (sec)
True
ALL STOP
STOP
50

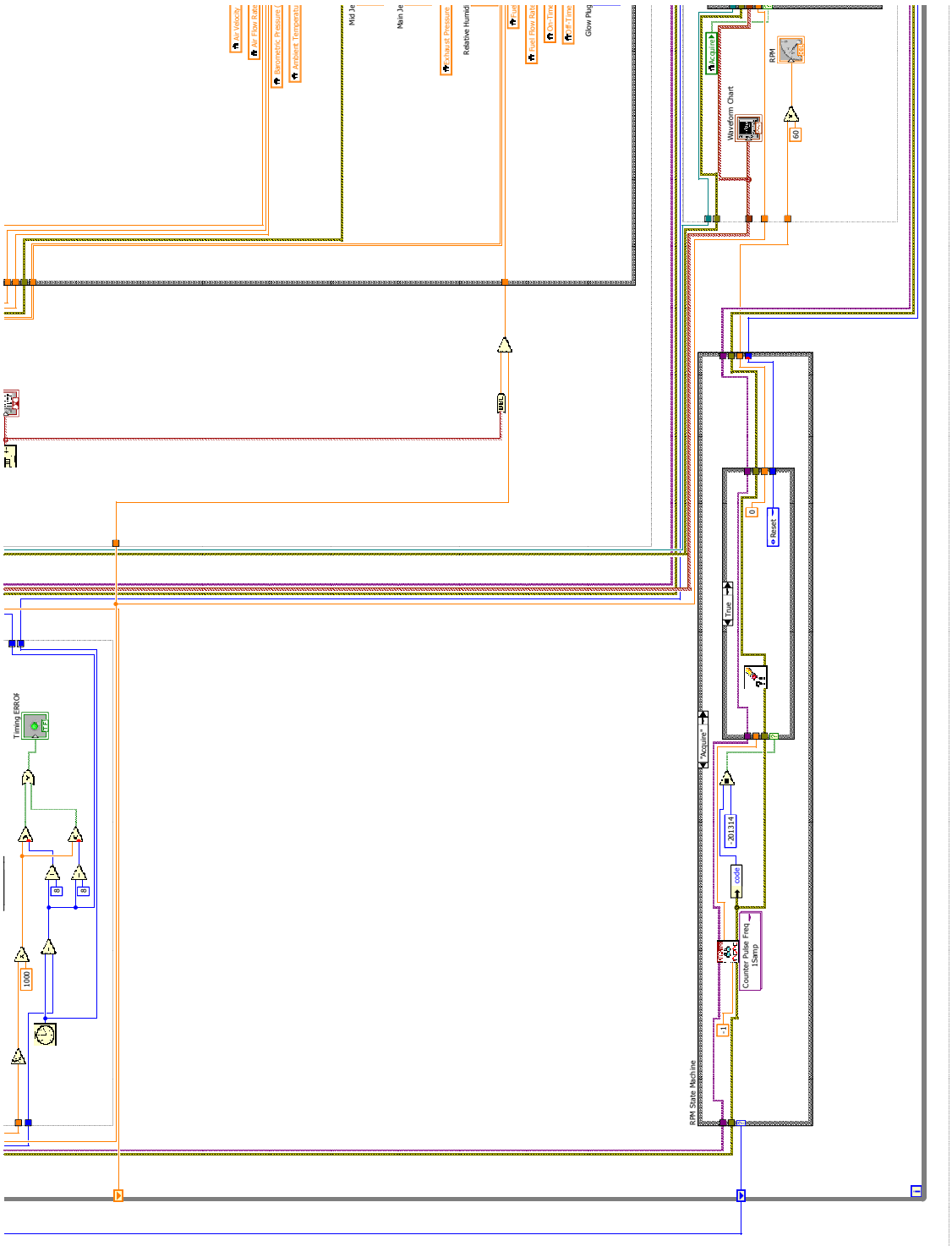
Air Velocity
Air Flow Rate
Barometric Pressure
Ambient Temperatu
Exhaust Pressure
Relative Humidi
Fuel
Fuel Flow Rate
Inj Time
IP T Time
Glow Plug
Acquire
RPM
Waveform Chart
60
Reset
True
"Acquire"
20134
code
Counter 1 Pulse Freq
1-samp
-1
RPM State Machine
Timing ERROR
1000

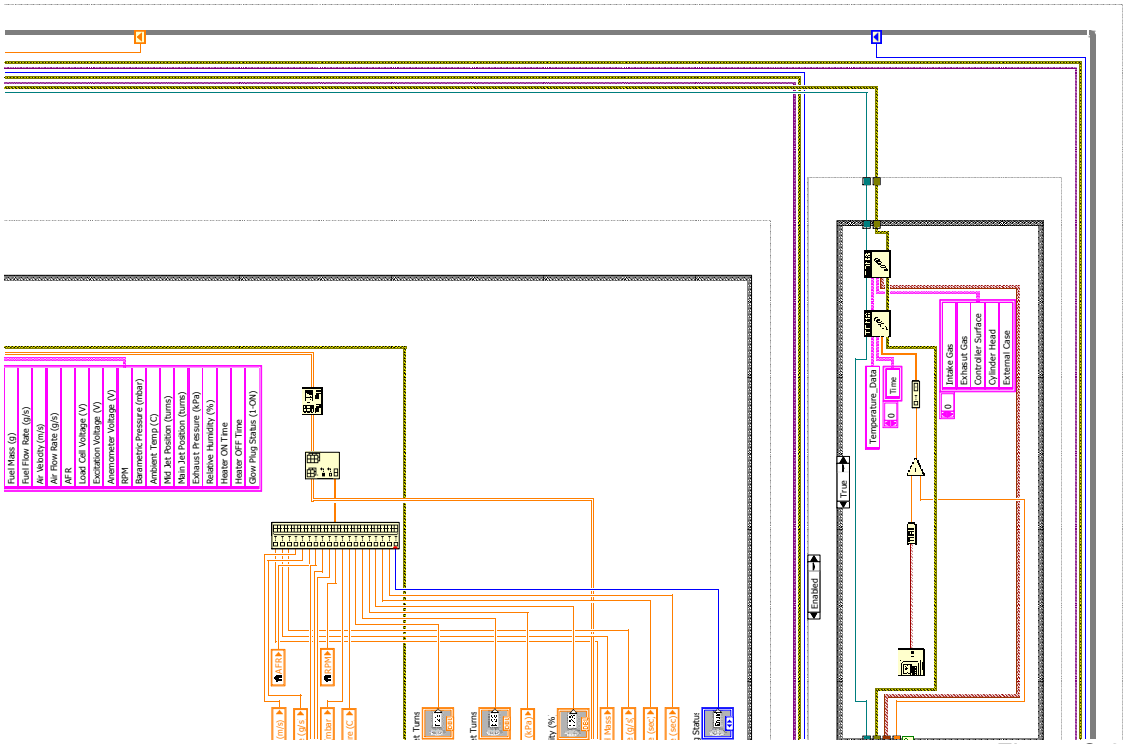
Fuel Mass (g)
Fuel Flow Rate (g/s)
Air Velocity (m/s)
Air Flow Rate (g/s)
AFR
Load Cell Voltage (V)
Excitation Voltage (V)
Anemometer Voltage (V)
RPM
Barometric Pressure (mbar)
Ambient Temp (C)
Mid Jet Position (turns)
Main Jet Position (turns)
Exhaust Pressure (kPa)
Relative Humidity (%)
Heater ON Time
Heater OFF Time
Glow Plug Status (1-ON)
Enabled
True
Temperature_Data
Time
Intake Gas
Exhaust Gas
Controller Surface
Cylinder Head
External Case

Figure C-2

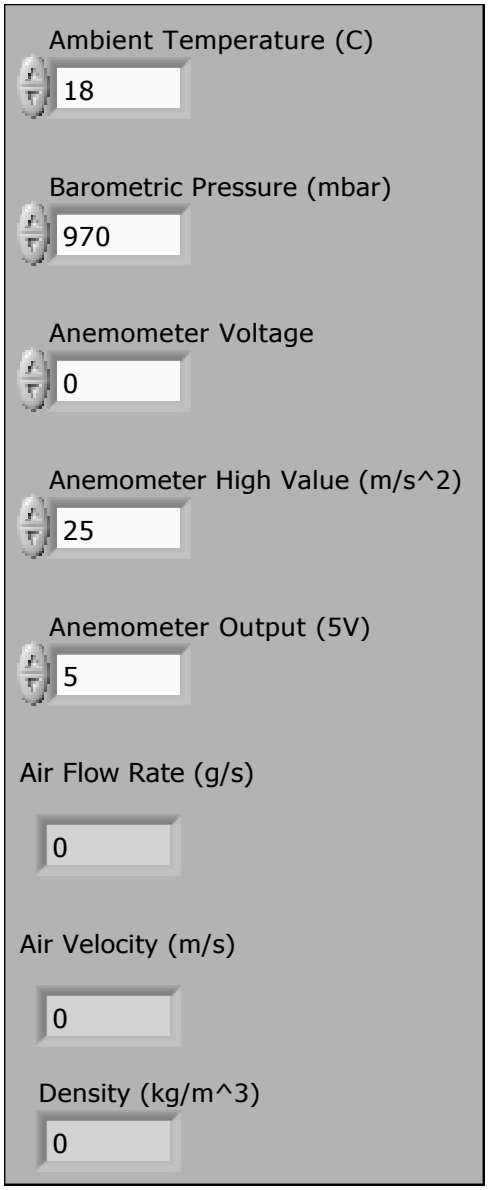
Ambient Temperature (C)
18
Barometric Pressure (mbar)
970
Anemometer Voltage
0
Anemometer High Value (m/s^2)
25
Anemometer Output (5V)
5
Air Flow Rate (g/s)
0
Air Velocity (m/s)
0
Density (kg/m^3)
0

Figure C-3

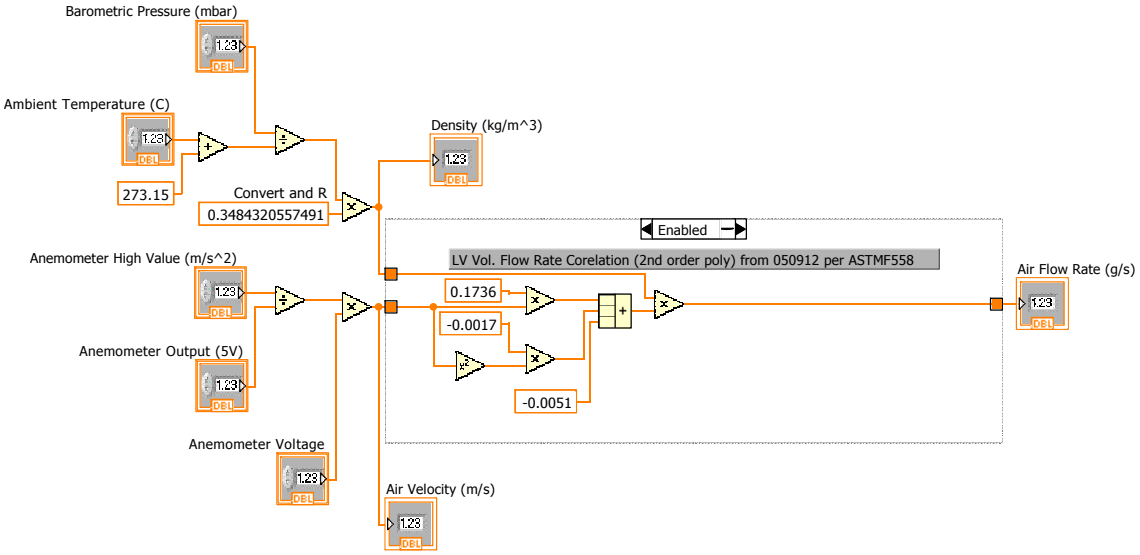
Barometric Pressure (mbar)
Ambient Temperature (C)
273.15
Convert and R
0.3484320557491
Density (kg/m^3)
Enabled
LV Vol. Flow Rate Corelation (2nd order poly) from 050912 per ASTMF558
Anemometer High Value (m/s^2)
Anemometer Output (5V)
Anemometer Voltage
0.1736
-0.0017
-0.0051
Air Velocity (m/s)
Air Flow Rate (g/s)

Figure C-4

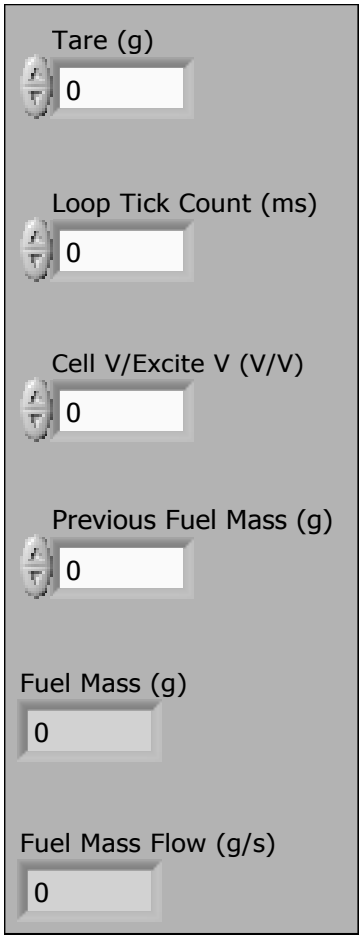

Figure C-5

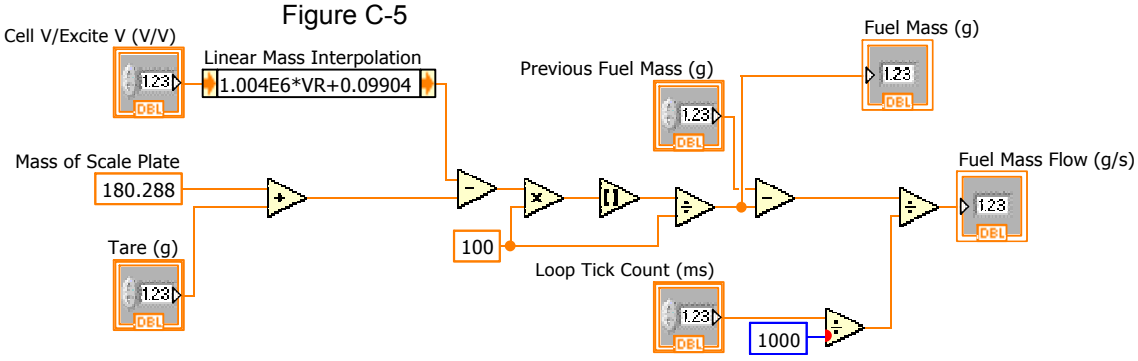

Figure C-6

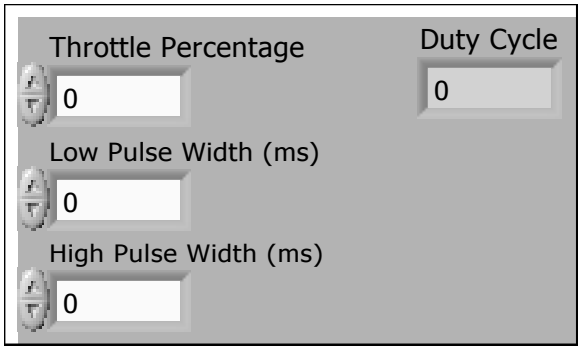

Figure C-7

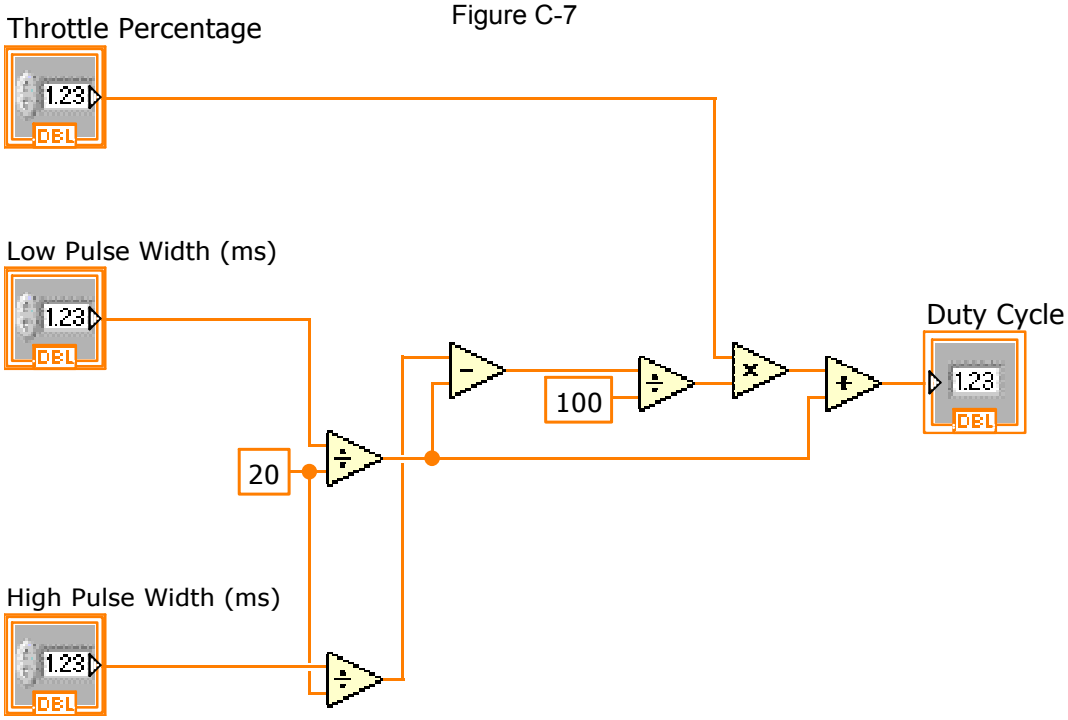

Figure C-8

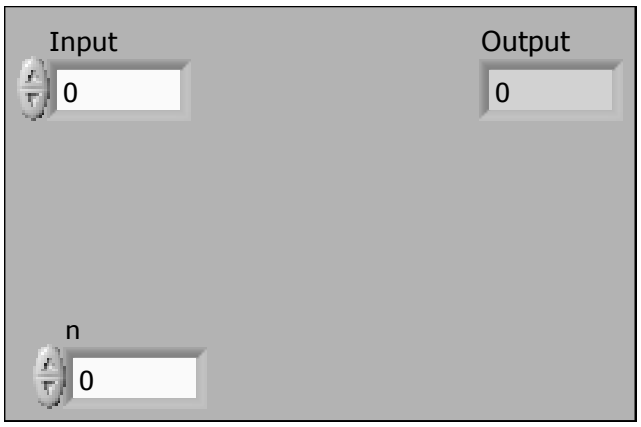

N Point Running Average
Nic Linley, Wendell Hull & Associates Inc.
01/30/2006

Usage: use in a loop that is aquiring or displaying data. Supply the current value and window size and the output will be the running average of the current window size.

So if "i" is the current sample then

Output[i] = (Input[i] + Input[i-1] + input[i-2] + ...+ input[i-n-1])/n

The VI is "reentrant," so you can have multiple ones place in a single VI.

The array being passed between the shift registers needs to be initilized to the windows size, "n." The condition for initializaiton is either the array size is less then 1 or the previous value of "n" != the current value of "n."

Figure C-9

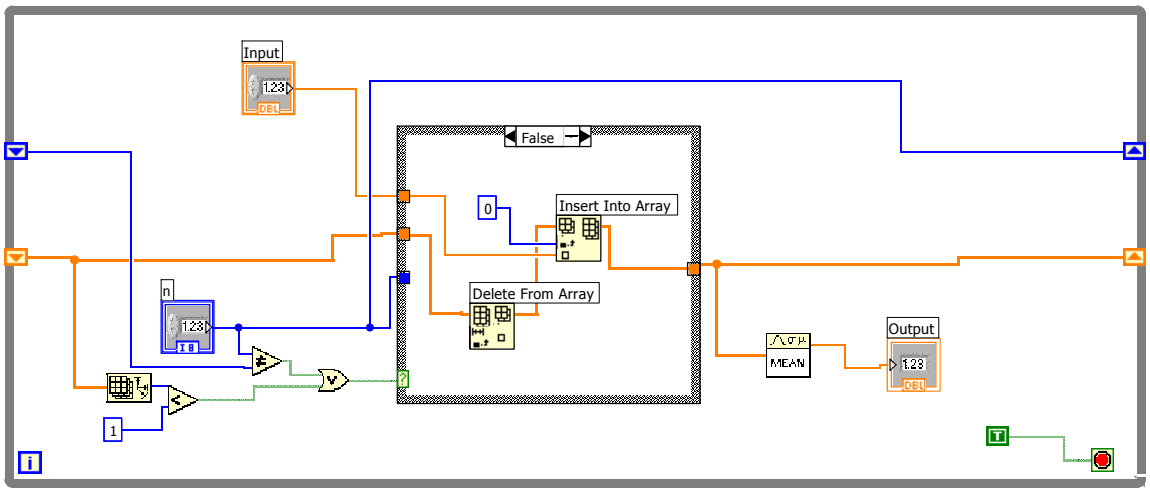

Figure C-10